DOCTORAL THESIS

# RENORMALIZATION GROUP FLOWS IN GAUGE-YUKAWA THEORIES, COMPOSITENESS & THE HIGGS

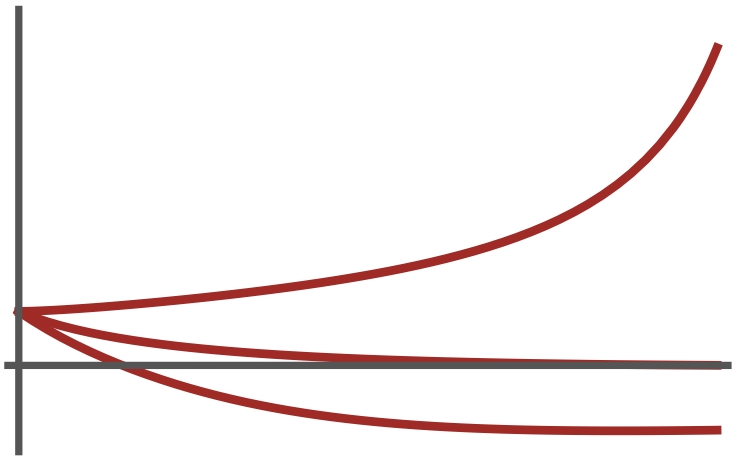

JENS KROG

# Renormalization Group Flows in Gauge-Yukawa Theories, Compositeness & the Higgs


| | |
|---|---|
| Author | Jens F. C. Krog |
| Advisor | Francesco Sannino |
| Co-Advisor | Claudio Pica |


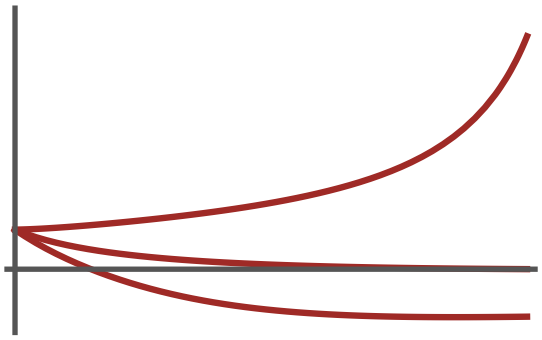

*Dissertation for the degree of Doctor of Philosophy*


CP$^3$-Origins
Centre for Cosmology and Particle Physics Phenomenology,
Department of Physics, Chemistry, and Pharmacy



Submitted to the University of Southern Denmark
October 28, 2015

# Acknowledgements

For the duration of my Ph.D. studies, I have had the pleasure of being part of the $CP^3$-Origins center, which has offered me a great community for scientific work as well as a valuable social interactions. I wish to thank current as well as former members of the $CP^3$ group for contributing to this experience, and in particular my advisor Francesco Sannino, who invited me to be part of the group.

Part of my studies were spent at the Fermilab National Accelerator Laboratory. The stay at Fermilab was very fruitful, and I owe thanks to Chris Hill for hosting me as well as the rest of the theory group for their generous hospitality.

# Abstract

The discovery of a bosonic resonance at the Large Hadron Collider (LHC) has forced the scientific community to take the theory for electroweak symmetry breaking including a Higgs scalar seriously, if not to accept it all together. The Higgs boson is now incorporated in the standard model (SM), and in this work we will mainly focus on the behavior of this or similar theories at small length scales.

Besides from the inherent hierarchy problem in scalar theories, these also may suffer from other complications. The isolated scalar $\phi^4$ theory may prove to be "trivial" due a the positive sign of its beta function, while the incorporation of Yukawa couplings threaten to drive the coupling negative and invoke instability of the electroweak vacuum. One should either make sure that the theory stays consistent at least until the Planck scale, where unknown gravitational effects should appear, or abandon the idea of fundamental scalars. These two possibilities are the motivation for the results presented here.

In this thesis we investigate the ultra violet (UV) behavior for the standard model and a set of extensions with respect to the issues mentioned above. We elucidate on previously unknown relations between the renormalization group (RG) equations of the standard model stemming from the required abelian nature of the Weyl anomaly, and propose a new lowest order calculation that satisfies the consistency conditions. We investigate the issue of instability in certain extensions of the standard model, and find that the electroweak vacuum may be stable in these extension where the parameters for the dark matter sector are constrained. Additionally we find that the extensions, in the same way as the standard model, are consistent with the idea of asymptotic safety, where the quartic scalar coupling vanishes at the Planck scale.

By instead allowing a divergence of the scalar coupling, one may interpret the gauge-Yukawa theory as being the low-energy description of a theory of fermions with a four-fermion interaction. We demonstrate that a large class of gauge-Yukawa theories may be equivalent to a theory of fermions and composite scalars, and determine the allowed parameter space for the gauge-Yukawa theory. We finally show that the Higgs boson may arise from such a theory as composite of neutrinos provided extra scalars are present. We show that the observed vacuum expectation value (VEV) and mass for the Higgs field arise naturally in specific extensions utilizing the Coleman-Weinberg mechanism while including viable dark matter candidates.

# Sammenfatning

Opdagelsen af en bosonlignende resonans ved eksperimenterne ved partikelacceleratoren "Large Hadron Collider" (LHC) har tvunget det videnskabelige miljø til enten at tage teorien for det elektrosvage symmetribrud via en Higgs-boson seriøst eller blot direkte acceptere den. Higgs-bosonen er nu indført i standardmodellen (SM), og i det følgende vil vi hovedsageligt fokusere på denne og lignende teoriers karakteristik ved små længdeskalaer.

Udover det, til teorier med skalarpartikler, tilhørende hierarkiproblem, kan teorierne også indeholde yderligere komplikationer. Isoleret set kan en skalar $\phi^4$-teori vise sig at være "triviel" grundet betafunktionen positive fortegn, hvorimod tilføjelse af Yukawakoblinger truer med at drive den kvartiske kobling til negative værdier og medføre ustabilitet af den elektrosvage grundtilstand. Enten bør teorien forblive konsistent ned til Planckskalaen, hvor ukendte gravitationseffekter bør dukke op, eller også må man opgive klassen af teorier med fundamentale skalarpartikler til at beskrive naturen. Disse to muligheder er motivationen for de resultater, som her vil blive præsenteret.

I denne afhandling undersøges den ultraviolette (UV) opførsel af standardmodellen og en mængde udvidelser af denne med henblik på de nævnte problemer. Vi belyser relationer imellem ligningerne for renormeringsgruppen(RG) for standardmodellen, som tidligere var ukendte, stammende fra den abelske egenskab af Weyl-anomalien og foreslår en ny førsteordens beregning, som overholder de tilhørende konsistenskrav. Vi undersøger problemet vedrørende ustabilitet i visse udvidelser af standardmodellen og finder at den elektrosvage grundtilstand kan være stabilt i disse udvidelser, hvilket sætter begrænsninger for de tilhørende nye parametre og de nye partikler i modellen herunder en kandidat til mørkt stof. Ydermere finder vi at denne klasse af udvidelser, ligesom standardmodellen, kan være konsistente med konceptet "asymptotisk sikkerhed", hvor den kvartiske kobling ved Planckskalaen er nul.

Hvis man istedet tillader en divergens af den kvartiske kobling, kan den tilhørende gauge-Yukawa teori ses som værende en beskrivelse af en teori bestående af fermioner med en firefermion-kobling ved store skalaer. Vi demonstrerer at en betydelig klasse af gauge-Yukawa-teorier kan være ækvivalente til teorier med fermioner og sammensatte skalarpartikler, og kortlægger de tilladte parameterrum for gauge-Yukawa-teorien. Slutteligt viser vi at den observerede vakuumforventningsværdi (VEV) og masse for Higgsfeltet fremkommer naturligt i specifikke udvidelser af standardmodellen hvor Coleman-Weinberg-mekanismen er anvarlig for symmetribruddet og som indeholder kandidater til mørkt stof.

# Preface

This dissertation is based mainly on results obtained through my Ph.D. studies, during which I have contributed to the following publications:


[1] O. Antipin, M. Gillioz, J. Krog, E. Mølgaard and F. Sannino,
"Standard Model Vacuum Stability and Weyl Consistency Conditions,"
JHEP **1308**, 034 (2013), [arXiv:1306.3234 [hep-ph]].

[2] O. Antipin, J. Krog, M. Mojaza and F. Sannino,
"Stable E$\chi$tensions with(out) gravity,"
Nucl. Phys. B **886**, 125 (2014), [arXiv:1311.1092 [hep-ph]].

[3] J. Krog, M. Mojaza and F. Sannino,
"Four-Fermion Limit of Gauge-Yukawa Theories,"
Accepted for publication in Phys.Rev.D, arXiv:1506.02642 [hep-ph].

[4] J. Krog and C. T. Hill,
"Is the Higgs Boson Composed of Neutrinos?,"
Accepted for publication in Phys.Rev.D, arXiv:1506.02843 [hep-ph].

[5] O. Antipin, J. Krog, E. Mølgaard and F. Sannino,
"Standard Model-like corrections to Dilatonic Dynamics,"
JHEP **1309**, 122 (2013), [arXiv:1303.7213 [hep-ph]].


To keep the line of reasoning coherent, only the results from [1–4] will be presented in the following.

# CONTENTS

# CHAPTER 1

# INTRODUCTION: A GAME OF INFINITIES

Trying to grasp the structure of our physical world at the length scales small enough to be beyond human perception has been a primary goal of many physicists over the last several centuries. The development of the theory of electromagnetism and quantum mechanics has given us increasingly impressive insights into the Nature of small scale phenomena. In order to incorporate quantum mechanics and special relativity into the same theory, quantum field theory was invented, and with it a wonderfully intuitive (though somewhat simplified) picture was invented to describe processes at the smallest scales: The Feynman diagrams. With Feynman diagrams, any process can be described with diagrams that intuitively visualize the interactions while giving a unambiguous recipe for calculating physical observables connected to the process. In Fig. 1.1 we show a diagram corresponding to the interaction between two fermions through the electromagnetic force. The main flaw in such pictures is that the spacial visualization in the diagram does not correspond to actual separation, but the horizontal axis should be though of as being the time evolution of the system, while any particles that only propagate internally in the diagram do not necessarily have the same properties as they would in a process where they were part of either the initial or final state of the system.

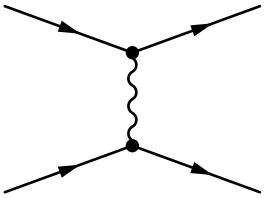

Figure 1.1: The electromagnetic interaction between two fermions represented via a Feynman diagram. The horizontal axis should be thought of as representing difference in time rather than in space.

The only ingredients one has to know to calculate the contribution to the cross section coming from a specific diagram are the propagators of the diagram and the vertices that connect these propagators. These quantities are defined in the

underlying quantum field theory, and once they are known, the calculation of the amplitude of a diagram follows directly from the expressions connected to them.

In the quantum field theory for a single scalar field $\phi$ governed by the Lagrangian density

$$\mathscr{L} = \frac{1}{2}\left(\partial_\mu \phi\right)^2 - \frac{1}{2} m_0 \phi^2 - \frac{\lambda_0}{4!}\phi^4, \tag{1.1}$$

the propagation of a scalar particle is given by

$$\text{----------} = \frac{i}{p^2 - m_0^2 + i\epsilon}, \tag{1.2}$$

and is related to the amplitude for a particle to propagate from $x$ to $y$ in a free theory (where $\lambda_0 = 0$) through the Fourier transform:

$$\langle 0|T\phi(x)\phi(y)|0\rangle = \int \frac{d^4p}{(2\pi)^4} \frac{i}{p^2 - m^2 + i\epsilon} e^{-ip\cdot(x-y)}. \tag{1.3}$$

As for the interaction between scalar particles, the vertex is parametrized even simpler:


$= -i\lambda_0$ (1.4)

Combining these ingredients into a diagram that corresponds to a given physical process yields an unambiguous result for the contribution from that diagram.

The picture is intuitive and straightforward at this level. The remainder of this chapter will deal with a specific problem that arises in this picture: To compute a cross section or correlation function, we should sum the contributions of all (connected and amputated) diagrams that correspond to the quantity in question. In the scalar field theory of (1.1) some of the extra diagrams that need to be taken into account will contain loops which will include extra factors of the interaction $\lambda_0$. In this case, we might argue that $\lambda_0$ is small, such that only the lowest order diagrams containing no loops should be relevant. As it turns out, the loop diagrams carry integrals over the momentum going around the loop which often are divergent quantities. That the corrections coming from diagrams of higher order in a small expansion parameter seem to be infinite naturally led to some frustration in the particle physics community; it seemed that the intuitive picture described above had fatal flaws which might invalidate the procedure all together. Luckily solutions were found for the problem, and in modern particle physics the juggling of infinities in divergent diagrams has been turned into a valuable tool through the process of *renormalization*, which forms the basis of most of the results presented in this thesis. In this section we will follow the logic of renormalization as presented in [6].

## 1.1 RENORMALIZATION IN PARTICLE PHYSICS

When we allow for interactions, like the term proportional to $\lambda_0$ in (1.1), the Hamiltonian of the theory is changed, and so is the ground state of the theory. Instead of the simple amplitude for propagation in (1.3), we consider the two-point Green's function,

$$\langle\Omega|T\phi(x)\phi(y)|\Omega\rangle, \tag{1.5}$$

where we have exchanged the original ground state $|0\rangle$ for the ground state of the interacting theory $|\Omega\rangle$. The physical interpretation of this expression is still the amplitude for propagation between $y$ and $x$, but the value changes due to the interactions of the theory.

Specifically, the propagation between the two points can now take place in several ways, and we define a corrected propagator:

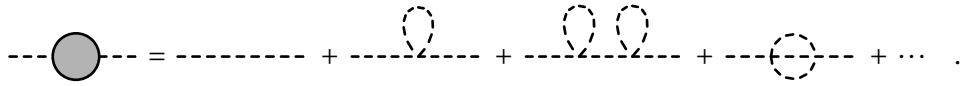

(1.6)

A further analysis of the two point function reveals that, in the interacting theory, its Fourier transform is given by

$$\int d^4x e^{ip\cdot x}\langle\Omega|T\phi(x)\phi(0)|\Omega\rangle = \frac{iZ}{p^2-m^2+i\epsilon} + \text{terms regular at } p^2=m^2. \tag{1.7}$$

Performing the same Fourier transform on (1.3) leads directly to the propagator (1.2). Two things should be noted from the corrected result: First, $m_0$ has been replaced by $m$ thereby shifting the pole of the propagator, and second the residue of the pole is $Z$ in the interacting theory. We call $Z$ the field renormalization, $m_0$ the bare mass, and $m$ the physical mass of the $\phi$ boson. On the same note, we will expect that the physical coupling constant $\lambda$ will differ from $\lambda_0$. So far we have not directly encountered any of the infinites mentioned in the beginning. They are present in the shift between the physical mass and the bare mass and in $Z$, and we shall see how to handle them shortly.

In order to recover the intuitive picture presented in the beginning, we will have to renormalize the theory, which loosely put is to trade divergences with unobservable shifts of the parameters in the theory. In order to recover the original form of the propagator (1.2), we rescale the $\phi$ field:

$$\phi = Z^{1/2}\phi_r. \tag{1.8}$$

Defining the theory in terms of $\phi_r$, will then lead to the same residue for the pole in the propagator as usual, although with a different pole.

After the rescaling, the Lagrangian has the form

$$\mathscr{L} = \frac{1}{2}Z\left(\partial_\mu\phi_r\right)^2 - \frac{1}{2}Zm_0\phi^2 - \frac{\lambda_0}{4!}Z^2\phi_r^4. \tag{1.9}$$

To define the theory in terms of the physical parameters we define

$$\delta_Z = Z - 1, \qquad \delta_m = m_0 Z^2 - m^2, \qquad \delta_\lambda = \lambda_0 Z^2 - \lambda. \tag{1.10}$$

With this redefinition, the Lagrangian becomes

$$\begin{aligned}\mathscr{L} = &\frac{1}{2}\left(\partial_\mu \phi_r\right)^2 - \frac{1}{2} m \phi_r^2 - \frac{\lambda}{4!}\phi_r^4 \\ &+ \frac{1}{2}\delta_Z \left(\partial_\mu \phi_r\right)^2 - \frac{1}{2}\delta_m \phi_r^2 - \frac{\lambda}{4!}\delta_\lambda \phi_r^4,\end{aligned} \tag{1.11}$$

where the second line is normally called the *counter terms* of the theory. These terms will contribute with new Feynman rules like the physical parameters, and are what we use to cancel divergences that arise in any process, making the theory well defined.

Since we have defacto introduced three new parameters in the Lagrangian through (1.10), we should define them by relating them to some quantity in the theory, to keep the number of free parameters constant. In $\phi^4$ theory, this may be done through the diagrams[1]

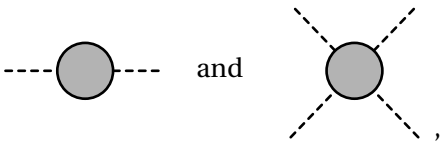


, (1.12)

where the grey circles imply that all connected diagrams with the same external legs have been summed to yield the total contribution. The defining conditions are called *renormalization conditions*, and specify the value of the above diagrams at some specific value of the external momenta in the diagrams. Different renormalization conditions may be chosen, and this fact is what may turn the divergence cancellation into a tool rather than a problem, as we will see.

### 1.1.1 A one loop example

To exemplify the notions presented in the beginning of this section, we examine the renormalization of $\phi^4$ theory at one loop order, to see where divergences may arise, and how to eliminate them from physical predictions.

We start off by setting the renormalization conditions

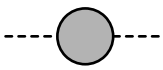

$$= \frac{i}{p^2 - m^2} + \quad \text{(terms regular at } p^2 = m^2\text{)};$$

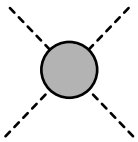

$$= -i\lambda \quad \text{(at } s = 4m^2\,,\ t = u = 0.\text{)} \tag{1.13}$$

[1] The procedure is very similar for theories with fermions and vector bosons. We will stick to $\phi^4$ theory so as to give the clearest picture of the logic of the renormalization procedure.

where the first condition defines both the mass and the residue of the propagator, and the last defines the physical coupling.

We may now look at a specific amplitude, namely the two particle scattering amplitude:

$i\mathcal{M}(p_1 p_2 \to p_3 p_4) =$ 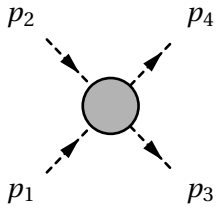


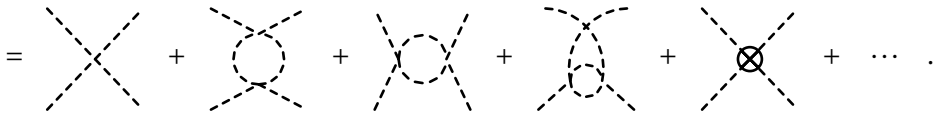

(1.14)

The first and last diagram displayed in the series have simple Feynman rules connected to them (the latter related to the counterterm $\delta_\lambda$ from (1.11)), while the loop diagram

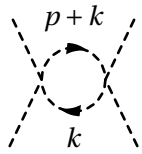


$$= \frac{(-i\lambda)^2}{2}\int \frac{d^4k}{(2\pi)^4}\frac{i}{k^2-m^2}\frac{i}{(k+p)^2-m^2} \equiv (-i\lambda)^2 \cdot iV(p^2). \quad (1.15)$$

Utilizing the Mandelstam variables, we note that in this diagram $p^2 = s$, and for the other two one loop diagrams, the same expression appears, but where $s$ is replaced by $t$ and $u$. At one loop, the entire amplitude is then

$$i\mathcal{M} = -i\lambda + (-i\lambda)^2\left[iV(s) + iV(t) + iV(u)\right] - i\delta_\lambda \quad (1.16)$$

Our renormalization conditions tell us that at $s = 4m^2, u = t = 0$, the entire amplitude must equal $-i\lambda$, so we must have

$$\delta_\lambda = -\lambda^2\left[V(4m^2) + 2V(0)\right]. \quad (1.17)$$

The definition coming from the renormalization condition then defines our physical coupling and at the same time, makes sure that any divergences coming from the terms on the right of (1.17) will be cancelled by our proper choice of the bare parameters through $\delta_\lambda$.

Calculating the contribution $V(p^2)$, one finds that the integral diverges as expected. We may perform a *dimensional regularization* and calculate the result in $d$ space-time dimensions, which yields

$$V(p^2) = -\frac{1}{2}\int_0^1 dx \frac{\Gamma(2-\frac{d}{2})}{(4\pi)^{d/2}} \frac{1}{\left[m^2 - x(1-x)p^2\right]^{2-d/2}} \quad (1.18)$$

where $\Gamma(z) = \int_0^\infty dx\, x^{z-1} e^{-x}$. The function $\Gamma(z)$ has poles at $z = 0, -1, -2, \ldots$, which gives rise to the expected divergence when $d = 4$, but is finite for $d = 4 - \epsilon$ with $\epsilon \ll 1$. Thus, invoking a small shift from four dimensions, we can cancel the divergent term by the counter term through (1.17), and only a finite momentum dependent correction remains for the amplitude.

Having fixed the counter term $\delta_\lambda$, we turn to the renormalization condition for the propagator to determine $\delta_Z$ and $\delta_m$. To find the correct pole behavior of the propagator, we must perform a sum over an infinite amount of diagrams, which equals a geometric series. Defining the sum of all *one-particle-irreducible* insertions into the propagator, i. e. all the diagram insertions with two external legs that cannot be cut into two such diagrams by removing a single line, by

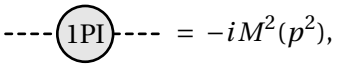


$$= -iM^2(p^2), \tag{1.19}$$

we can find the full two point propagator by the sum


$$= \frac{i}{p^2 - m^2 - M^2(p^2)}. \tag{1.20}$$

Requiring that the pole of this propagator is at $p^2 = m^2$ and that the residue is 1, is equivalent to requiring

$$M^2(p^2)\big|_{p^2=m^2} = 0 \quad \text{and} \quad \frac{d}{dp^2} M^2(p^2)\big|_{p^2=m^2} = 0. \tag{1.21}$$

We can directly calculate $M^2(p^2)$ to this one loop order, where the only possible insertions in the bare propagator is a one loop diagram and the counter term, and find with dimensional regularisation

$-iM^2(p^2) =$ 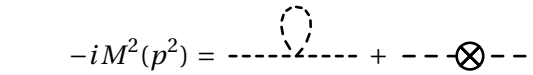

$$= -\frac{i\lambda}{2} \frac{1}{(4\pi)^{d/2}} \frac{\Gamma(1-\frac{d}{2})}{(m^2)^{1-d/2}} + i(p^2\delta_Z - \delta_m). \tag{1.22}$$

Since only one term depends on $p^2$, satisfying the conditions (1.21) is done simply by setting

$$\delta_Z = 0 \quad \text{and} \quad \delta_m = -\frac{\lambda}{2} \frac{1}{(4\pi)^{d/2}} \frac{\Gamma(1-\frac{d}{2})}{(m^2)^{1-d/2}}. \tag{1.23}$$

Having thus fixed the physical parameters $m$ and $\lambda$, the theory is once again well defined and the infinities lurking in the loop diagrams have been cancelled with the proper counter terms. The infinities have only provided a shift between the bare parameters of the theory, which are not accessible to experiments, and measuring the coupling $\lambda$ and mass $m$ in an experiment will fully define the link between theory and the corresponding physical system. As we saw, the renormalization conditions were in this case slightly trivial to satisfy, since we could set $\delta_Z = 0$. Adding higher loop orders or adding a Yukawa interaction with a fermion would however force both $\delta_Z$ and $\delta_m$ nonzero.

## 1.2 RENORMALIZATION SCALES AND THE CALLAN-SYMANZIK EQUATION

Renormalization conditions, like the ones in (1.13), will make sure, that the divergences in loop diagrams do not appear in the physical parameters for our theory. We could however have chosen other similar renormalization conditions, that would have accomplished the same thing. When taking the limit $d \to 4$ ($\epsilon \to 0$) in an expression like (1.18), the $\Gamma$ function will produce terms like $\frac{1}{\epsilon} + \gamma + \log(4\pi) + \ldots$. When enforcing the cancellation with the counter term, all of these terms will be cancelled, but the only problematic term is the divergent $\frac{1}{\epsilon}$ term. One could chose another *renormalization scheme*, in which only this term is cancelled by the counter term. This scheme is known as the *minimal subtraction (MS)* scheme. A third possibility is to also cancel the $\gamma$ and $\log(4\pi)$ terms and replace accompanying $\log(m^2)$ by $\log(m^2/M^2)$ to ensure that the dimensionality of the final expression is correct. The mass parameter $M$ is arbitrary and different values will correspond to different renormalization scheme. This procedure is known as the *modified minimal subtraction* ($\overline{MS}$) scheme.

The freedom we have when picking renormalization schemes will be the key to turning the renormalization procedure into a valuable tool for investigations of quantum field theories. To see how, we will modify the renormalization conditions

from the previous section to the form

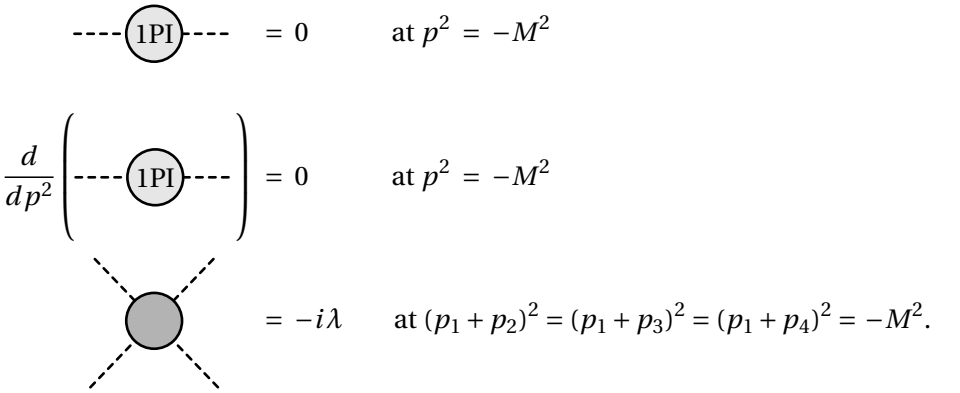


(1.24)

Here we have once again included an arbitrary scale $M$ which we denote as the *renormalization scale* (note also, that the theory is defined for the spacelike momentum $p^2 = -M^2$). $M$ is of course completely unphysical, but as will see, examining how the theory changes under variations of this scale will give us physical insights to the theory at hand. Using such a scheme with such a renormalization scale is particularly useful when the physical mass $m = 0$, since the scheme used in (1.13) produces terms proportional to $\log(m)$. For simplicity, we will in the following assume exactly that $m = 0$.

As our starting point, we will thus take a theory with some bare coupling $\lambda_0$ as well as some cutoff scale $\Lambda$ (used to enforce a cutoff regularization). We could in principle carry out the evaluation of the corrections to the bare parameters of the theory (with the inherent cutoff dependence) and not carry out the renormalization. As we have seen, however, it is practical to eliminate the cutoff dependence through the renormalization conditions and thus the counter terms. Should we wish so, we could reverse the operation from the knowledge of the renormalization conditions, physical couplings, and counter terms to recover the original bare theory. In this sense we could enforce different renormalization conditions for the same theory, for example by using a different renormalization scale $M'$. The two renormalized theories would then correspond to the same underlying bare theory.

By the same bare theory we mean the one with the same set of Green's functions

$$\langle\Omega|T\phi(x_1)\phi(x_2)\dots\phi(x_n)|\Omega\rangle \tag{1.25}$$

given by the same functions of the bare parameter $\lambda_0$ and cutoff $\Lambda$. As we have seen, we can remove the cutoff dependence by rescaling the fields and defining renormalization conditions at some scale $M$. The Green's functions are numerically the same up to a factor of the field strength renormalization $Z$:

$$\langle\Omega|T\phi_r(x_1)\phi_r(x_2)\dots\phi_r(x_n)|\Omega\rangle = Z^{-n/2}\langle\Omega|T\phi(x_1)\phi(x_2)\dots\phi(x_n)|\Omega\rangle. \tag{1.26}$$

The left hand side now depends on the physical coupling $\lambda$ and the renormalization scale $M$. Had we used another set of conditions, we would have another scale $M'$, another field strength rescaling $Z'$, and another physical coupling $\lambda'$ (at this point, it should be clear that the renormalized coupling is not really a physical quantity either, since different renormalization conditions lead to different values.)

We denote by $G^{(n)}(x_1,\ldots,x_n)$ the connected $n$-point function after a renormalization:

$$G^{(n)}(x_1,\ldots,x_n) = \langle\Omega|T\phi_r(x_1)\phi_r(x_2)\ldots\phi_r(x_n)|\Omega\rangle_{\text{connected}}. \tag{1.27}$$

A small shift in the renormalization scale $M$ will distort the relation to the bare theory, but it should be possible to make a simultaneous shift of the field strength and coupling constant to keep the bare theory corresponding to our renormalized theory fixed. The infinitesimal transformation we would like to impose is then of the form

$$\begin{aligned} M &\to M+\delta M \\ \lambda &\to \lambda+\delta\lambda \\ \phi_r &\to (1+\delta\eta)\phi_r. \end{aligned} \tag{1.28}$$

Since the renormalized Green's function is always related to the bare one with the appropriate power of the field strength renormalization associated, this transformation will induce the rescaling

$$G^{(n)} \to (1+n\delta\eta)G^{(n)}. \tag{1.29}$$

We can then relate the change in $G^{(n)}$ due to the shifts in $\lambda$ and $M$ with this rescaling through the relation

$$dG = \frac{\partial G^{(n)}}{\partial M}\delta M + \frac{\partial G^{(n)}}{\partial\lambda}\delta\lambda = n\delta\eta G^{(n)}. \tag{1.30}$$

We now define the dimensionless parameters

$$\beta \equiv \frac{M}{\delta M}\delta\lambda, \quad \gamma \equiv -\frac{M}{\delta M}\delta\eta, \tag{1.31}$$

which makes us able to rewrite (1.30) via a multiplication of $M/\delta M$ into

$$\left[M\frac{\partial}{\partial M} + \beta\frac{\partial}{\partial\lambda} + n\gamma\right]G^{(n)} = 0. \tag{1.32}$$

This equation is known as the Callan-Symanzik equation. This equation relates the shift of the different parameters in the to each other while the renormalization scale is changed. It should be noted, that since we are working with a renormalized theory, $\beta$ and $\gamma$ are independent of the cutoff for the bare theory. Indeed they are only functions of the values of the coupling constants of the given theory, which in

this case is just $\lambda$. The functions $\beta$ and $\gamma$ will become the main focus for the later chapters of this work, even though they at this point seem to be an unphysical manifestation of the changes of the arbitrary renormalization scale.

To see the importance of the $\beta$ and $\gamma$, we will look for solutions to the Callan-Symanzik equation, and we will begin with the one for the two point function, $G^2(p)$, in the scalar theory described above. The two point function is then the sum of all connected diagrams with two external legs and must carry dimension $(\text{mass})^{-2}$, We can then express its dependence on the two scales $p$ and $M$ as follows

$$G^{(2)}(p) = \frac{i}{p^2} g(-p^2/M^2). \tag{1.33}$$

Given the way in which the Green's function depends on the ratio between $M$ and $p$, we may trade one for the other in the Callan-Symanzik equation. Redefining $p$ to be the magnitude of the spacelike momentum $p = (-p^2)^{1/2}$ we rewrite the Callan-Symanzik equation for the two point function:

$$\left[ p\frac{\partial}{\partial p} - \beta\frac{\partial}{\partial \lambda} + 2 - 2\gamma \right] G^{(2)}(p) = 0. \tag{1.34}$$

The equation is now defined with respect to the physical scale $(p)$, which is the argument of the Green's function.

The Callan-Symanzik equation for the two point function is solved by

$$G^{(2)}(p,\lambda) = \frac{i}{p^2}\mathcal{G}(\bar{\lambda}(p,\lambda)) \cdot \exp\left( 2\int_{p'=M}^{p'=p} d\log(p'/M)\,\gamma\left(\bar{\lambda}(p,\lambda)\right)\right), \tag{1.35}$$

where we have defined a new function $\bar{\lambda}$ which solves

$$\frac{d}{d\log(p/M)}\bar{\lambda}(p) = \beta(\bar{\lambda}), \quad \bar{\lambda}(M) = \lambda. \tag{1.36}$$

The function $\mathcal{G}(\bar{\lambda}(p,\lambda))$ must be determined by computing $G^{(2)}(p)$ via a perturbation series in $\lambda$ and matching the terms to an expansion of (1.35).

In (1.36) we have defined a new coupling constant, $\bar{\lambda}$, which can be viewed as depending on the momentum defining the scale at which the 2-point function is evaluated, instead of the arbitrary renormalization scale. We call this quantity the *running coupling constant*, and we usually say that we define it at the scale $M$ with the *renormalization group equation* (1.36). By knowing the scale where the coupling is defined, its value at that scale, and the expression for $\beta$, the coupling is defined uniquely[2].

To see the importance of this parameter, one can repeat the exercise above for the four-point function $G^{(4)}(p)$, which yields an expression similar to (1.35), where we now have a factor $\mathcal{G}^{(4)}(\bar{\lambda}(p,\lambda))$ in front. To leading order in perturbation theory,

[2] If there are more than one coupling in the theory, one trades the one differential equation for a set of them, and uniqueness is in general not guaranteed.

we know that $G^{(4)}(p) = \frac{-i\lambda}{p^8}$, and by matching this to the first term in the expansion of the full solution

$$G^{(4)}(p,\lambda) = \frac{1}{p^8}\mathcal{G}^{(4)}(\bar{\lambda}(p,\lambda)) \cdot \exp\left(4\int_{p'=M}^{p'=p} d\log(p'/M)\,\gamma\left(\bar{\lambda}(p,\lambda)\right)\right), \tag{1.37}$$

it can be seen that the factor in front of the exponential is on the form

$$\mathcal{G}^{(4)} = -i\bar{\lambda} + \mathcal{O}(\bar{\lambda}^2). \tag{1.38}$$

We see that the factors in front of the exponentials in (1.35) and (1.37) are functions of the running coupling and indeed we see that by replacing the ordinary coupling $\lambda$ with the running $\bar{\lambda}$ at the appropriate energy scale we improve the results we would have gotten form an ordinary expansion in the coupling constants using Feynman diagrams. The running coupling constant measures the effective coupling constant modified by the change of scale between the one where the coupling is defined and the one were the correlation function or amplitude is evaluated.

The framework discussed here thus gives us information about the evolution of the coupling constant when the scale of the system is changed. To obtain the coupling constant at one scale, one needs only to measure the coupling at some other scale and the renormalization group equation for that coupling, which amounts to knowing the form of $\beta$. The functions $\beta$ and $\gamma$ can be obtained by calculating the 2-point and 4-point functions to a given order in perturbation theory like in the previous section. The dependence of the renormalization scale $M$ will then be introduced via the counter terms and the beta function, $\beta$ ,can be found through use of the Callan-Symanzik equation. Loosely speaking, the beta function will contain the factors in front of the divergent loop diagrams, since these are the ones that are cancelled through adjustment of the counter terms at the scale $M$.

The beta functions for a given theory are of great use, when one wishes to investigate how the theory evolves when the relevant scale is changed, as will be evident from the following chapters. For low values of the coupling constant, such that only one loop terms are relevant to the problem, the sign of the beta function is of great importance. A negative sign thus signals the presence of *asymptotic freedom*, where the theory becomes free in the far UV, while a positive sign hints that the theory becomes free in the infrared. A zero in the beta function is called a fixed point, and signals scale independent behavior for the theory. In the next section, we will see, that the first two situations are common in particle physics.

## 1.3 THE STANDARD MODEL AT HIGH ENERGIES

The list of results in high energy theory stemming from the knowledge of the beta functions of a given theory is not a short one, and the remaining chapters of this work will add a couple of points to that list. To appreciate the context of this work, we will mention a few of the other results in the following. Of specific interest

to us will be the results regarding the quartic coupling for the Higgs boson in the standard model, which has been indirectly measured [7].

### 1.3.1 Asymptotic freedom

Perhaps the most renowned result in the framework of RG equations is the discovery of asymptotic freedom in a large class of nonabelian gauge theories due to Gross & Wilczek [8], and Politzer [9]. These authors found that Yang-Mills theory, having a non-abelian symmetry group, had a negative one loop beta function. Since the one loop terms in the beta function dominates for small couplings, this meant that the theory had a UV stable fixed point at zero coupling. It was found that even when fermions were added, this feature might persist, and specifically it was there when the symmetry group was $SU(3)$ and less than sixteen triplets were added in the fundamental representation. Since this was exactly the proposed theory for strong interactions, QCD, it was predicted that given a "small enough" coupling constant for the strong interactions at some energy scale, the coupling would run to zero when the energy was increased; QCD would be *asymptotically free*. Thus perturbation theory should be applicable for QCD at high enough energies, while the coupling would grow stronger in the IR, and potentially lead to the confinement of quarks due to some unknown mechanism.

### 1.3.2 The fate of the Higgs coupling

The behavior of a quartic coupling in scalar theories is the opposite, and in $\phi^4$ theory given by (1.11), the beta function is given to one loop by

$$\frac{d\lambda}{d\log(p/M)} = \beta_{\bar{\lambda}} = \frac{3\bar{\lambda}^2}{(4\pi)^2}. \tag{1.39}$$

Since the one loop term is positive, the coupling increases with the energy scale, and indeed the solution to this equation is given by

$$\bar{\lambda} = \frac{\lambda}{1 - \frac{3\lambda}{(4\pi)^2}\log\left(\frac{p}{M}\right)}, \tag{1.40}$$

which diverges when $p = M \cdot \exp\left(\frac{(4\pi)^2}{3\lambda}\right)$ (at which point perturbation theory is clearly not valid). While the divergence cannot be trusted, the form of the solution does put an upper bound on the energy scales where perturbation theory is valid. If we wanted to extend the range of validity for perturbation theory to very large energies, we would need to have very small initial values for the coupling. In the limit where the range of validity goes to infinity, it is sometimes said that $\phi^4$ theory suffers from *triviality*, since this requires $\lambda_M \to 0$.

In the case of the standard model, where a scalar doublet with a similar $\phi^4$ interaction is present, the picture is slightly different. The presence of Yukawa couplings between the Higgs doublet and the fermion of the standard model together

with electroweak interactions for the Higgs doublet modifies the beta function for the quartic coupling. Taking only the top Yukawa ($y_t$) and electroweak ($g_1, g_2$) couplings into account, the RG equation is given by

$$\beta_\lambda = \frac{1}{(4\pi)^2}\left[3(4y_t^2 - 3g_2^2 - g_1^2)\lambda - 6y_t^4 + \tfrac{3}{8}[2g_2^4 + (g_1^2+g_2^2)^2] + 24\lambda^2\right]. \tag{1.41}$$

Naturally, the coupling $y_t, g_1$, and $g_2$ have beta functions of their own, and the entire system does not have a simple analytic solution like the one above. However, since the top coupling has long been known to be large compared to the gauge couplings (even before its measurement, the non-discovery of the top quark hinted towards a large coupling), some predictions could be made:

**A:** If the quartic coupling $\lambda$ was sufficiently small, the top coupling would dominate the beta function and eventually drive the Higgs coupling to negative values at high energies.

**B:** If the Higgs coupling was very large, then the triviality picture above might be relevant once more.

These two asymptotic scenarios were both troublesome. The first would lead to a possible instability of the electroweak vacuum, since the $\phi^4$ term in the potential would become negative. The second would mean that perturbation theory would break down at some higher energy scale.

Turning these considerations around, such that the quartic coupling neither becomes negative or diverges between the electroweak scale and the Planck scale, where gravitational effects are expected to appear, one can make a prediction for the value of the scalar coupling at the weak scale and hence a prediction of the Higgs boson mass [10]. As it turns out, the predicted range for the Higgs mass is pretty narrow considering the large hierarchy between the two scales in the problem. This is due to the appearance of an approximate fixed point when only the quartic and top Yukawa couplings are considered, and the weaker gauge couplings[3] are ignored, at which point the system of RG equations takes the form

$$\beta_\lambda \simeq \frac{1}{(4\pi)^2}\left[12y_t^2\lambda - 6y_t^4 + 24\lambda^2\right] \tag{1.42}$$

$$\beta_{y_t} \simeq \frac{1}{(4\pi)^2}\left[\frac{9}{2}y_t^3\right]. \tag{1.43}$$

Defining a new "coupling" $\lambda/y_t^2$, we can calculate its beta function and find

$$\beta_{\frac{\lambda}{y_t^2}} = \frac{y_t^2}{(4\pi)^2}\left[24\left(\frac{\lambda}{y_t^2}\right)^2 + 3\frac{\lambda}{y_t^2} - 6\right], \tag{1.44}$$

[3] As mentioned, the strong gauge coupling is small at large energies.

which has a fixed point such that $\beta_{\lambda/y_t^2} = 0$ when

$$\frac{\lambda}{y_t^2} = \frac{1}{2}\sqrt{\frac{65}{64}} - \frac{1}{16} \approx 0.44. \tag{1.45}$$

This approximate fixed point for the ratio $\lambda/y_t^2$ is attractive in the IR, such that any initial ratio between the couplings at high energies will lead to something close to the fixed point value, if the high energy scale is well separated from the electroweak scale. The flow of the two couplings is shown in Fig. 1.2

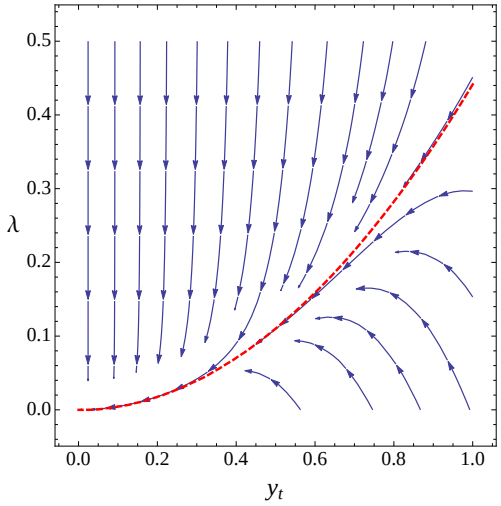


Figure 1.2: The renormalization group flow for the top Yukawa and quartic scalar coupling towards the IR for $g_1, g_2, g_3 \simeq 0$. The red dashed line shows the fixed point for the ratio $\lambda/y_t^2$

Specifying conditions on the value of $\lambda$ at the Planck scale ($M_P$) leads to predictions for the mass of the Higgs particle ($m_H$) (which had not been measured at the time), and specifically translating the requirement of absolute stability of the electroweak vacuum as well as validity of perturbation theory into the constraint $0 < \lambda(M_P) < 6$ leads to the somewhat narrow mass prediction [11]

$$126\ \text{GeV} < m_H < 173\ \text{GeV}.$$

The lower bound of this window has been used as a prediction in theories, where gravitational interactions above the Planck scale drives the Higgs couplings to very small but positive values [12].

Of course, this prediction of the Higgs mass relied on the specific assumptions of absolute stability and perturbative validity. Smaller Higgs masses were allowed, but the requirement that the electroweak vacuum should be at least so long lived that the universe could exist as it does, might require new physics to show up at some energy scale below the Planck scale to alter the potential.

On the other hand, the possible divergence of the quartic Higgs could also be seen as a sign of new physics. Specifically, divergent behavior is compatible with a scenario where the Higgs is a composite particle, and it was thus expected that the Yukawa coupling to the fermion constituents should diverge in a similar fashion. Theories where the Higgs is a top quark condensate have been around for a while, and though the earliest models predicted too high masses for both the Higgs and the top quark [13], viable theories are still being considered [14].

While the Higgs mass is currently well established, its value poses many interesting theoretical and phenomenological questions. In particular, the questions of vacuum stability, relation to gravitational physics and compositeness are still relevant today, and we will spend the remainder of this work discussing them.

# CHAPTER 2

# RG FLOW AND VACUUM STABILITY IN THE STANDARD MODEL

Any reasonably thorough analysis of a given quantum field theory must include an analysis of the behavior induced by a change of the renormalization scale, i.e the renormalization group flow. For some theories, such a change will not have any effect on the theory, and we call these theories *scale invariant* field theories, a subclass of the *conformal* field theories[1]. For the well known theories of QCD and QED, however, a change of the RG scale induces a change in the coupling constants of the theory; the coupling constants "run". The description of this running of the coupling constants is an important tool in characterizing essential features of a theory, and theories may be associated with different features like fixed points, asymptotic freedom and -safety, triviality, and unification etc. based on this description.

Theories featuring only a single coupling constant, which we will take to be dimensionless, offer a simple recipe for a perturbative expansion when calculating the effects of the RG evolution; an expansion in the coupling constant itself. Taking the coupling constant to be small enables a reliable expansion and we may say that perturbation theory is valid for analysis. As we shall see in the following, theories with multiple different coupling constants offer the use of a similar approach to the lowest order, albeit not exactly the one conventionally considered.

## 2.1 THE WEYL ANOMALY

We shall take as a starting point a conformal field theory to which we will add terms with dimensionless coupling constants that break the scale invariance such that these couplings start running. The line of reasoning roughly follows the work

[1] In addition to the symmetry under a rescaling of the coordinates, a conformal symmetry also implies invariance under the *special conformal transformations* containing a combination of translations and inversions

of Osborn [15]. The Lagrangian for such a theory may be summarized by

$$\mathscr{L} = \mathscr{L}_{CFT} + g_i \mathscr{O}^i, \tag{2.1}$$

where $\mathscr{O}^i$ are the operators that break the conformal symmetry, $g_i$ are the corresponding dimensionless couplings, and $\mathscr{L}_{CFT}$ contains the kinetic terms for the quantum fields of the theory. Since we only added dimensionless couplings to the theory, it is still classically scale invariant.

Our aim will be to deduce a set of relations between the RG equations of the theory, and we will therefore introduce a tool in the form of a nontrivial background metric $\gamma^{\mu\nu}$ as well as space time dependence for the coupling constants:

$$\begin{aligned} \gamma^{\mu\nu} &= \gamma^{\mu\nu}(x), \\ g_i &= g_i(x). \end{aligned}$$

Our next move will be to perform a *local* scale transformation signified by the parameter $\sigma(x)$, which transforms the metric as

$$\gamma^{\mu\nu} \to e^{2\sigma(x)} \gamma^{\mu\nu}. \tag{2.2}$$

Just as we saw in the previous chapter, a change of the scale of the system could be related to a rescaling of the couplings along with the anomalous dimensions for the fields of the theory. We can thus "compensate" for the local change of the metric by simultaneously changing the couplings

$$g_i(\mu) \to g_i(e^{-\sigma(x)}\mu), \tag{2.3}$$

up to a number of terms for $g_i$ that vanish in flat space.

This transformation can be expressed via the variation of the generating functional at the quantum level, which is defined by

$$W = \log\left[\int \mathscr{D}\Phi\, e^{i\int \mathrm{d}^4 x\, \mathscr{L}}\right]. \tag{2.4}$$

This variation is usually referred to as the *Weyl anomaly*, and it quantifies the deviation from true scale invariance due to quantum effects as described by

$$\begin{aligned} \Delta_\sigma W &\equiv \int \mathrm{d}^4 x\, \sigma(x) \left(2\gamma_{\mu\nu}\frac{\delta W}{\delta \gamma_{\mu\nu}} - \beta_i \frac{\delta W}{\delta g_i}\right) \\ &= \sigma\left(aE(\gamma) + \chi^{ij}\partial_\mu g_i \partial_\nu g_j G^{\mu\nu}\right) + \partial_\mu \sigma \omega^i \partial_\nu g_i G^{\mu\nu} + \ldots \end{aligned} \tag{2.5}$$

Here, $G^{\mu\nu} = R^{\mu\nu} - \frac{1}{2}\gamma^{\mu\nu}R$ is the Einstein tensor, $E = R^{\mu\nu\rho\sigma}R_{\mu\nu\rho\sigma} - 4R^{\mu\nu}R_{\mu\nu} + R^2$ is the Euler density, $\beta_i$ is the beta functions for the coupling $g_i$, and $a$, $\omega^i$, and $\chi^{ij}$ are functions of the couplings $g_i$. Naturally, reverting to constant values for $g_i$ and a trivial metric, would trivialize this equation somewhat[2], but what we are

[2] It would reduce to the Callan-Symanzik equation.

interested in is mainly the structure to be found in the functions $a$, $\omega^i$, and $\chi^{ij}$ and their relation to the beta functions. These functions are completely determined by the theory and can be explicitly computed in a perturbative expansion in the couplings $g_i$.

An important feature of the group of Weyl transformations is that it is abelian, such the order of two successive transformations is irrelevant:

$$\Delta_\sigma \Delta_\tau W = \Delta_\tau \Delta_\sigma W. \tag{2.6}$$

When applying this property to the anomaly (2.5), a set of consistency conditions arise, among which the one we will focus on is

$$\frac{\partial \tilde{a}}{\partial g_i} = \left(-\chi^{ij} + \frac{\partial \omega^i}{\partial g_j} - \frac{\partial \omega^j}{\partial g_i}\right)\beta_j \equiv -\tilde{\chi}^{ij}\beta_j, \tag{2.7}$$

where we have defined a new function $\tilde{a} = a - \omega^i \beta_i$. At the lowest order in perturbation theory, the functions $\omega^i$ turn out to be one forms [16], such that $\frac{\partial \omega^i}{\partial g_j} - \frac{\partial \omega^j}{\partial g_i} = 0$ and at this order $\tilde{\chi}^{ij} = \chi^{ij}$. Regarding $\tilde{\chi}^{ij}$ as a metric in coupling constant space, we may define a contravariant

$$\beta^i \equiv \tilde{\chi}^{ij}\beta_i, \tag{2.8}$$

and we see that at the lowest order,

$$\beta^i = \chi^{ij}\beta_i, \tag{2.9}$$

thus relating all beta functions to the function $\tilde{a}$ through (2.7), and making the changes in $\tilde{a}$ under scale transformations a gradient flow described by $\beta^i$. Applying a second derivative to (2.7) yields the result central to this chapter:

$$\frac{\partial^2 \tilde{a}}{\partial g_i \partial g_j} = -\frac{\partial \beta^i}{\partial g_j} \quad \Leftrightarrow \quad \frac{\partial \beta^i}{\partial g_j} = \frac{\partial \beta^j}{\partial g_i}. \tag{2.10}$$

Evidently, the abelian nature of the Weyl group is reflected through the deviation from absolute scale invariance, namely the Weyl anomaly, in to a set of conditions linking the "contravariant" beta functions to each other. These will henceforth be referred to as the Weyl consistency conditions. Specifically, these conditions are relations between cross terms in the beta functions, that is terms in $\beta^i$ containing $g_j$ and vice versa. This set of relations will also be present in the limit where the couplings are restored to constants and the metric goes becomes of the Minkowski type, and is fundamentally present in any field theory which contains only marginal couplings[3].

In the following, we will use the standard model (in an $\overline{\text{MS}}$ scheme, where the Higgs mass is ignored) as an example, and show that these relations are explicitly fulfilled to lowest order.

[3]This statement can be generalized to theories where dimensional couplings are present, but where the renormalization procedure is a mass independent one, as in $\overline{\text{MS}}$.

## 2.2 PERTURBATIVE COUNTING FOR GAUGE-YUKAWA THEORIES

To see the consequences of the relations described above, we now turn to the standard model. Ignoring the Higgs mass, i.e working with a renormalization scale that is considerably larger than the Higgs mass, such that we may regard all SM particles to be massless will approximate the theory with the classically scale invariant type described above and justify the use of the previous results. With this in mind, the marginal operators and the corresponding couplings will arise from the interaction terms in the SM which counts gauge as well as Yukawa and scalar couplings. To simplify the picture, we will restrict the space of coupling constants to be that of the three gauge couplings $(g_1, g_2, g_3)$, the top Yukawa coupling $(y_t)$ and the quartic self interaction coupling of the Higgs $(\lambda)$ while taking the rest to be zero. This approximation is widely used for RG analysis of the SM in the UV [17].

Due to the nature of the perturbative corrections it is convenient to redefine the coupling set $\{g_i\}$ as $\{\alpha_1, \alpha_2, \alpha_3, \alpha_t, \alpha_\lambda\}$, where

$$\alpha_1 = \frac{g_1^2}{(4\pi)^2}, \quad \alpha_2 = \frac{g_2^2}{(4\pi)^2}, \quad \alpha_3 = \frac{g_3^2}{(4\pi)^2}, \quad \alpha_t = \frac{y_t^2}{(4\pi)^2}, \quad \alpha_\lambda = \frac{\lambda}{(4\pi)^2}\,. \tag{2.11}$$

To specify, $g_1, g_2, g_3$ are the $U(1)_Y$, $SU(2)_\mathrm{w}$ and $SU(3)_c$ gauge couplings respectively. Similarly, we denote by $\beta_1, \beta_2, \beta_3, \beta_t$, and $\beta_\lambda$ their respective beta functions, defined as $\beta_i \equiv \mu^2 \frac{d\alpha_i}{d\mu^2}$.

At leading order in the couplings, the matrix $\chi$ is diagonal, and reads [16]

$$\chi = \mathrm{diag}\left(\frac{1}{\alpha_1^2}, \frac{3}{\alpha_2^2}, \frac{8}{\alpha_3^2}, \frac{2}{\alpha_t}, 4\right). \tag{2.12}$$

The most important property of this expression for the "metric" is that when calculating the "contravariant" $\beta^i$ which enter into the relation with $\tilde{a}$, (2.10), the power of the coupling constants in the equations differ from the one in the regular beta functions. One finds that any gauge $\beta^g$ compared to the original $\beta_g$ features two powers fewer in $\alpha_g$; the Yukawa $\beta^t$ is related to $\beta_t$ with one less power of $\alpha_t$ while $\beta^\lambda$ carries the same powers in $\alpha_\lambda$ as $\beta_\lambda$. The condition (2.10) therefore plays an important role, since it relates coefficients of different beta functions at different loop order. Explicitly, the lowest order consistency conditions that we obtain

are

$$2\frac{\partial}{\partial\alpha_t}\beta_\lambda = \frac{\partial}{\partial\alpha_\lambda}\left(\frac{\beta_t}{\alpha_t}\right)+\mathcal{O}\left(\alpha_i^2\right) \tag{2.13}$$

$$4\frac{\partial}{\partial\alpha_1}\beta_\lambda = \frac{\partial}{\partial\alpha_\lambda}\left(\frac{\beta_1}{\alpha_1^2}\right)+\mathcal{O}\left(\alpha_i^2\right) \tag{2.14}$$

$$\frac{4}{3}\frac{\partial}{\partial\alpha_2}\beta_\lambda = \frac{\partial}{\partial\alpha_\lambda}\left(\frac{\beta_2}{\alpha_2^2}\right)+\mathcal{O}\left(\alpha_i^2\right) \tag{2.15}$$

$$2\frac{\partial}{\partial\alpha_1}\left(\frac{\beta_t}{\alpha_t}\right) = \frac{\partial}{\partial\alpha_t}\left(\frac{\beta_1}{\alpha_1^2}\right)+\mathcal{O}\left(\alpha_i^2\right) \tag{2.16}$$

$$\frac{2}{3}\frac{\partial}{\partial\alpha_2}\left(\frac{\beta_t}{\alpha_t}\right) = \frac{\partial}{\partial\alpha_t}\left(\frac{\beta_2}{\alpha_2^2}\right)+\mathcal{O}\left(\alpha_i^2\right) \tag{2.17}$$

$$\frac{1}{4}\frac{\partial}{\partial\alpha_3}\left(\frac{\beta_t}{\alpha_t}\right) = \frac{\partial}{\partial\alpha_t}\left(\frac{\beta_3}{\alpha_3^2}\right)+\mathcal{O}\left(\alpha_i^2\right) \tag{2.18}$$

$$\frac{1}{3}\frac{\partial}{\partial\alpha_2}\left(\frac{\beta_1}{\alpha_1^2}\right) = \frac{\partial}{\partial\alpha_1}\left(\frac{\beta_2}{\alpha_2^2}\right)+\mathcal{O}\left(\alpha_i^2\right) \tag{2.19}$$

$$\frac{1}{8}\frac{\partial}{\partial\alpha_3}\left(\frac{\beta_1}{\alpha_1^2}\right) = \frac{\partial}{\partial\alpha_1}\left(\frac{\beta_3}{\alpha_3^2}\right)+\mathcal{O}\left(\alpha_i^2\right) \tag{2.20}$$

$$\frac{3}{8}\frac{\partial}{\partial\alpha_3}\left(\frac{\beta_2}{\alpha_2^2}\right) = \frac{\partial}{\partial\alpha_2}\left(\frac{\beta_3}{\alpha_3^2}\right)+\mathcal{O}\left(\alpha_i^2\right) \tag{2.21}$$

What should be noted, as evident from the structure of (2.12), is that the relations are not between terms in the beta function of the same loop order, but rather connects terms of different loop orders for different types of couplings. Explicitly, one can see from (2.13), (2.14), and (2.15), that the consistency conditions (2.10) relate the mixed terms in the one loop beta function for the quartic coupling to the two loop terms in the Yukawa beta function and to the three loop gauge beta functions. A test of the relations above can readily be made from the knowledge of the beta functions for the standard model, which we will take from Ref. [18–20], without using the $SU(5)$ normalization for the hypercharge:

$$\beta_\lambda = \underbrace{\frac{9}{16}\alpha_2^2-\frac{9}{2}\alpha_\lambda\alpha_2}_{Eq.\ (2.15)}+\underbrace{\frac{3}{16}\alpha_1^2-\frac{3}{2}\alpha_\lambda\alpha_1}_{Eq.\ (2.14)}+\underbrace{\frac{3}{8}\alpha_1\alpha_2}_{Eqs.\ (2.14\&2.15)}+12\alpha_\lambda^2 +\underbrace{6\alpha_\lambda\alpha_t-3\alpha_t^2}_{Eq.\ (2.13)}. \tag{2.22a}$$

$$\beta_t = 2\alpha_t\Big\{\frac{9}{4}\alpha_t - \underbrace{4\alpha_3}_{Eq.\ (2.18)} - \underbrace{\frac{17}{24}\alpha_1}_{Eq.\ (2.16)} - \underbrace{\frac{9}{8}\alpha_2}_{Eq.\ (2.17)} + \underbrace{3\alpha_\lambda^2 - 6\alpha_t\alpha_\lambda}_{Eq.\ (2.13)} - 6\alpha_t^2$$
$$+ 18\alpha_3\alpha_t + \alpha_3^2\Big(-\frac{202}{3} + \frac{40n_G}{9}\Big) + \alpha_t\Big(\frac{131}{32}\alpha_1 + \frac{225}{32}\alpha_2\Big) \tag{2.22b}$$
$$+ \frac{1187}{432}\alpha_1^2 - \frac{3}{8}\alpha_1\alpha_2 + \frac{19}{18}\alpha_1\alpha_3 - \frac{23}{8}\alpha_2^2 + \frac{9}{2}\alpha_3\alpha_2\Big\},$$

$$\beta_1 = 2\alpha_1^2\Big\{\frac{1}{12} + \frac{10n_G}{9} + \Big(\frac{1}{4} + \frac{95n_G}{54}\Big)\alpha_1 + \underbrace{\Big(\frac{3}{4} + \frac{n_G}{2}\Big)\alpha_2}_{Eq.\ (2.19)} + \underbrace{\frac{22n_G}{9}\alpha_3}_{Eq.\ (2.20)}$$
$$+ \Big(\frac{163}{1152} - \frac{145n_G}{81} - \frac{5225n_G^2}{1458}\Big)\alpha_1^2 + \Big(\frac{87}{64} - \frac{7n_G}{72}\Big)\alpha_1\alpha_2 - \frac{137n_G}{162}\alpha_1\alpha_3$$
$$+ \Big(\frac{3401}{384} + \frac{83n_G}{36} - \frac{11n_G^2}{18}\Big)\alpha_2^2 + \Big(\frac{1375n_G}{54} - \frac{242n_G^2}{81}\Big)\alpha_3^2 \tag{2.22c}$$
$$- \frac{n_G}{6}\alpha_2\alpha_3 + \underbrace{\alpha_\lambda\Big(\frac{3}{4}\alpha_1 + \frac{3}{4}\alpha_2 - \frac{3}{2}\alpha_\lambda\Big)}_{Eq.\ (2.14)}$$
$$+ n_t\alpha_t\Big[\underbrace{-\frac{17}{12}}_{Eq.\ (2.16)} - \frac{785}{64}\alpha_2 - \frac{29}{6}\alpha_3 + \Big(\frac{113}{32} + \frac{101n_t}{16}\Big)\alpha_t\Big]\Big\},$$

$$\beta_2 = 2\alpha_2^2\Big\{-\frac{43}{12} + \frac{2n_G}{3} + \underbrace{\Big(\frac{1}{4} + \frac{n_G}{6}\Big)\alpha_1}_{Eq.\ (2.19)} + \Big(-\frac{259}{12} + \frac{49n_G}{6}\Big)\alpha_2$$
$$+ \underbrace{2n_G\alpha_3}_{Eq.\ (2.21)} + \Big(\frac{163}{1152} - \frac{35n_G}{54} - \frac{55n_G^2}{162}\Big)\alpha_1^2 + \Big(\frac{187}{64} + \frac{13n_G}{24}\Big)\alpha_1\alpha_2$$
$$- \frac{n_G}{18}\alpha_1\alpha_3 + \Big(-\frac{667111}{3456} + \frac{3206n_G}{27} - \frac{415n_G^2}{54}\Big)\alpha_2^2 \tag{2.22d}$$
$$+ \frac{13n_G}{2}\alpha_2\alpha_3 + \Big(\frac{125n_G}{6} - \frac{22n_G^2}{9}\Big)\alpha_3^2 + \underbrace{\alpha_\lambda\Big(\frac{1}{4}\alpha_1 + \frac{3}{4}\alpha_2 - \frac{3}{2}\alpha_\lambda\Big)}_{Eq.\ (2.15)}$$
$$+ n_t\alpha_t\Big[\underbrace{-\frac{3}{4}}_{Eq.\ (2.17)} - \frac{593}{192}\alpha_1 - \frac{729}{64}\alpha_2 - \frac{7}{2}\alpha_3 + \Big(\frac{57}{32} + \frac{45n_t}{16}\Big)\alpha_t\Big]\Big\},$$

$$\begin{aligned}\beta_3 = 2\alpha_3^2\Big\{ &-\frac{11}{2}+\frac{2n_G}{3}+\underbrace{\frac{11n_G}{36}\alpha_1}_{Eq.\ (2.20)}+\underbrace{\frac{3n_G}{4}\alpha_2}_{Eq.\ (2.21)}+\left(-51+\frac{38n_G}{3}\right)\alpha_3\\ &+\left(-\frac{65n_G}{432}-\frac{605n_G^2}{972}\right)\alpha_1^2-\frac{n_G}{48}\alpha_1\alpha_2+\frac{77n_G}{54}\alpha_1\alpha_3\\ &+\left(\frac{241n_G}{48}-\frac{11n_G^2}{12}\right)\alpha_2^2+\frac{7n_G}{2}\alpha_2\alpha_3+\left(-\frac{2857}{4}+\frac{5033n_G}{18}-\frac{325n_G^2}{27}\right)\alpha_3^2\\ &+n_t\alpha_t\Big[\underbrace{-1}_{Eq.\ (2.18)}-\frac{101}{48}\alpha_1-\frac{93}{16}\alpha_2-20\alpha_3+\left(\frac{9}{4}+\frac{21n_t}{4}\right)\alpha_t\Big]\Big\},\end{aligned} \tag{2.22e}$$

Here $n_G$ is the number of generations which we set to 3 and $n_t$ is the number of top quarks, i.e. 1. Note that although we considered the gauge beta functions to three loops, we show only the two-loop top Yukawa and the one-loop Higgs quartic beta functions. This, as we will demonstrate momentarily, leads to a Weyl consistent expansion in the couplings up to $\mathcal{O}(\alpha_i^3)$.

To help the reader immediately identify the terms in the beta functions that must satisfy the Weyl consistency conditions given in Eqs. (2.13-2.21), we have color-coded the contributions. Furthermore, beneath each relevant term we have noted the equation number of the Weyl consistency condition it refers to. Specifically, the red color is associated to Eq (2.13), green to Eq. (2.14), blue to Eq. (2.15), cyan to Eq. (2.16), magenta to Eq. (2.17), orange to Eq. (2.18), purple to Eq. (2.19), brown to Eq. (2.20), and finally gray to Eq. (2.21). Note that the term $\frac{3}{8}\alpha_1\alpha_2$ in $\beta_\lambda$ enters into both Eq. (2.14) and Eq. (2.15).

This illustrates that the one-loop coefficients of the quartic $\beta_\lambda$-function is related to the two-loop coefficient of the Yukawa $\beta_t$-function, and to the three-loop beta functions of the electroweak gauge couplings. Restricting the computation to these orders, namely adopting a 3-2-1 loop counting in the gauge, Yukawa and quartic beta functions, corresponds to a truncation of the function $\tilde{a}$ at order $\alpha_i^3$. For illustration, we show the terms in the function $\tilde{a}$ which contribute to the one-loop quartic $\beta_\lambda$-function:

$$-\tilde{a} = \ldots+\underbrace{\frac{9}{4}\alpha_2^2\alpha_\lambda-9\alpha_\lambda^2\alpha_2}_{Eq.\ (2.15)}+\underbrace{\frac{3}{4}\alpha_1^2\alpha_\lambda-3\alpha_\lambda^2\alpha_1}_{Eq.\ (2.14)}+\underbrace{\frac{3}{2}\alpha_1\alpha_2\alpha_\lambda}_{Eqs.\ (2.14-2.15)}+16\alpha_\lambda^3+\underbrace{12\alpha_\lambda^2\alpha_t-12\alpha_t^2\alpha_\lambda}_{Eq.\ (2.13)}+\ldots \tag{2.23}$$

In order to ensure that the Weyl anomaly, measuring the departure from scale invariance, is correctly of abelian nature, we thus see that the for the lowest non-trivial order calculation one needs the quartic beta functions calculated to one loop, the Yukawa beta functions to two loops, and the gauge beta functions to three loops ("3-2-1" ordering). In this setup then, a conventional calculation to one loop in all couplings is not a complete lowest order calculation at all! In addition, in order to specify a consistent NLO counting, one needs to calculate corrections to the lowest order "metric", and it is not certain that a consistent order

expansion can be found. In any case, it can be said that under the "3-2-1" ordering, the requirement of an abelian Weyl anomaly is satisfied to lowest order, while a conventional ordering leads to a departure from Weyl consistency.

## 2.3 VACUUM STABILITY REVIEWED

As we have described a new lowest order ordering which respects the Weyl consistency conditions, we should investigate how big the effect from departure from this ordering is. If departing from Weyl consistency means large changes in the predictions for the theory in question, it becomes vital to understand which result should be trusted. For the standard model, the UV behavior of the theory has been studied in great detail, and specifically the (in)stability of the Higgs vacuum has been questioned.

The analysis of the vacuum stability requires the knowledge of the effective potential of the model at hand. The standard model effective potential is known up to two loops [21]. Its explicit form is given in the appendix of Ref. [17, 21]. For large field values $\phi \gg v = 246$ GeV, the potential is very well approximated by its RG-improved tree-level expression,

$$V_{\text{eff}}^{tree} = \frac{\lambda(\mu)}{4}\phi^4 \,. \tag{2.24}$$

with $\mu = \mathcal{O}(\phi)$. Therefore if one is simply interested in the condition of absolute stability of the potential, it is possible to study the RG evolution of $\lambda$ and determine the scale $\Lambda < M_{pl}$, with $M_{pl}$ the Planck scale, above which the coupling is negative.

We now calculate the RG flow as the renormalization scale changes from the electroweak scale to the Planck scale. We show the evolution of the Higgs quartic coupling $\lambda$ in three cases:

**(1-1-1)** The conventional leading order result, where all beta functions are calculated to one loop.

**(3-2-1)** The lowest order calculation respecting the Weyl consistency conditions, using the three loop gauge beta functions, the two loop top Yukawa beta function, and the one loop quartic beta function.

**(3-3-3)** The conventional "NNLO" calculation using three loop beta functions for all couplings.

The resulting evolutions are shown in Fig. 2.1 for the central values of the Higgs and top mass, and for the value of the top mass which results in $\lambda = 0$ at the Planck scale.

Evidently, there is a large difference when upgrading from the conventional lowest order (1-1-1) to the Weyl consistent lowest order (3-2-1), which gives $\Lambda \approx 10^8$ GeV and $\Lambda \approx 10^{10}$ GeV, respectively, for the central value top mass. Note that this is despite the fact, that the beta function for the quartic coupling is identical

in the two orderings. It is harder to draw conclusions when comparing to the full three loop analysis (3-3-3). Clearly the two methods yield approximately the same result for the running of the quartic coupling, even though the quartic beta function for the latter has a considerably larger amount of terms. This feature may be due to large cancellations in the higher order terms for the quartic coupling, which has already been pointed out by the authors of [22]. This tells us that the influence of the extra loops in the gauge and top Yukawa beta functions is greater than the higher order terms of the quartic itself, even on the quartic evolution.

However, an accurate analysis of the potential has to take into account the full structure of the Higgs potential. As was shown in [23, 24], one can always define an effective coupling $\lambda_{\text{eff}}$ such that for $\phi \gg v$ the effective potential assumes the form

$$V_{\text{eff}} = \frac{\lambda_{\text{eff}}(\mu)}{4}\phi^4 \,. \tag{2.25}$$

The explicit expression for $\lambda_{\text{eff}}$, up to two-loop order, can be found in [17, 21]. Within the 3-2-1 counting scheme, we have to take into account $\lambda_{\text{eff}}$ only to one-loop order, which is consistent with the one-loop running of the quartic coupling. On the other hand for the 3-3-3 scheme we keep the full two-loop expression. The direct comparison between the running of the effective quartic couplings in the two schemes is shown in Fig. 2.2. We note a pattern very similar to the one for $\lambda$ given in Fig. 2.1. The difference is, however, that the scale where $\lambda_{\text{eff}}$ crosses zero is roughly one order of magnitude larger, $\Lambda \approx 10^{11}$GeV for the 3-3-3 and 3-2-1 orderings with a central top mass.

In addition to the question of total stability addressed above, we consider the possibility of a metastable vacuum state, from which a decay can in principle occur via tunnelling. The key to the validity of such a description is the expected lifetime of such a state. If the system can be expected to stay in the metastable state for a period longer than the current age of the universe, then this description does not encounter any immediate tension with reality. We invoke standard ap-

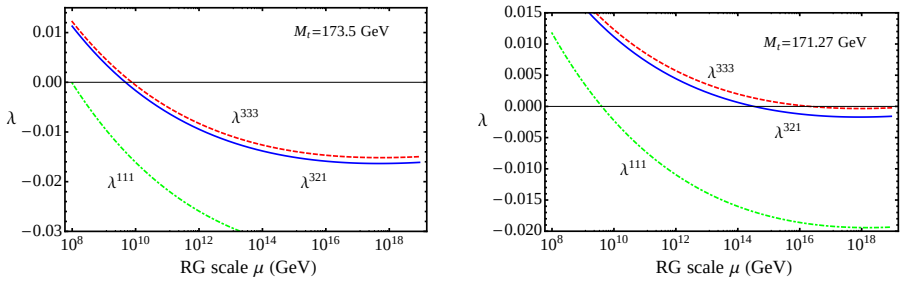


Figure 2.1: The RG evolution of the quartic Higgs coupling in different orderings, where the Higgs mass is set at its central value $M_H = 125.7$ GeV and the top mass is set to $M_t = 173.5(171.261)$ GeV to the left(right).

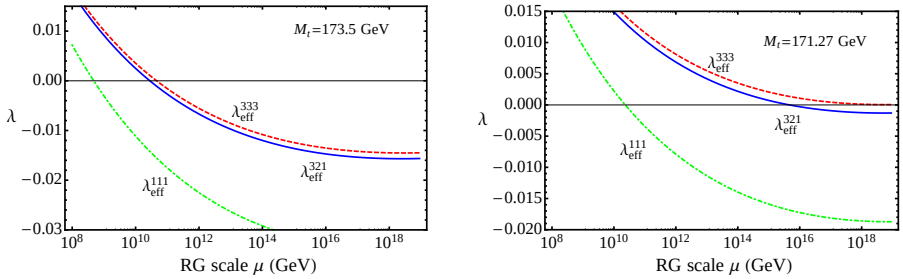


Figure 2.2: The RG evolution of the quartic Higgs coupling in different orderings, where the Higgs mass is set at its central value $M_H = 125.7$ GeV and the top mass is set to $M_t = 173.5(171.27)$ GeV to the left(right).

proximations [25] for the metastability of such a vacuum, which require that the approximated probability of the false vacuum decaying within the lifetime of the universe is less than one. This can be expressed mathematically as

$$\lambda(\phi) > -\frac{8\pi^2/3}{4\log[\phi T_U e^{\gamma_E}/2]}, \tag{2.26}$$

where $T_U$ is the age of the universe, $\gamma_E$ is the Euler-Mascheroni constant and the field value $\phi$ plays the role of the renormalization scale, so the equation must be valid for all scales (at least up to the Planck scale). We invoke this division between the metastable and unstable vacuum state, and compare the 3-3-3 results to the 3-2-1 as a function of the top and Higgs mass in Fig. 2.3

In addition to the vacuum stability analysis, we consider the case where the electroweak vacuum is the true ground state, but an unstable minimum exists at higher values of the Higgs field. The condition for such a second vacuum close to the point when $\lambda_{\rm eff}$ vanishes is the simultaneous vanishing of $\beta_{\rm eff} = d\lambda_{\rm eff}/d\ln\phi$ on the new minimum. Typically these two conditions are met by lowering the value of the top mass. To verify this possibility we show in the right panels of Figs. 2.1 and 2.2, where we adopt a lower value of the top mass, i.e. $M_t = 171.27$ GeV. It is clear from the picture, that for this value of the top mass and within the 3-3-3 counting scheme, the conditions for the existence of a second vacuum, degenerate in energy with the electroweak one, are met. Indeed, in the right panel of Fig. 2.2 we observe that $\lambda^{333}_{\rm eff}$ crosses zero at $\Lambda \approx 10^{19}$ GeV with a near zero slope, i.e. $\beta_{\rm eff} \approx 0$. However, within the 3-2-1 counting scheme, the situation differs as $\lambda^{321}_{\rm eff}$ crosses zero about three orders of magnitude earlier, with non-vanishing $\beta_{\rm eff}$, for the same value of the top mass. We have to lower the top mass to circa $M_t \approx 171.05$ GeV in this Weyl consistent scheme to accommodate the emergence of a degenerate minimum, giving a deviation of the order $2\sigma$ from the central value of the top mass.

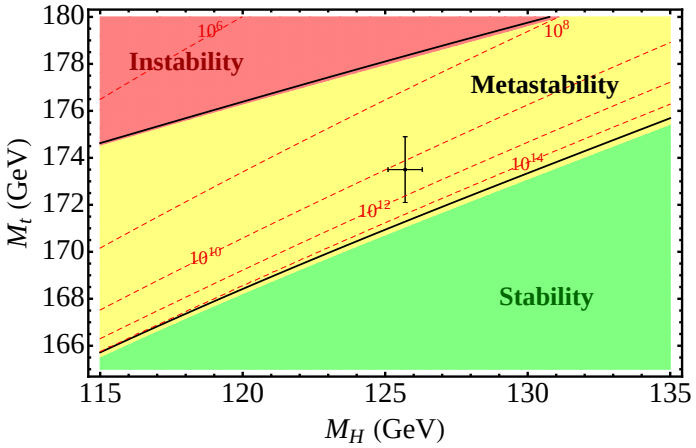


Figure 2.3: Standard model stability analysis based on the effective standard model Higgs quartic coupling. The red region indicates instability, the yellow metastability and the green absolute stability following the 3-2-1 counting. For comparison, the black lines indicate the bounds from the 3-3-3 counting. The point with error bars shows the experimental values of the top [26] and Higgs [7] masses. The red dashed lines show the value in GeV at which $\lambda_{\text{eff}}^{321}$ crosses zero.

## 2.4 IMPACT FROM RE-ORDERING

As is evident from the previous section, the results on the question of absolute stability of the standard model vacuum state is only altered slightly when switching from the 3-3-3 ordering to the 3-2-1 ordering, and as such does not change the conclusion. For the question of metastability, the differences are also small, but it should be noted that the difference might become crucial once the uncertainties on the Higgs and top masses are reduced, and in this case the nature of the conclusion might depend on the chosen ordering. The same is true for the question regarding the possibility of and unstable vacuum around the Planck scale.

Even though the conclusions in the phenomenological example displayed here does not seem be very sensitive to whether the 3-2-1 or 3-3-3 ordering is used, we did see a large effect when converting from the conventional 1-1-1 leading order result to the 3-2-1 leading Weyl consistent ordering. The exact origin for this effect cannot with certainty be attributed to the Weyl consistency, but it certainly does beg the question whether a conventional "L-L-L" type of ordering which is bounded in the counting of $\hbar$s is as consistent as we have taken it to be. Perhaps the additional structure in the RG equations given by the Weyl consistency conditions will become the key the precision.

# CHAPTER 3

# STABILITY BY EXTENSION AND GRAVITY

While the instability in the Higgs potential of the standard model as described above is not directly inconsistent with the low energy vacuum state which our part of the universe seem to be in, it might lead to inconsistencies in the cosmological picture describing the earliest period for the universe [27, 28]. The presence of an instability in the Higgs potential coupled with fluctuations of the Higgs field value due to inflation could thus lead to bubbles where the Higgs field is at its true minimum, which would fill most of the universe.

The main assumption made in the previous chapter, however, is the absence of new physics between the electroweak scale and the Planck scale. Since many questions are left unanswered by the standard model, even though there is very little tension with particle experiments, physics at higher energy scale are often invoked to offer explanations for such questions. Specifically, the standard model does not offer any candidates for dark matter (DM), and must as such be extended in some way to enable a proper description of the astronomical and cosmological observations that point to the existence of such. These extensions may lead to different conclusions regarding the vacuum stability question depending on the nature of the new physics.

The low value of the quartic Higgs coupling at large energies has also been proposed as consequence of gravitational interactions at transplanckian energies. In the following we investigate whether vacuum stability may be restored with the introduction of dark matter and the effects on the possible connection to gravitational dynamics.

## 3.1 STABLE DARK MATTER EXTENSIONS OF THE STANDARD MODEL

We investigate dark matter motivated extensions [29, 30] of the SM, where dark matter is magnetically interacting. Here, for the first time we investigate their possible simultaneous ability to save the electroweak vacuum from being metastable, provide a dark matter candidate, and their compatibility with the asymptotically safe gravity framework [12, 31].

The new sector consists of a vectorlike heavy electron ($E$), a complex heavy scalar electron ($S$) and a SM singlet Dirac fermion ($\chi$). The associated renormalizable Lagrangian is

$$\begin{aligned}\mathscr{L} &= \mathscr{L}_{\rm SM} + \bar{\chi} i\partial\!\!\!/ \chi - m_\chi \bar{\chi}\chi + \overline{E} i D\!\!\!/ E - m_E \overline{E} E - (S\overline{E}\chi y_\chi + \text{h.c.}) \\ &\quad + D_\mu S^\dagger D^\mu S - m_S^2 S^\dagger S - \lambda_{HS} H^\dagger H S^\dagger S - \lambda_S (S^\dagger S)^2 \,, \end{aligned} \tag{3.1}$$

where $H$ is the SM Higgs doublet and $D^\mu = \partial^\mu - i g_1 Q_D B^\mu$, with $g_1$ the hypercharge coupling and $Q_D$ denoting the hypercharge of $E$ and $S$. We assume the new couplings $y_\chi, \lambda_{HS}$ and $\lambda_S$ to be real and the bare mass squared of the $S$ field, $m_S^2$, to be positive so that electroweak symmetry breaks via the Higgs doublet. The interactions among $\chi$, our potential magnetic dark matter candidate, and the SM fields occur via loop-induced processes involving the $S\bar{E}\chi y$-operator. Only the scalar field $S$ feels the Higgs directly. This is true provided we do not mix the new electron with the SM leptons via generalized Yukawa interactions. Due to this property and the requirement of the renormalizability of the theory, the $S$ sector is a portal sector and can be probed directly using processes involving the Higgs.

The phenomenological signatures of this model were studied in Ref. [29], where it was constructed in the search for a theory that is able to alleviate the tension between the different direct-detection dark matter searches [32–35].

This model, without the explicit mass parameters, was also recently considered as a *perturbatively natural conformal* extension of the SM [36], where electroweak symmetry breaking is generated via the Coleman-Weinberg mechanism without any quadratic divergences to the perturbative order considered. This scenario, in fact, predicts the mass of $S$ to be around $m_S \approx 383$ GeV, close to the benchmark value used in [29].

A more detailed analysis of the dark matter properties and constraints of these theories appeared in [30]. Here it was shown that the basic model is constrained dominantly by direct detection experiments and its parameter space can be nearly entirely covered by up-coming ton-scale direct detection experiments. Adding the vacuum stability analysis and the interplay with gravitational interactions allows us to get one step closer to a more complete extension of the SM.

## 3.2 RG FLOW ANALYSIS

To study the vacuum stability and possible compatibility with the asymptotically safe gravity scenario under the influence of the new dark matter interactions, we turn to the RG equations for the couplings of the theory. The relevant couplings to consider are assumed to be: The gauge couplings $g_1, g_2$, and $g_3$, associated to the $U(1), SU(2)$ and $SU(3)$ gauge symmetry respectively, as well as the top Yukawa coupling $y_t$, the Yukawa coupling of the dark sector $y_\chi$, and the three quartic couplings $\lambda_H, \lambda_{HS}$, and $\lambda_S$.

Without gravitational corrections, i.e. in the low-energy region (as compared to the Planck scale), their respective beta functions are given to one loop order by:

$$\beta_{g_1} = \frac{1}{(4\pi)^2}\left(\frac{41}{6}+\frac{5}{3}Q_D^2\right)g_1^3 \quad , \quad \beta_{g_2} = -\frac{19}{96\pi^2}g_2^3 \quad , \quad \beta_{g_3} = -\frac{7}{(4\pi)^2}g_3^3 \, , \tag{3.2}$$

$$\beta_{y_t} = \frac{1}{(4\pi)^2}\left[\frac{9}{2}y_t^3 - (\frac{17}{12}g_1^2+\frac{9}{4}g_2^2+8g_3^2)y_t\right] \, , \tag{3.3}$$

$$\beta_{y_\chi} = \frac{1}{(4\pi)^2}3y_\chi(y_\chi^2 - Q_D^2 g_1^2) \, , \tag{3.4}$$

$$\beta_{\lambda_H} = \frac{1}{(4\pi)^2}\left[3(4y_t^2-3g_2^2-g_1^2)\lambda_H - 6y_t^4 + \tfrac{3}{8}[2g_2^4+(g_1^2+g_2^2)^2] + 24\lambda_H^2 + \lambda_{HS}^2\right] \, , \tag{3.5}$$

$$\beta_{\lambda_{HS}} = \frac{1}{(4\pi)^2}\left[\frac{3}{2}(4y_t^2-3g_2^2-g_1^2+8\lambda_H)\lambda_{HS} + (4y_\chi^2 - 6Q_D^2 g_1^2 + 8\lambda_S + 4\lambda_{HS})\lambda_{HS} + 3Q_D^2 g_1^4\right] \, , \tag{3.6}$$

$$\beta_{\lambda_S} = \frac{1}{(4\pi)^2}\left[2\lambda_{HS}^2 + 6Q_D^4 g_1^4 - 12Q_D^2 g_1^2\lambda_S + 20\lambda_S^2 + 8y_\chi^2\lambda_S - 4y_\chi^4\right] \, , \tag{3.7}$$

where $Q_D$ is the hypercharge of the $E$ and $S$ fields.

Perturbative values of the couplings are within the phenomenological constraints presented for the theory in [29], and therefore the one loop beta functions should be applicable around the Fermi scale. Admittedly, the use of only one loop beta functions not in line with the logic employed in the previous chapter, and we should therefore anticipate that some corrections may present themselves if a Weyl consistent first order calculation would be performed where one must take into account the three loop beta functions for the gauge couplings and the two loop beta functions for the Yukawa couplings. We regard the present analysis to be no more than a good qualitative estimate of the dynamics of the theory, especially so if the couplings remain small along the RG flow. We will assume, that the DM candidate $\chi$ has a mass around $m_\chi \sim 10$ GeV, and that the mass of the scalar and vector like electron have masses $m_S \sim m_E \sim 500$ GeV.

Due to the decoupling theorem, the SM couplings will run as in the SM, until the mass scale $m_S$ of the new scalar $S$ (and electron $E$) is reached. To lowest order in perturbation theory, there is no threshold effects on the couplings at this scale, since the vacuum expectation value of $S$ is at the origin. Beyond the $m_S$ scale the running couplings are influenced by the new sector. In particular, at one loop, the beta function for the $U(1)$ gauge coupling, $g_1$, is modified since the new scalar $S$ appears in the loop corrections to the $g_1$ coupling, and the beta function for the Higgs self-coupling $\lambda_H$ receives corrections from the portal coupling, $\lambda_{HS}$. Defining values of $\lambda_S$, $\lambda_{HS}$ and $y_\chi$ at the $m_S$ scale as well as choosing a value for the hypercharge $Q_D$, will then uniquely dictate the evolution of the theory, at least until gravitational corrections should be taken into account.

In order to constrain the parameter space of the theory, we will look for fixed point structures in the new sector. Upon inspection of (3.2) and (3.4), we see that the system of $g_1$ and $y_\chi$ can be considered in isolation, and as in the case of the

$(\lambda_H, y_t)$ system described in Chapter 1 we find that the ratio $\frac{y_\chi}{g_1}$ has an *approximate* IR fixed point, which reads:

$$r \equiv \left.\frac{y_\chi}{g_1}\right|_{IR} = \sqrt{\tfrac{41}{18} + \tfrac{14}{9} Q_D^2}\,. \tag{3.8}$$

Assuming that $y_\chi$ reaches small values in the IR of order $g_1$ (at the $m_S$ scale), we can expect that the ratio of these couplings in the IR is close to this value. We impose this assumption in our analysis to determine $y_\chi(m_S)$ from $g_1(m_S)$.

Moving on to the beta function for $\lambda_S$, we see that upon replacing $g_1$ via (3.8), it only depends on the couplings $\lambda_S$, $y_\chi$, and $\lambda_{HS}$. If we assume small values for the $\lambda_{HS}$ coupling ($\lambda_{HS} < y_\chi^2$), then the system of the $\lambda_S$ and $y_\chi$ couplings can be considered separate from the rest of the theory to this order. Reminiscent of the situation for the $(\lambda_H, y_t)$ system in the standard model, we find an approximate fixed point, after defining $\kappa = (Q_D/r)^2$, in the IR:

$$\left.\frac{\lambda_S}{y_\chi^2}\right|_{IR} = \frac{3\kappa - 1}{20} + \frac{\sqrt{81 - 6\kappa - 111\kappa^2}}{20} + \mathcal{O}(\lambda_{HS})\,, \tag{3.9}$$

where we explicitly remind ourselves that nonzero values of $\lambda_{HS}$ at low energies will lead to corrections to this estimate. Interestingly, insertion of (3.8), such that the leading estimate on the ratio only depends on $Q_D$ ensures that the ratio is always between 0.32 and 0.42 regardless of the value of $Q_D$!

All that is left in order to perform a stability analysis is the choice of the values of the parameters $\lambda_{HS}(m_S)$ and $Q_D$, with which we will determine the values of $y_\chi(m_S)$ from $g_1(m_S)$ and in turn $\lambda_S(m_S)$ from $y_\chi(m_S)$ together with the choice for $\lambda_{HS}(m_S)$ by assuming a constant value for $\lambda_{HS}$ for the calculation (3.9) (Since $\lambda_{HS}$ enters with a positive sign in (3.7), nonzero values for the portal coupling will lead to a decrease in the predicted IR value for $\lambda_S$). With this procedure in mind, we vary $\lambda_{HS}(m_S)$ for different values of $Q_D$ to determine the minimal value needed to make $\lambda_H$ positive between the Fermi and Planck scale, a sign for absolute stability of the Higgs potential.

For $Q_D = 1$ we deduce from Eq. (3.8) and (3.9) that $y_\chi(m_S) \approx 0.69$, and $\lambda_S(m_S) \approx 0.20$ up to corrections from $\lambda_{HS}$. The smallest value for $\lambda_{HS}$ that ensures stability of the electroweak vacuum is $\lambda_{HS}(m_S) \gtrsim 0.26$. A nonzero value of $\lambda_{HS}$ leads, in the full analysis, to a slightly smaller $\lambda_S(m_S) \lesssim 0.19$. The running couplings are shown in Figure 3.1. The quartic couplings run to large values around the Planck scale. Thus the lower boundary on the coupling $\lambda_{HS}$ corresponds to a Landau pole close to the Planck scale. For higher values of $\lambda_{HS}$ the Landau pole is shifted toward lower energy scales.

For $Q_D = 2$ we have $y_\chi(m_S) \approx 1.03$ and the lower boundary on $\lambda_{HS}$ is slightly lowered; $\lambda_{HS}(m_S) \gtrsim 0.2$ with $\lambda_S(m_S) \lesssim 0.41$. The Landau pole, however, is also lowered to around the value $10^{15}$ GeV. For even higher values of $Q_D$ this trend continues and the value of $y_\chi(m_S)$ quickly becomes non-perturbative.

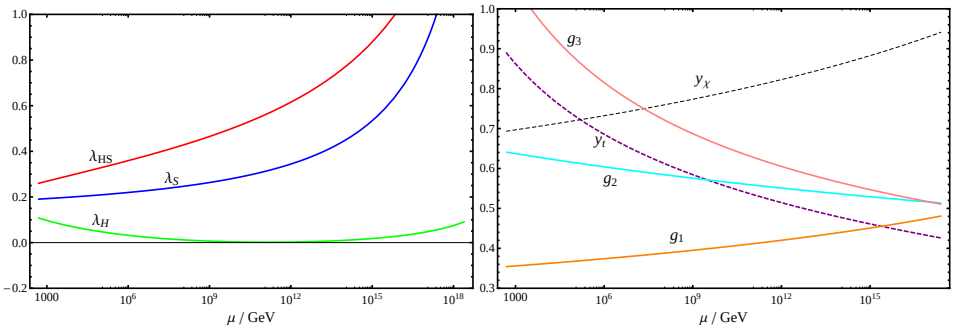


Figure 3.1: RG evolution of the couplings, where $Q_D = 1$, $m_S = 500$ GeV, $\lambda_{HS}(m_S) = 0.26$, $y_\chi(m_S) = 0.69$ and $\lambda_S(m_S) = 0.19$. The Higgs self coupling is stabilized due to the portal coupling $\lambda_{HS}$, which is here at its lower bound to ensure stability.

For $Q_D \sim 0$ i.e. for millicharged dark scalar and electron, the trend goes in the opposite direction; the lower bound becomes $\lambda_{HS} \gtrsim 0.28$ with $y_\chi(m_S) \approx 0.53$ and $\lambda_S(m_S) \lesssim 0.11$ and the Landau pole moves beyond the Planck scale.

For the case $Q_D = 1$ we make an elaborate study of the Higgs potential stability in the phase space of couplings. The electroweak vacuum is not stable if the Higgs self-coupling $\lambda_H$ runs to negative values. We can, however, distinguish metastability from instability. This is done by considering the probability of tunneling to the true vacuum during the evolution of the Universe. If the probability is bigger than some value $p$, we say that the electroweak vacuum is unstable. Otherwise it is metastable, and thus physical (see Refs. [25, 37, 38] for details). In our study, we choose the value $p = 0.1$, which means that most of the universe (more precisely $e^{-p} \sim 90\%$) is in the metastable phase at current times.

In Fig. 3.2 we show the results of this analysis as a function of the top-quark mass $M_t$ and $\lambda_{HS}(m_S)$, where we kept fixed all other parameters fixed to their central experimental value, in particular $m_H = 125.9$ GeV, as given by the Particle Data Group [26]. Varying $m_H$ within the experimental uncertainty does not generate any numerically significant difference in the figure.

So far we concentrated on the stability analysis. By combining it with the request of a viable dark matter candidate [30], typically needing large values of $\lambda_{HS}$ and $y_\chi$ at the electroweak scale, we conclude that the model is able to solve the dark matter problem while remaining stable. However, the scalar couplings are expected to generate a Landau pole before reaching the Planck scale. Possible interpretations coming from this feature will be discussed in Chapters 4 and 5.

## 3.3 CROSSING THE GRAVITY SCALE

At this stage we will make a leap beyond what is usually attempted in phenomenological studies of DM models and investigate possible consequences from extend-

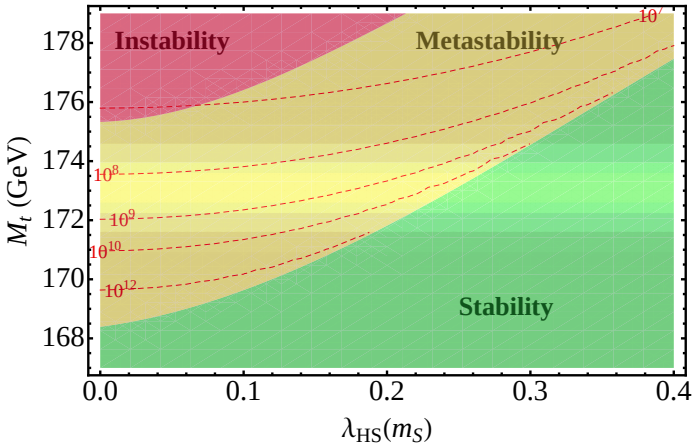


Figure 3.2: The Higgs potential stability as a function of the top-quark mass $M_t$ and $\lambda_{HS}(m_S)$. The shadings show the normal distribution of the top-mass with mean value 173.1 GeV and standard deviation $\sigma = 0.9$ GeV, as given by the Particle Data Group [26]. All other parameters were fixed to their central experimental values, in particular $m_H = 125.9$ GeV [26]. The dashed contours indicate the scale (in GeV) where $\lambda_H = 0$.

ing the analysis to RG scales beyond the Planck mass. Near the Planck scale we can no longer ignore the gravitational corrections, but currently there is no universal consensus on how quantum gravitational corrections have to be dealt with. To progress here we will make use of the intriguing scenario according to which quantum gravity becomes asymptotically safe, and therefore nonperturbatively renormalizable due to the occurrence of a strongly coupled UV fixed point [39]. The literature on the subject is vast and we refer to [40] for a review. To determine the gravitational corrections we follow [41].

The authors in [12, 31] noticed an intriguing feature of the SM when assuming the electroweak vacuum to be the true vacuum; i.e. they showed that a lower bound on the Higgs mass consistent with asymptotic safe gravity is $129 \pm 6$ GeV. These results seem to imply that the electroweak scale is somehow determined by Planck scale physics.

Here we test whether this picture survives, when including the effects of the candidate dark sector. Denoting collectively the set of dimensionless couplings by $x_i$ it follows from pure dimensional grounds that the gravitational contribution, $\beta_i^{grav}$, to the beta function of $x_i$ reads:

$$\beta_{x_i}^{grav} = \frac{a_i}{8\pi} \frac{\mu^2}{M_P^2(\mu)} x_i \,, \tag{3.10}$$

where the Planck scale, $M_P(\mu)$, is a dynamical quantity and scales due to asymptotic safety as [12]:

$$M_P^2(\mu) = M_P^2 + 2\xi_0 \mu^2 \tag{3.11}$$

where $M_P = (8\pi G_N)^{-1/2} = 2.4 \times 10^{18}$ GeV is the usual (low energy) Planck mass. The parameter $\xi_0$ is a model and scheme dependent number. Its exact value is not important for this work and we fix its numerical value to $\xi_0 = 0.024$ based on numerical studies in certain (FRGE) gravity models [41–43].

Also the coefficients $a_i$ are scheme and model dependent and are furthermore dynamical. For our study only their sign near the Planck scale will be important. The full one loop beta functions for the couplings $x_i$ thus read:

$$\mu \frac{dx_i}{d\mu} = \beta_{x_i} + \frac{a_i}{8\pi} \frac{\mu^2}{M_P^2(\mu)} x_i \,. \tag{3.12}$$

The corrections to the beta functions from gravity are negligible until we reach $\mu^2 \sim M_P^2$. If the couplings stay perturbative in the high energy regime, they are well described by Eq. (3.12) with $a_i$ constant. For $\mu^2 > M_P^2$ the gravitational corrections become increasingly important. In particular, for $a_i < 0$ the couplings will run towards zero in the UV, making them all asymptotically free. In Ref. [12] it was argued[1] that $a_i$ for the gauge and Yukawa couplings are indeed expected to be negative, while explicit computations for $\beta_{\lambda_H}^{grav}$ yields $a_\lambda > 0$ [41, 43]. One should note that different results have been obtained in the literature [46], so a positive $a_\lambda$ is at this point an explicit assumption. Due to the universal nature of gravitational interactions, these arguments apply equally to the couplings of the extended sector and therefore we assume the sign of the gravitational coefficient $a_i$ of each type of coupling to be: $a_{gauge} < 0$, $a_{Yukawa} < 0$ and $a_{quartic} > 0$. Thus also $y_\chi$ becomes asymptotically free beyond the Planck scale, while the quartic couplings $\lambda_H$ and $\lambda_S$ must both be positive or zero at the Planck scale to ensure that the potential stays bounded from below beyond the Planck scale.

To investigate whether the asymptotically safe scenario agrees with the value of the discovered Higgs mass, we assume that $\lambda_H(M_P) \approx 0$ and $\beta_{\lambda_H}|_{M_P} = 0$, as prescribed in [12, 31]. This effectively sets $\lambda_{HS}(M_P) \approx 0$. The couplings $y_\chi$ and $\lambda_S$ are determined as in the previous section at the $m_S$ scale using Eq. (3.8) and (3.9). We restrict the analysis of this section to $Q_D = 1$. This fully constrains the parameter space and leads to the evolution of the couplings shown in Fig. 3.3.

The first thing to note is that $\lambda_S$ stays positive and perturbative all the way to the Planck scale as required by consistency of the asymptotically safe scenario. The next thing to note is that $\lambda_{HS}$ stays very small (and negative) all the way down to the $m_S$ scale. This means that its effect on the running of $\lambda_H$ is negligible in the entire region from the Planck scale and down to the Fermi scale. Moreover, it does not ruin stability of the electroweak vacuum, since the potential is bounded from below as long as $2\sqrt{\lambda_H \lambda_S} + \lambda_{HS} > 0$. Thus the Higgs mass prediction from the pure

[1] The argument for $a_{gauge} < 0$ follows from explicit calculations in [44, 45]. The argument for $a_{Yukawa} < 0$ follows by negation, since positive values lead to trivial IR fixed points with $y_{t,IR} = y_{\chi,IR} = 0$ (where IR is now the Planck scale as seen from the asymptotically safe UV fixed point), up to contributions from the gauge sector, which are not able to explain the large value of the top Yukawa coupling. Negative values of $a_{Yukawa}$ are moreover supported by explicity computations [46].

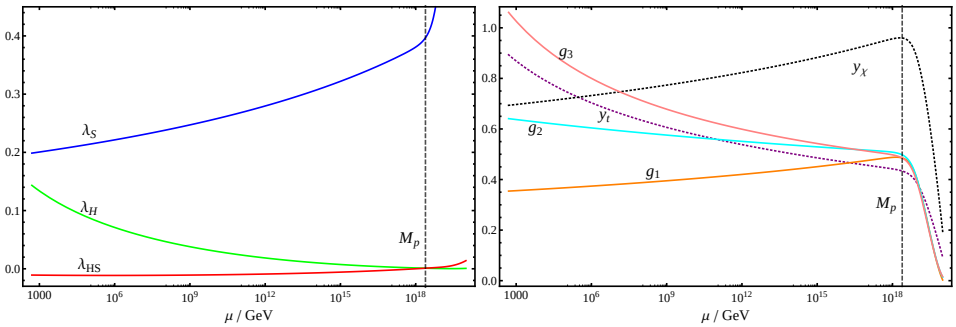


Figure 3.3: RG evolution of the couplings, where we fixed $Q_D = 1$ and $m_S = 500$ GeV, and used the initial conditions $\lambda_H(M_P) \approx 0$, $\lambda_{HS}(M_P) \approx 0$, $y_\chi(m_S) = 0.69$ and $\lambda_S(m_S) = 0.21$ as given in the text. The numerical values for the gravity coefficient were taken universally to be $\xi_0 = 0.024$, $a_\lambda = 1$, $a_y = -1$, and $a_g = -1$. Large variations on these parameters have been investigated with no relevant differences on the results.

SM within asymptotic safe scenario stays intact. We recall that the prediction is $m_H = 129 \pm 6$ GeV [12,31]. In fact, the effect from the presence of $\lambda_{HS}$ is to push the Higgs mass prediction slightly down (< 1 GeV). Since we have fixed the top mass to its experimental central value and allowed the Higgs mass, at the electroweak scale, to be determined by the UV conditions above, the stability regions of Fig. 3.2 will change slightly.

So far we have insisted in reducing the parameter space by using the low energy boundary conditions coming from (3.8) and (3.9) to determine $\lambda_S$ and $y_\chi$. One could argue, however, that a more consistent choice from the point of view of asymptotic safe gravity would be to require the vanishing of $\lambda_S$ and its beta function near the Planck scale, as done for $\lambda_H$. This corresponds to assuming $\lambda_S(M_P) \approx 0$ and $y_\chi^2(M_P) = \sqrt{\frac{3}{2}} Q_D^2 g_1^2(M_P)$ to ensure that $\beta_{\lambda_S}|_{M_P} = 0$. In this case, the prediction for the values $\lambda_S(m_S)$ and $y_\chi(m_S)$ changes to smaller values, while the effects on $\lambda_{HS}$ and thus $\lambda_H$ remains effectively unchanged. This scenario is shown in Fig. 3.4, where again the electroweak vacuum remains stable since $2\sqrt{\lambda_H \lambda_S} + \lambda_{HS} > 0$ along the entire energy range (using very small, but positive values for the quartic couplings at the Planck scale).

Our study shows that the prediction of the Higgs mass from the interplay with asymptotic safe gravity, put forward in [12, 31], apply to a wider class of extensions of the SM. These models generically contain new perturbative scalar and fermionic sectors. The key ingredients are to require, as done for the SM, that the Higgs self-coupling $\lambda_H$ and its beta function to be zero just below the Planck scale. The vanishing of the beta function guarantees the absence of a Landau pole immediately above the Planck scale. We note that the Higgs mass prediction presented here, and in [12, 31] for the SM, are lower bounds compatible with the asymptotic

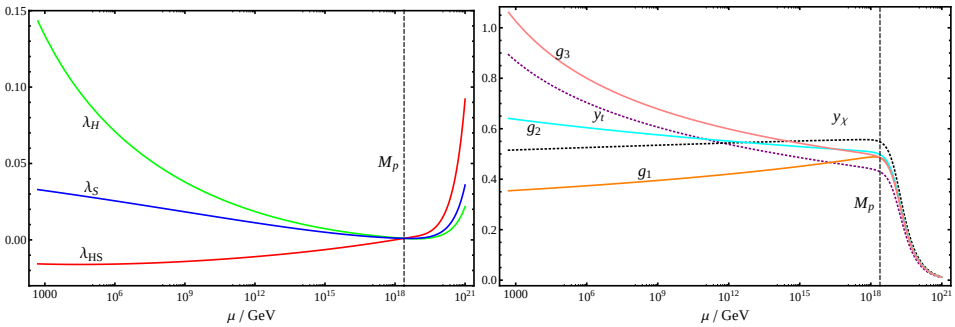


Figure 3.4: RG evolution of the couplings, where we fixed $Q_D = 1$ and $m_S = 500$ GeV and used the Planck boundary conditions $\lambda_H(M_P) \approx 0$, $\lambda_{HS}(M_P) \approx 0$, $\lambda_S(M_P) \approx 0$ and $y_\chi(M_P) = 0.54$, such that $\beta_{\lambda_H}\big|_{M_P} \approx 0$ and $\beta_{\lambda_S}\big|_{M_P} \approx 0$. The numerical values for the gravity coefficient were taken universally to be $\xi_0 = 0.024$, $a_\lambda = 1$, $a_y = -1$, and $a_g = -1$. Large variations on these parameters have been investigated with no relevant differences on the results.

safety scenario[2].

An asymptotically safe scenario as the one depicted above, albeit being perfectly compatible with these kind of stable extensions of the SM, may be at odds with the further requirement to also feature a phenomenologically viable DM candidate. If it is assumed that $a_\lambda > 0$ to ensure a highly predictive model, then the scalar couplings must vanish at the Planck scale. This assumption stems from certain quantum gravity computations. If, however, a negative sign is assumed this would enable the combination of asymptotic safety and large scalar couplings around the Planck scale that can accommodate the correct DM thermal relic density at low energies [30].

The extensions considered here yielded small deviations for the evolution of the SM coupling constants up to the Planck scale. While both the asymptotic safety scenario and absolute stability of the Higgs potential are interesting options, another venue has yet to be explored. If the Higgs coupling was to diverge before the Planck scale, nonperturbative methods would be needed to make sense of the theory. Alternatively, such a divergence might signal that the Higgs boson has internal structure, and that the high energy theory might be one of only fermionic matter. We turn our attention to this scenario for the remainder of this work.

[2] If there were tree level threshold effects on the quartic Higgs self-coupling, like in Ref. [47], the bound on the Higgs mass could be lowered further. Note that this is not possible in the current setup, since it would require $\langle S \rangle \neq 0$ which would break the electroweak gauge symmetry completely.

# CHAPTER 4

# COMPOSITENESS A LA NJL

While our treatment of the Higgs particle so far has implicitly assumed that the Higgs is a fundamental particle, and as such the only known fundamental scalar, the this is not necessarily the case. While a gauge-Yukawa theory is successfully used to describe the particle physics experiments that has been conducted so far, it might be that this theory should be replaced by one without fundamental scalars at high energies, which yields the same effective description at low energies. In this chapter, we dedicate ourselves to the study of a general set of gauge-Yukawa theories, inspired by the the global symmetries of QCD and electroweak theory. Keeping the initial discussion general we will then argue that it is possible to reinterpret and make use of a certain class of gauge-Yukawa theories that are not asympotically safe or free, and thus usually could not be considered as complete descriptions of nature. These theories thus have Landau poles that cannot be tamed controllably, at least within perturbation theory, but which instead herald the energy scale at which the scalars must be viewed as being composite objects.

## 4.1 THE COMPOSITE FACET OF GAUGE-YUKAWA THEORIES

A gauge-Yukawa theory can be described by a Lagrangian of the general form

$$\mathscr{L} = -\frac{1}{4g^2}F_{\mu\nu}F^{\mu\nu} + i\bar{\Psi}\not{D}\Psi + D_\mu\Phi D^\mu\Phi^\dagger + (Y\bar{\Psi}\Phi\Psi + h.c) - V(\Phi)\,, \tag{4.1}$$

$$V(\Phi) = {m_0}^2\Phi^\dagger\Phi + \lambda(\Phi^\dagger\Phi)^2, \tag{4.2}$$

where $Y$, $m_0^2$, and $\lambda$ may be tensors in the fermion $\Psi$ and scalar $\Phi$ field space. To define the theory the appropriate gauge group(s) and corresponding representations must be specified, while the choice of the Yukawa and scalar couplings determine the global symmetries of the theory. This class of theories are renormalizable and have been extensively studied. When quantum effects are considered and counter terms are added to remove the ultraviolet divergences, all of the terms in the Lagrangian Eq. (4.1) receive corrections. Focussing on the fermionic

and scalar sector of the theory the changes to the Lagrangian are given by

$$i\bar{\Psi}\not{D}\Psi \to i(1+\delta_{Z_\Psi})\bar{\Psi}\not{D}\Psi, \quad D_\mu\Phi D^\mu\Phi^\dagger \to (1+\delta_{Z_\Phi})D_\mu\Phi D^\mu\Phi^\dagger\,, \tag{4.3}$$

$$m_0^2 \to m_0^2+\delta_{m^2}=m_r^2, \quad Y\to Y+\delta_Y=Y_r, \quad \lambda\to\lambda+\delta_\lambda=\lambda_r, \tag{4.4}$$

where $\delta_{Z_\Phi}$ and $\delta_{Z_\Psi}$ are the corrections from field-strength renormalization of the scalars and fermions. Through the renormalization procedure, a renormalization scale $\mu$ is introduced, and when the operators above change as the renormalization scale is varied, the theory moves along a renormalization group flow in the space of couplings. Defining the couplings at a given energy scale picks out a unique RG trajectory of the flow. Therefore in principle, a specific gauge-Yukawa theory has an infinite number of physically different paths in the RG flow.

To retain the canonical form of the renormalized Lagrangian, the field-strength renormalizations may be absorbed by a redefinition of the fields, $\Phi\to\Phi/(1+\delta_{Z_\Phi})^{1/2}$, and $\Psi\to\Psi/(1+\delta_{Z_\Psi})^{1/2}$, giving:

$$\mathscr{L}=-\frac{1}{4g^2}F_{\mu\nu}F^{\mu\nu}+i\bar{\Psi}\not{D}\Psi+D_\mu\Phi D^\mu\Phi^\dagger+(\tilde{Y}\bar{\Psi}\Phi\Psi+h.c)-V(\Phi)\,, \tag{4.5}$$

with

$$V(\Phi)=m_\Phi^2\Phi^\dagger\Phi+\tilde{\lambda}(\Phi^\dagger\Phi)^2\,. \tag{4.6}$$

The renormalized canonical parameters are in terms of the renormalized non-canonical ones given by:

$$\tilde{Y}=\frac{Y_r}{(1+\delta_{Z_\Psi})\sqrt{(1+\delta_{Z_\Phi})}}, \qquad m_\Phi^2=\frac{m_r^2}{(1+\delta_{Z_\Phi})}, \quad and \quad \tilde{\lambda}=\frac{\lambda_r}{(1+\delta_{Z_\Phi})^2}\,. \tag{4.7}$$

In standard perturbation theory the denominators in the above expressions can be taken to unity, such that to lowest order $\tilde{Y}=Y_r$, $m_\Phi^2=m_r^2$ and $\tilde{\lambda}=\lambda_r$. However, this identification breaks down if at strong-coupling the field-strength renormalizations grow big. This is the situation we would like to investigate.

In particular, we want to consider in this work gauge-Yukawa theories, where the scalars are composite fields appearing only below a certain energy scale $\Lambda_{\rm UV}$. Above that scale, one should recover a theory of only fermions and gauge bosons. This means that the scalars must cease to propagate at the scale $\Lambda_{\rm UV}$, and there we must set $\delta_{Z_\Phi}=-1$. This physical requirement on the scalar field translates into requirements for the scalar and Yukawa couplings as well as the mass term of the renormalized Lagrangian in Eq. (4.5), which we call *the compositeness conditions*. It is convenient to express these conditions in the following form:

$$\lim_{\mu\to\Lambda_{\rm UV}}\tilde{Y}^{-2}=0\,, \qquad \lim_{\mu\to\Lambda_{\rm UV}}\frac{\tilde{\lambda}}{\tilde{Y}^4}\approx\frac{\lambda_r}{Y_r^4}\,, \qquad \lim_{\mu\to\Lambda_{\rm UV}}\frac{m_\Phi^2}{\tilde{Y}^2}\approx\frac{m_r^2}{Y_r^2}\,, \tag{4.8}$$

where by the limit an inverse transformation from Eq. (4.5) to Eq. (4.1) is implied at the scale $\Lambda_{\rm UV}$. This transformation is necessary, because the canonical couplings

diverge at the scale $\Lambda_{\rm UV}$. In perturbation theory such a divergence is associated with the occurrence of a Landau pole. The approximation used requires also that the fermion wave function renormalization correction does not spoil Eq. (4.8).

We show now a particularly important case, where these conditions are matched onto a purely fermionic gauge theory at the composite scale. Consider the case when $\lambda_r = 0$ at the scale $\Lambda_{\rm UV}$. The Lagrangian at the scale $\Lambda_{\rm UV}$ in this case reads:

$$\mathscr{L} = -\frac{1}{4g_r^2} F_{\mu\nu}F^{\mu\nu} + i\bar{\Psi}\not{D}\Psi + (Y_r\bar{\Psi}\Phi\Psi + h.c) - m_r^2\Phi^\dagger\Phi, \tag{4.9}$$

where we assume that $\delta_{Z_\Psi} \ll 1$, or equivalently that the interactions are very weak at $\Lambda_{\rm UV}$. Since there is no kinetic term for the scalars, we may eliminate them via their equations of motion, and the resulting Lagrangian is

$$\mathscr{L} = -\frac{1}{4g_r^2} F_{\mu\nu}F^{\mu\nu} + i\bar{\Psi}\not{D}\Psi + \frac{Y_r^2}{m_r^2}(\bar{\Psi}\Psi)^2, \tag{4.10}$$

which has the structure of a generalized gauged Nambu-Jona-Lasinio (gNJL) model [48]. The link between the four fermion theory described above and a low energy gauge-Yukawa theory was first demonstrated in [13]. To connect the picture to the effective field theory language, we may choose as renormalization conditions $m_r^2(\Lambda_{\rm UV}) = \Lambda_{\rm UV}^2$ and $Y_r^2(\Lambda_{\rm UV}) = G$, with $G$ being the dimensionless four-fermion coupling. Then the above Lagrangian takes the form of the following effective field theory:

$$\mathscr{L} = -\frac{1}{4g_r^2} F_{\mu\nu}F^{\mu\nu} + i\bar{\Psi}\not{D}\Psi + \frac{G}{\Lambda_{\rm UV}^2}(\bar{\Psi}\Psi)^2\,. \tag{4.11}$$

The attentive reader would have realised that to derive the gNJL effective theory from the gauge-Yukawa system we used not only the compositeness conditions Eq. (4.8) but also that $\lambda_r = 0$. It is therefore important to know when this requirement may be satisfied starting from the gauge-Yukawa theory. Consider the following limit:

$$\lim_{\mu\to\Lambda_{\rm UV}} \frac{\tilde{\lambda}}{\tilde{Y}^2} \approx \lim_{\mu\to\Lambda_{\rm UV}} \frac{\lambda_r}{(1+\delta_{Z_\Phi})Y_r^2}\,. \tag{4.12}$$

One observes that if $\lambda_r$ does not vanish at the composite scale the above quantity diverges at $\Lambda_{\rm UV}$. If, however, $\lambda_r \to 0$ in this limit, the ratio of $\frac{\lambda_r}{(1+\delta_{Z_\Phi})}$ may go to a constant value, thus yielding

$$\lim_{\mu\to\Lambda_{\rm UV}} \frac{\tilde{\lambda}}{\tilde{Y}^2} = \text{ constant}\,. \tag{4.13}$$

This new condition will be added to the list of compositeness conditions given in Eq. (4.8), further reducing the number of gauge-Yukawa theories that may admit a composite realization of the gNJL-type.

The previous conditions are non-perturbative in nature and can be exploited to investigate also the correspondence between the two types of theories. In particular, as we shall see, the correspondence enables us to study certain aspects of theories of composite dynamics through gauge-Yukawa theories that feature a RG region, where the theories can be treated perturbatively. This result shows that weakly coupled gauge-Yukawa theories at some intermediate energy scale are, de facto, composite theories. It is therefore tantalising to speculate that the standard model with its perturbative Higgs sector could hide, in plain sight, a composite theory. Beyond perturbation theory one can use first principle lattice studies [49–53] for which our results can be viewed exploratory in nature.

To display how the compositeness conditions work out in a specific theory, we introduce a concrete example which elucidates the main points. It consists of an $SU(N_C)$ gauge theory featuring $N_F$ Dirac fermions transforming according to the fundamental representation of the gauge group. They further interact, via Yukawa interactions, with a gauge-singlet $N_F \times N_F$ complex scalar field that at intermediate energies self-interact. We show that it is possible to enforce the compositeness conditions in this theory while simultaneously discovering a controllable perturbative regime along the RG flow. This situation is similar to the SM, where at and around the electroweak scale all the couplings can be treated in perturbation theory. Following the Weyl consistent coupling constant ordering described in Chapter 2 and thus organize the analysis coupling by coupling and such order by order.

## 4.2 THE COMPOSITE TEMPLATE

We start with an $SU(N_C)$ gauge theory with $N_C > 2$. The associated gauge fields $A^a_\mu$ have field strength $F^a_{\mu\nu}$ ($a = 1, \cdots N_C^2 - 1$). We add $N_F$ Dirac fermions $Q^c_i$ with $i = 1, \cdots N_F$ and $c = 1, \cdots N_C$ transforming according to the fundamental representation of $SU(N_C)$. The fermions further interact with an $N_F \times N_F$ complex scalar $H$. The fundamental interaction Lagrangian reads:

$$\mathscr{L} = -\frac{1}{2}\,\mathrm{Tr}\left[F^{\mu\nu}F_{\mu\nu}\right] + \mathrm{Tr}\left[\overline{Q}\, i\not{D} Q\right] + \mathrm{Tr}\left[\partial_\mu H^\dagger \partial^\mu H\right] + y\,\mathrm{Tr}\left[\overline{Q}\, H Q\right] - V[H]\ , \quad (4.14)$$

with $\mathrm{Tr}\left[\overline{Q}\, H Q\right] = \mathrm{Tr}\left[\overline{Q}_L H Q_R + \overline{Q}_R H^\dagger Q_L\right]$ and

$$V[H] = m_H^2\,\mathrm{Tr}\left[H^\dagger H\right] + u\,\mathrm{Tr}\left[H^\dagger H H^\dagger H\right] + v\left(\mathrm{Tr}\left[H^\dagger H\right]\right)^2 . \quad (4.15)$$

We trace over both color and flavour indices. The theory has been studied earlier in connection with top-quark condensate models in [54, 55], albeit in a different setup and limit that we here are taking.

The model has four classically marginal coupling constants given by the gauge coupling, the Yukawa coupling $y$, and the quartic scalar couplings; the single-trace coupling $u$ and the double-trace coupling $v$. From these we define new rescaled

couplings, useful in the large $N_C$ and $N_F$ limit, which read

$$\alpha_g = \frac{g^2 N_C}{(4\pi)^2}, \quad \alpha_y = \frac{y^2 N_C}{(4\pi)^2}, \quad \alpha_u = \frac{u N_F}{(4\pi)^2}, \quad \alpha_v = \frac{v N_F^2}{(4\pi)^2}. \tag{4.16}$$

These are the appropriately normalized couplings which enables us to study the Veneziano limit of the theory, where $N_F, N_C \to \infty$, while $N_F/N_C$ is kept constant. Note the additional power of $N_F$ in the definition of the scalar double-trace coupling, which makes $v/u$ go as $\alpha_v/(\alpha_u N_F)$.

Having defined the gauge-Yukawa theory under investigation, we specify the connection to a fermion theory with composite scalars as described above. The resulting compositeness conditions introduced in the previous section specialize to

$$\lim_{\mu\to\Lambda_{\rm UV}} \alpha_y^{-1} = 0\,, \qquad \lim_{\mu\to\Lambda_{\rm UV}} \frac{\alpha_u}{\alpha_y^2} = \lim_{\mu\to\Lambda_{\rm UV}} \frac{\alpha_v}{\alpha_y^2} = 0\,, \qquad \lim_{\mu\to\Lambda_{\rm UV}} \frac{y^2}{m_H^2} = \frac{G}{\Lambda_{\rm UV}^2}, \tag{4.17}$$

where the last requirement gives the matching to the high energy four fermion theory. The two first conditions can be investigated in any renormalization scheme, while the last one involving the mass, only applies to mass-dependent schemes. In mass-independent schemes there will be corrections to the right-hand-side of the latter condition [56], which are, however, unimportant to this work. The matching to the high-energy theory is achieved in the following way: At the scale $\Lambda_{\rm UV}$, where the couplings of the Lagrangian Eq. (4.14) formally diverge, the theory should instead be rewritten through the transformations given in Eq. (4.7). Assuming furthermore that

$$\lim_{\mu\to\Lambda_{\rm UV}} \frac{\alpha_{u/v}}{\alpha_y} = \text{constant}\,. \tag{4.18}$$

as explained in the previous section, it then follows that the scalar sector of the theory is described by

$$\mathscr{L}^H_{\rm Composite} = \sqrt{G}\,\mathrm{Tr}\left[\overline{Q}_L H Q_R + \overline{Q}_R H^\dagger Q_L\right] - \Lambda_{\rm UV}^2\,\mathrm{Tr}\left[H^\dagger H\right], \tag{4.19}$$

where the fields $Q_{L/R}$ and $H$ now are the inversely transformed ones, like in Eq. (4.3), where the kinetic term for $H$ has vanished. The renormalized mass parameter and Yukawa coupling are the inversely transformed ones defined in Eq. (4.4), where the renormalization conditions identifying them with the cut-off and the four-fermion coupling was imposed. By eliminating the auxiliary scalar degrees of freedom through their equation of motion, one obtains the four-fermion interaction[1]:

$$\mathscr{L}^H_{\rm Composite} = \frac{2G}{\Lambda_{\rm UV}^2}\,\mathrm{Tr}\left[\overline{Q}_L T^a Q_R\right]\mathrm{Tr}\left[\overline{Q}_R T^a Q_L\right], \tag{4.20}$$

[1] By using a Fierz identity, this can be recast into the form $G/\Lambda_{\rm UV}^2(\overline{Q}_L^{ic} Q_{Rc}^j)(\overline{Q}_{Rj}^{c'} Q_{Lic'})$.

Here $T^a$ was introduced through $H = h^a T^a$, with $a = 0, 1, \ldots, N_F^2 - 1$ which are the the generators of $SU(N_F)$, while $T^0 = \frac{1}{\sqrt{2N_F}}\mathbb{1}$. The normalization used is $\mathrm{Tr}\, T^a T^b = \frac{1}{2}\delta^{ab}$.

We are now ready to provide a consistent renormalization group investigation of this gauge-Yukawa system superimposed with the compositeness conditions derived above. Abiding the consistency conditions derived in Chapter 2, we will investigate the system by use of RG equations in the pattern:

$$\beta_g = \beta_g^{(1)}(g) + \beta_g^{(2)}(g, y) + \beta_g^{(3)}(g, y, \lambda) + \cdots , \tag{4.21}$$

$$\beta_y = \beta_y^{(1)}(g, y) + \beta_y^{(2)}(g, y, \lambda) + \cdots , \tag{4.22}$$

$$\beta_\lambda = \beta_\lambda^{(1)}(\lambda, g, y) + \cdots , \tag{4.23}$$

where the superscripts denote the loop order of the terms and the parenthesis shows which couplings they depend on. In our case the general quartic coupling $\lambda$ will be replaced by $u$ and $v$. Respecting the Weyl consistency conditions, one may consider the running of the gauge coupling at 1-loop consistently without taking into account the running of Yukawa and the quartic couplings (leading order). Likewise one may analyze the two-loop running of the gauge coupling taking into account the one-loop running of the Yukawa consistently without taking into account the running of the quartics (next-to-leading order). At three loops, running of all couplings must be taken into account and the lowest consistent counting order is 3-2-1 loops in the gauge-Yukawa-quartic beta functions (next-to-next-to-leading order). We will in this sense analyze the leading, next-to-leading and next-to-next-leading order corrections to the RG flow and their physical implications on the four-fermion theory described above. In particular, we will compute the distance in energy between the composite scale and the confinement scale of the theory, and show that large hierarchies are not only possible to establish, but seems to be a clear feature of these theories.

### 4.2.1 Leading order and weak compositeness conditions

The leading order analysis is an over simplified case, which is not able to capture the composite nature of gauge-Yukawa theories. Nevertheless, we make a leading order analysis in this section for completeness, since it allows us to define the infrared scale and furthermore provides a pedagogic step towards the following sections.

To the leading order one needs only to consider the gauge beta function at one-loop which reads:

$$\beta_g = \partial_t \alpha_g = -\beta_0 \alpha_g^2 = -\frac{2}{3}\alpha_g^2 \left(11 - 2\frac{N_F}{N_C}\right) . \tag{4.24}$$

Taking the Veneziano limit by letting $N_F, N_C \to \infty$, allows us to further take $x = N_F/N_C$ to be any real nonnegative number. Depending on the number of flavours,

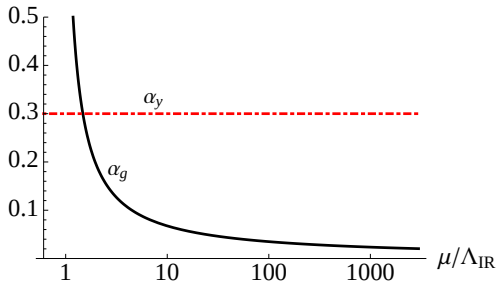


Figure 4.1: Renormalization group evolution for the lowest order analysis, where the Yukawa coupling is constant and nonzero, while the gauge coupling runs. We have here defined the scale $\Lambda_{IR}$ such that $\alpha_g(\Lambda_{IR}) = 1$. The scalar quartic couplings, not included here, are also constants to this order.

the double zero at $\alpha_g = 0$ can either be an infrared or an ultraviolet gaussian fixed point. The latter case is also known as asymptotic freedom. In the former case the ultraviolet theory is not well defined unless higher orders introduce an interacting ultraviolet fixed point, in which case the theory becomes asymptotically safe [57, 58].

Here we consider the case in which the theory is asymptotically free. This restriction allows us to assume that the wave-function renormalization of the fermions will stay small near the composite scale, since they are at one-loop produced by gauge interactions. As explained in the previous section, for consistency we should not consider the running of the scalar and Yukawa couplings at this order. According to the compositeness conditions Eq. (4.17) we should have

$$\lim_{\mu\to\Lambda_{UV}} {\alpha_y}^{-2} = 0\,. \tag{4.25}$$

To this order, a constant and formally divergent $\alpha_y$ is thus required. This is in clear tension with perturbation theory. Given that we want to avoid an uncontrollable nonperturbative analysis, to the leading order we therefore must take another approach by enforcing instead a weaker version of the compositeness conditions: Assuming that we are describing a four-fermion theory at a mass scale, which is at least a few times below the composite scale, we may consider $\alpha_y$ simply to some constant value smaller than one, as depicted in Fig. 4.1, to ensure validity of the pertubative analysis. We shall see that when next to leading order corrections are taken into account, this assumption is valid, since the Yukawa coupling will naturally grow at high energy and what we are describing here are boundary conditions in an energy range, where the Yukawa coupling is small enough for perturbation theory to hold. For the scalar self-interactions we assume a similar behaviour.

From this first oversimplified analysis one expects that the asymptotically free theory develops a mass gap associated with the divergence of the gauge coupling at low energies. At these energies chiral symmetry breaks leading to the formation

of the nonperturbative condensate

$$\langle \overline{Q}Q \rangle \propto \Lambda_{\rm IR}^3 \,. \tag{4.26}$$

The scale $\Lambda_{\rm IR}$ can be estimated to be (cf. Eq. (.39) in the appendix):

$$\Lambda_{\rm IR} = \mu_0 \exp\left(-\frac{1}{\beta_0 \alpha_g(\mu_0)}\right) . \tag{4.27}$$

This estimate is insensitive to the perturbative corrections from the Yukawa and scalar sectors, which contribute only at higher orders. Thus if the Yukawa and scalar sectors stay perturbative in the IR, the above expression provides a good estimate of the IR strong scale of the fully dynamical gauge-Yukawa theory.

### 4.2.2 Next-to-leading order analysis: The rise of the Yukawa coupling

For the next order in perturbation theory one needs to go to two loops in the gauge coupling and one loop in the Yukawa, while the evolution of the scalar couplings is still not relevant. To this order, therefore, the Yukawa coupling is no longer a constant and its running and consequent back-reaction on the gauge coupling are important. We have [2]:

$$\beta_g = -\frac{2}{3}\alpha_g^2 \left[ \left(11 - 2\frac{N_F}{N_C}\right) + \left(34 - \frac{N_F}{N_C}\left\{10 + 3\frac{N_C^2-1}{N_C^2}\right\}\right)\alpha_g + 3\frac{N_F^2}{N_C^2}\alpha_y \right] \tag{4.28}$$

$$\beta_y = \alpha_y \left[ 2\left(1 + \frac{N_F}{N_C}\right)\alpha_y - 6\frac{N_C^2-1}{N_C^2}\alpha_g \right] . \tag{4.29}$$

Working in the Veneziano limit by defining $x = N_F/N_C$ at large $N_F$ and $N_C$ yields:

$$\beta_g = -\frac{2}{3}\alpha_g^2 \left[ (11 - 2x) + (34 - 13x)\,\alpha_g + 3x^2 \alpha_y \right] , \tag{4.30}$$

$$\beta_y = 2\alpha_y \left[ (1+x)\,\alpha_y - 3\alpha_g \right] . \tag{4.31}$$

We restrict $x < 11/2$, ensuring asymptotic freedom for the gauge coupling. In the absence of the Yukawa interactions, a well known interacting infrared fixed point emerges at

$$\alpha_g^* = \frac{11-2x}{13x-34} , \qquad \text{for} \qquad \frac{34}{13} < x < \frac{11}{2} , \quad \text{and} \quad \alpha_y = 0 . \tag{4.32}$$

For $x$ very close to $11/2$ this is the Banks-Zaks perturbative infrared fixed point. This fixed point, however, disappears in the presence of the Yukawa interactions [3].

[2] The beta functions are in the $\overline{\rm MS}$-scheme [59–64]. It would also be interesting to investigate the compositeness conditions in other renormalisation schemes such as the momentum subtraction scheme [65–68], since different schemes can be more or less suitable to explore different facets of gauge-Yukawa theories.

[3] By setting $\beta_y = 0$ we derive $\alpha_y = \frac{3}{1+x}\alpha_g$ which can be substituted in $\beta_g$ yielding:

$$\beta_g \to -\frac{2}{3}\alpha_g^2 \left[ (11-2x) + \left(34 - 13x + 9\frac{x^2}{1+x}\right)\alpha_g \right] ,$$

showing that the presence of the Yukawa has eliminated the possibility of the infrared fixed point.

Therefore the next-to-leading-order effects on the gauge beta function strengthens the infrared QCD-like behaviour of the theory.

The RG flow of the gauge-Yukawa system for $x = 2$ is shown in Fig. 4.2. The arrows in the figure shows the flow from the ultraviolet (UV) to the infrared (IR) regime. In the UV two distinct phases form. The boundary between these two phases is approximately given by

$$\frac{\alpha_y}{\alpha_g} = \frac{2(x-1)}{3(x+1)}\,, \tag{4.33}$$

which is determined by the one-loop beta functions in both couplings (cf. Eq. (.56) in the appendix). Below the red trajectory both couplings are asymptotically free meaning that the theory is non-interacting and well defined in the UV. This RG region, therefore, does not support a composite limit of the theory. The composite limit emerges in the RG region above the red trajectory, where the Yukawa coupling diverges in the UV, thus allowing the compositeness conditions given in Eq. (4.17) to be satisfied. We notice that the boundary Eq. (4.33) for $x \leq 1$ is outside the physical parameter space of the couplings. Therefore the composite limit is supported by the entire perturbative region of the physical space of couplings, i.e. the Yukawa coupling will also diverge in the UV. Thus $x = 1$ defines a boundary in the external parameter space.

We show in Fig. 4.3, again for $x = 2$, the actual running of the two couplings in the composite region for one particular RG trajectory. Considering the flow from UV to IR, initially $\alpha_y \gg \alpha_g$ due to the compositeness condition. Since $\alpha_y$ will decrease, while $\alpha_g$ increases towards the IR, at some intermediate scale $\mu_0$, their val-

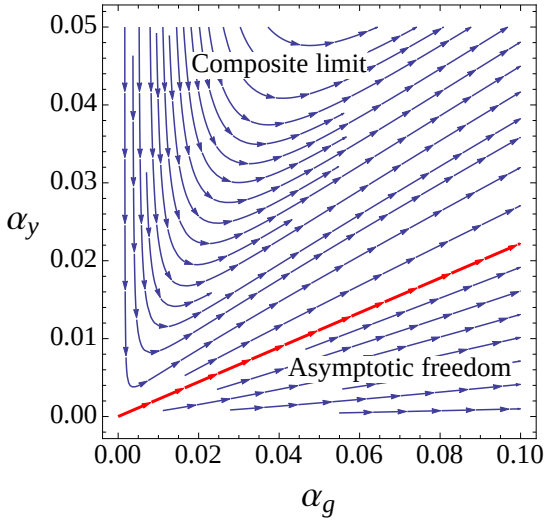


Figure 4.2: The RG flow in the $(\alpha_g, \alpha_y)$ plane for $x = 2$. Two distinct phases are present. The red trajectory indicates the phase boundary estimated from the one loop beta functions: $\frac{\alpha_y}{\alpha_g} = \frac{2(x-1)}{3(x+1)}$.

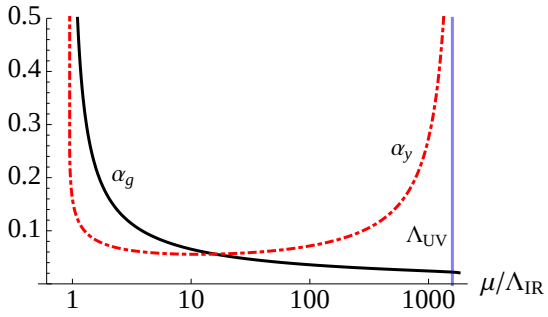


Figure 4.3: Renormalization group evolution for the next to leading order analysis, where the Yukawa and gauge couplings run. We define the scale $\Lambda_{\rm IR}$ and $\Lambda_{\rm UV}$ such that $\alpha_g(\Lambda_{\rm IR}) = \alpha_y(\Lambda_{\rm UV}) = 1$. The scalar quartic couplings are constants to this order and are not included here.

ues equal, and once $3\alpha_g > (1+x)\alpha_y$, the sign of the Yukawa beta function changes, making it grow again in the deep IR. This growth of $\alpha_y$ in the IR is therefore at most as fast as $3\alpha_g/(1+x)$.

The composite scale $\Lambda_{\rm UV}$ is identified with the Landau pole in the Yukawa coupling. We will fix our perturbative initial conditions at the crossing scale $\mu_0$, and we ensure perturbation theory to be valid by requiring $\alpha_g(\mu_0) = \alpha_y(\mu_0) = C \ll 1$. This condition is for any $x$ consistently above the boundary Eq. (4.33), ensuring the theory to be in the composite phase.

It is interesting to study the hierarchy between the composite scale and the chiral symmetry breaking one, as a function of both $C$ and $x$. At the one loop level, in both the gauge and Yukawa coupling, we can estimate it analytically to be

$$\log\left(\frac{\Lambda_{\rm UV}}{\Lambda_{\rm IR}}\right) = \frac{3\left(1+\frac{\alpha_g(\mu_0)}{\alpha_y(\mu_0)}\frac{2(1-x)}{3(1+x)}\right)^{\frac{11-2x}{2(1-x)}}}{2(11-2x)\alpha_g(\mu_0)}. \tag{4.34}$$

The expression is well-defined for any $x$, and it takes the following simple form at $x = 1$:

$$\lim_{x\to 1}\log\left(\frac{\Lambda_{\rm UV}}{\Lambda_{\rm IR}}\right) = \frac{1}{3\alpha_g(\mu_0)}\lim_{x\to 1}\left(1+\frac{\alpha_g(\mu_0)}{\alpha_y(\mu_0)}\frac{2(1-x)}{3(1+x)}\right)^{\frac{11-2x}{2(1-x)}} = \frac{\exp\left(\frac{3\alpha_g(\mu_0)}{2\alpha_y(\mu_0)}\right)}{3\alpha_g(\mu_0)}. \tag{4.35}$$

To set the initial values of the couplings we will use $\alpha_g(\mu_0) = \alpha_y(\mu_0) = C$ since in the composite phase there will always be a $\mu_0$ such that this condition is fulfilled.

In Fig. 4.4 we compare the approximate analytical one-loop result with the next-to-leading order numerical calculation. To numerically estimate the value of the IR(UV) scale we use the approximate relation $\alpha_{g(y)}(\Lambda_{\rm IR(UV)}) = 1$.

The ratio increases for small and large values of $x$ for a fixed value of $C$. This is so because, for small $x$, the first coefficient of the Yukawa beta function decreases, de facto, slowing the runaway behavior of the associated coupling in the

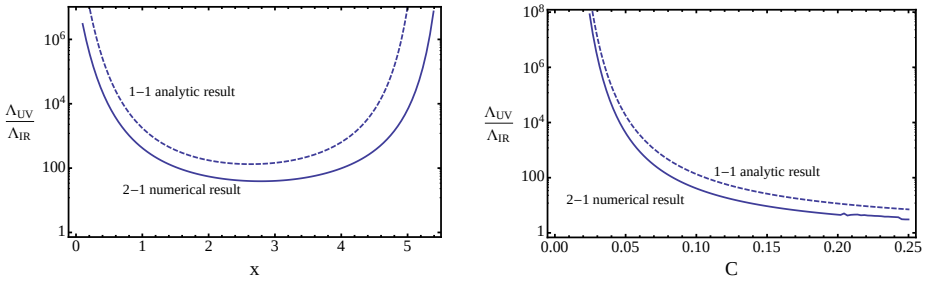


(a) $x$ is varied while $C = 0.1$ (b) $C$ is varied while $x = 2.5$

Figure 4.4: The ratio between the scale of UV compositeness ($\Lambda_{UV}$) and the one associated to infrared gauge coupling divergence ($\Lambda_{IR}$), as a function of the number of flavors/colors, parametrized by $x$ and the common value, $C$, of the gauge and Yukawa coupling at the scale where they are equal. We vary $x$ in (a) and $C$ in (b). The one loop estimate is presented in dashes while the NLO perturbative (2-1) numerical result is represented by the solid curve

UV. For large $x$, instead, the ratio becomes large since we are nearing the limit where asymptotic freedom is lost for the gauge coupling. Consequently the infrared scale is approaching zero.

Additionally, we explore the influence of the chosen value of the couplings $\alpha_y = \alpha_g = C$ at the scale where they are equal. Setting $x = 2.5$ associated to a region of $x$ that does not influence dramatically the ratio $\Lambda_{UV}/\Lambda_{IR}$, as it is clear from Fig. 4.4a, we vary the value $C$ and plot again the ratio in Fig. 4.4b. As one might have expected, smaller values of the couplings lead to a larger ratio of the scales since more RG running is needed to reach the UV and IR scales where the couplings become nonperturbative. We also observe that the approximate one-loop result overestimates the ratio.

Another interesting feature is that for the theory to remain perturbative in an intermediate regime, say $C < 0.1$, the ratio of the scales, as function of $x$, cannot be too small, and typically should be larger than 100, implying a hierarchy of scales of at least two orders of magnitudes. This means that theories in the extended technicolor class may also be expected to offer large separation between the extended technicolor scale, where four fermion interactions are relevant and the strong scale connected to electroweak symmetry breaking.

It is straightforward to see that the compositeness conditions in Eq. (4.17) are satisfied to this order. The conditions for the scalar sector are satisfied by imposing the weaker version of the conditions discussed in the previous leading-order case. Following that reasoning, thus to the next-to-leading order in perturbation theory, we have shown that gauge-Yukawa theories can be naturally viewed as stemming from a compositeness paradigm for a wide region of the RG phase diagram, e.g. the one in Fig. 4.2.

### 4.2.3 Next-to-Next-to-leading order: The awakening of the scalars

In the previous sections, we were able to draw a consistent picture of compositeness in the gauge-Yukawa sector, and we were furthermore able to provide estimates for the hierarchy between the ultraviolet composite scale and the infrared confinement scale. From the ultraviolet theory point-of-view, the scalars are merely auxiliary fields. For consistency of the analysis in the previous sections, they should therefore not play any physical role. In this section, we investigate the influence of the scalars on the above results, and provide the needed constraints on the scalar coupling phase space, needed to ensure consistency of the previous analysis.

The next order in the RG analysis requires the one loop beta functions for the quartic couplings, the two loop terms in the Yukawa beta function, and the three loop terms in the gauge beta function. This system of RG equations obeys the Weyl consistency conditions and reflects the back reaction from the scalars on the running of the Yukawa coupling, which in turn back reacts on the gauge coupling. Since the scalars do not carry gauge charge, they do not contribute to the three-loop terms for the gauge coupling. Additionally, since we are considering a mass-independent renormalization scheme, we can independently take into account the running of the mass, where one-loop is also sufficient. In the Veneziano limit, the beta functions to this order read [69, 70]:

$$\beta_g = -\frac{2}{3}\alpha_g^2\left[(11-2x)+(34-13x)\,\alpha_g+3x^2\alpha_y+\frac{81x^2}{4}\alpha_g\alpha_y\right.$$
$$\left.-\frac{3x^2(7+6x)}{4}\alpha_y^2+\frac{2857+112x^2-1709x}{18}\alpha_g^2\right], \tag{4.36}$$

$$\beta_y = 2\alpha_y\left[(1+x)\,\alpha_y-3\alpha_g+(8x+5)\alpha_g\alpha_y+\frac{20x-203}{6}\alpha_g^2\right.$$
$$\left.-8x\alpha_u-\frac{x(x+12)}{2}\alpha_y^2+4\alpha_u^2\right], \tag{4.37}$$

and for the scalar sector

$$\beta_u = 4\left[2\alpha_u^2+\alpha_u\alpha_y-\frac{x}{2}\alpha_y^2\right], \tag{4.38}$$

$$\beta_v = 4\left[\alpha_v^2+4\alpha_u\alpha_v+3\alpha_u^2+\alpha_v\alpha_y\right], \tag{4.39}$$

$$\beta_{m_H^2} = \partial_t m_H^2 = 4m_H^2[\alpha_y+\alpha_v+2\alpha_u]\,. \tag{4.40}$$

In this section we must show that the scalar self-interactions can be consistent with the compositeness picture emerged above and driven, so far, by the Yukawa interactions. Specifically, considering as in the above analysis an intermediate RG scale $\mu_0$, where perturbation theory is well-defined, we have to ensure that the scalar couplings stay perturbative up to the composite scale, where they furthermore have to satisfy the compositeness conditions given in Eq. (4.8) and Eq. (4.13). The reason for this requirement is that if the scalar couplings would grow strong before the composite scale, the analysis of the previous sections would be invalidated.

There are two other issues which may arise; the first is that according to the mass-independent scheme, the scalars remain dynamical as long as $m_H(\mu) < \mu$. For $m_H(\mu) = \mu$, the scalars will decouple before reaching the scale where they should be seen as auxiliary fields, and therefore this situation should be avoided. The second issue arises when the effective potential develops a global minimum away from the origin due to quantum corrections. For consistency of our analysis, this has to be avoided between the scales $\mu_0$ and $\Lambda_{\rm UV}$, since the vacuum expectation value of the scalar fields was earlier assumed to be zero in the analysis of the compositeness condition on the Yukawa coupling and in the calculation of the scale hierarchy. However, at lower scales there is no inconsistency of having a symmetry breaking through the scalar sector, rather than the gauge sector. This would correspond to another interesting possibility that we are, however, not considering here.

To summarize, the aim of this section is to understand and provide the criteria under which:

1. The scalar sector stays perturbative up to the composite scale, where it furthermore must satisfy the compositeness conditions.

2. The scalars do not decouple before the infrared confinement scale.

3. The minimum of the effective potential at the origin remains stable under quantum corrections between the composite and confinement scales.

We now demonstrate that there is a subset of theories which do obey the above three constraints on the scalar sector. First of all, we need to ensure that there is no Landau pole in the scalar couplings between $\mu_0$ and $\Lambda_{UV}$. To lowest order in perturbation theory, we have shown in the appendix (cf. Eq. (.67), (.68) and (.80)) that the initial conditions on the scalar couplings must satisfy the following inequality, to not become strong at intermediate scales:

$$\left\{|\alpha_u(\mu_0)|\,,\, 2|\alpha_v(\mu_0)|\right\} < \frac{2(11-2x)}{24}\,\frac{C}{\left(1-\frac{2}{3}\frac{x-1}{x+1}\right)^{\frac{11-2x}{2(1-x)}}-1}\,, \tag{4.41}$$

where we used the renormalization condition of the previous section $\alpha_g(\mu_0) = \alpha_y(\mu_0) = C$.

There is another subtle effect, which can lead to a Landau pole, due to tangential divergence, as explained in the appendix (cf. Eq. (.70)-(.71)). Here we can in the general case at best impose an overconstraint inequality, ensuring no Landau poles. For the $\alpha_u$ coupling it reads:

$$-1-\sqrt{1+4x} < 4\frac{\alpha_u(\mu_0)}{C} < -1+\sqrt{1+4x}\,. \tag{4.42}$$

For the $\alpha_v$ coupling, the situation is more complex (cf. Eq. (.79)). The following constraints, however, will ensure no Landau poles at intermediate scales:

$$\alpha_v(\mu_0) > \frac{\alpha_y(\mu_0)+4\alpha_u(\mu_0)}{2}\left(-1+\sqrt{1-\frac{12}{\left(4+\frac{\alpha_y(\mu_0)}{\alpha_u(\mu_0)}\right)^2}}\right), \tag{4.43}$$

$$\alpha_v(\mu_0) < \frac{\alpha_y(\mu_0)+4\alpha_u(\mu_0)}{2}\left(-1-\sqrt{1-\frac{12}{\left(4+\frac{\alpha_y(\mu_0)}{\alpha_u(\mu_0)}\right)^2}}\right). \tag{4.44}$$

If $\alpha_u(\mu_0)$ is negative, the additional constraint, $\left(4+\frac{\alpha_y(\mu_0)}{\alpha_u(\mu_0)}\right)^2 > 12$, must be imposed, which can be expressed more clearly as:

$$\alpha_u(\mu_0) > -\frac{\alpha_y(\mu_0)}{4+\sqrt{12}} \approx -0.13\,\alpha_y(\mu_0) \quad \text{and} \quad \alpha_u(\mu_0) < \frac{\alpha_y(\mu_0)}{\sqrt{12}-4} \approx -1.87\,\alpha_y(\mu_0)\,. \tag{4.45}$$

To ensure that there are no Landau poles in the infrared regime, before the confinement scales, similar constraints can be put, which are also provided in the appendix (cf. Eq. (.68) and (.80)).

At high scales the coupling $\alpha_v$ may also exhibit tangential divergence, as explained in the appendix (cf. Eq. (.76)). This is avoided by imposing the following constraint on the theory parameters:

$$x > -4+3\sqrt{3}-\sqrt{6\left(7-4\sqrt{3}\right)} \approx 0.54\,. \tag{4.46}$$

The constraint does not depend on the initial perturbative values of the scalar couplings and must be satisfied regardless. Thus we can conclude that for $x < 0.54$, the perturbative theory cannot show a composite nature of the type we are considering, but for any other values $0.54 < x < 5.5$, there are well defined regions where compositeness is expected.

When these constraints are satisfied, the only Landau pole appearing in the UV regime is the one driven by the Yukawa coupling. It is then clear that in perturbation theory the running of the scalar couplings at the composite scale may only diverge as fast as the Yukawa coupling, and thus the extra condition in Eq. (4.13), in agreement with an NJL-type four-fermion theory interpretation, is automatically satisfied. In appendix 5.5 we have furthermore showed that the value of Eq. (4.13) are at one-loop exactly fixed by the theory parameters, and independent of the initial values of the couplings (cf. Eq. (.63) and (.77)). In particular, near the composite scale the sign of $\alpha_u$ is always negative, while the sign of $\alpha_v$ is always positive. The consequence of this on the stability of the potential will be analyzed at the end of this chapter.

Intuitive understanding of the constraints for the quartic couplings may most easily be obtained from a visualization, and in Fig. 4.5 we display the constraints

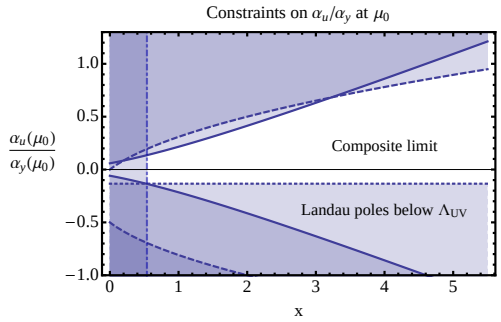


Figure 4.5: The constraints on $\alpha_u(\mu_0)$ in terms of $\alpha_y(\mu_0)$ for different values of $x$. The strong coupling constraint Eq. (4.41) is shown in solid, while the perturbative tangential divergence constraints on $\alpha_u$ Eq. (4.42), and on $\alpha_v$ Eq. (4.45)-(4.46) are shown in dashes, dots, and dotdashes, respectively.

Eq. (4.41), (4.42), (4.45) and (4.46) in terms of the ratio $\frac{\alpha_u(\mu_0)}{\alpha_y(\mu_0)}$. From the figure we see that, although the absence of unwanted Landau poles is strongly constraining the parameter space, a range of initial values for $\alpha_u$ is still consistent with the composite picture. We note in particular that the quartic coupling $\alpha_u$ is always constrained to be smaller than the Yukawa coupling, and that for any $x$, the coupling $\alpha_u$ cannot be smaller than $-0.13\alpha_y$.

As mentioned, the picture for the other coupling, $\alpha_v$, is more involved, and the constraints depend on the values of $x$ and $\alpha_y$ as well as the ratio $\frac{\alpha_u}{\alpha_y}$. We start by examining the latter dependence, coming from Eq. (4.43) and (4.44), which is depicted in Fig 4.6a.

The allowed regions for $\alpha_v(\mu_0)$ depend on the ratio $\alpha_u/\alpha_y$ in a nontrivial way, but notice that this dependence only constrains $\alpha_v$ in the region of negative values, while leaving positive values for $\alpha_v(\mu_0)$ unconstrained. For values of $\alpha_u/\alpha_y$ larger than $\sim 0.7$ the region excluded by Eq. (4.43) is fully contained within the absolute lower bound coming from the strong coupling constraints Eq. (4.41), making the former constraint irrelevant. The region where Eq. (4.43) and Eq. (4.44) are most relevant, is the one where $\alpha_u/\alpha_y$ takes small values, the lowest value allowed from Eq. (4.45) being $\frac{\alpha_u(\mu_0)}{\alpha_y(\mu_0)} \simeq -0.13$. In Fig. 4.6b we therefore display the strong coupling constraints Eq. (4.41) (independent of $\alpha_u/\alpha_y$) alongside the constraints Eq. (4.43) and (4.44), evaluated at $\frac{\alpha_u(\mu_0)}{\alpha_y(\mu_0)} = -0.13$. For larger values of $\alpha_u/\alpha_y$, the horizontal band in Fig. 4.6b moves downwards and closes the small window of allowed parameter space in the lower right corner for $\frac{\alpha_u(\mu_0)}{\alpha_y(\mu_0)} = -0.05$, as one can infer from Fig. 4.6a.

To test the validity of the approximations made in the calculations of the constraints above, we perform a full RG running of the coupled system of equations including the scalar couplings. As a benchmark model, we choose $x = 2.5$ (giving the smallest hierarchy between $\Lambda_{UV}$ and $\Lambda_{IR}$, cf. Fig. 4.4a), and $\alpha_g(\mu_0) =$

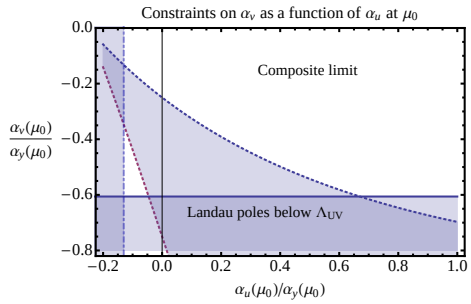


(a) $x$-independent bounds on compositeness.

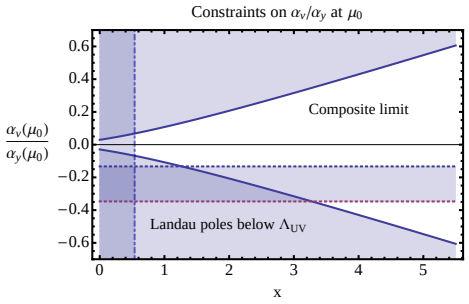


(b) $x$-dependent bounds on compositeness for $\frac{\alpha_u(\mu_0)}{\alpha_y(\mu_0)} = -0.13$.

Figure 4.6: Constraints on the initial value of the coupling $\alpha_v$ in terms of $\alpha_y$. (a) displays the $x$-independent constraints coming from Eq. (4.43), (4.44) (dots), and Eq. (4.45) (dotdashes), while the lowest $x$-dependent bound is also displayed (solid), which can be inferred from (b). (b) displays the $x$-dependent strong coupling constraints Eq. (4.41) (solid), and Eq. (4.46) (dotdashes), while the $x$-independent constraints Eq. (4.43) and (4.44) (dots) are displayed for $\frac{\alpha_u(\mu_0)}{\alpha_y(\mu_0)} = -0.13$. For larger values of $\frac{\alpha_u(\mu_0)}{\alpha_y(\mu_0)}$ the horizontal band moves downwards and closes the small window in the lower right corner for $\frac{\alpha_u(\mu_0)}{\alpha_y(\mu_0)} = -0.05$, as one can infer from (a).

$\alpha_y(\mu_0) = 0.1$, guaranteeing composite behavior in the gauge-Yukawa sector, as well as $\alpha_u(\mu_0)/\alpha_y(\mu_0) = 0.3$ and $\alpha_v(\mu_0)/\alpha_y(\mu_0) = 0.1$ to respect the constraints for the quartics. A numerical solution to the RG equations at one loop in all beta functions generates the running couplings shown in Fig. 4.7, where also the running of the ratios $\alpha_u/\alpha_y$ and $\alpha_v/\alpha_y$ is shown.

The result shows that the quartic couplings are well behaved between $\Lambda_{IR}$ and $\Lambda_{UV}$, where respectively the gauge and the Yukawa coupling poles are located. The plot of the running of ratios demonstrates that they run to a unique constant at the composite scale, which signals that a possible composite UV completion is of four-fermion NJL-type. Including the complete NNLO information in the RG equations, given at the beginning of this section, we find a very similar picture for the benchmark model, as shown in Fig. 4.8a. As predicted, we thus see that the initial conditions for the scalar couplings in this setup are not relevant for the UV behavior, in contrast to the situation for the simplest standard model extensions tailored for compositeness [4].

Next we consider the running of the mass and note that from its beta function the mass-squared parameter cannot change sign in perturbation theory. We further require the sign of $m_H^2$ to be positive to match the ultraviolet gNJL theory and to ensure stability of the scalar vacuum at the origin (for the Coleman-

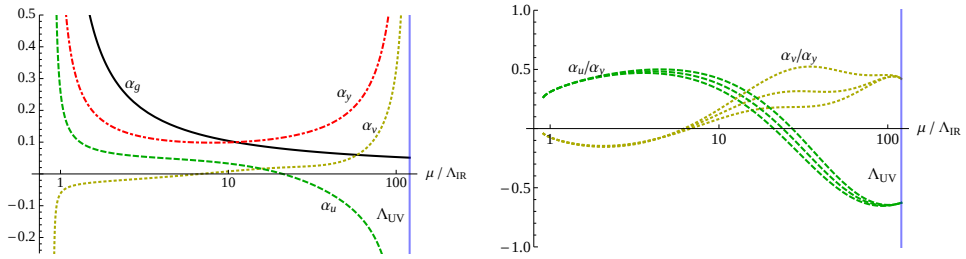


(a) 1-loop running couplings

(b) 1-loop running of coupling ratios

Figure 4.7: The RG evolution of the one loop system of gauge, Yukawa, and quartic couplings for a benchmark model, which respects the constraints for composite theories, where $x = 2.5$ giving the smallest hierarchy between $\Lambda_{\rm UV}$ and $\Lambda_{\rm IR}$ (see Fig. 4.4a). Fig. 4.7a shows the composite signature, where the divergence of the Yukawa and scalar couplings at $\Lambda_{\rm UV}$ is expected, and implies a possible composite interpretation of the theory. Fig. 4.7b shows that the ratios $\alpha_v/\alpha_y$ and $\alpha_u/\alpha_y$ are well-behaved in the entire region and run for different initial conditions to a unique fixed value at $\Lambda_{\rm UV}$, implying the possible composite theory to be of NJL-type.

Weinberg instabilities concerning the case $m_H^2 = 0$ see [55]). The compositeness conditions tell us that the mass parameter must also diverge at the composite scale. At perturbative values, however, it must be ensured that $m_H(\mu) < \mu$ for every $\mu > \mu_0$, since otherwise the scalar fields would decouple at a scale $\mu^*$, where $m_H(\mu^*) = \mu^*$. In the perturbative regime, however, this can be easily achieved by choosing $m_H(\mu_0) < \mu_0$, since the growth in $m_H$ is logarithmic in $\mu/\mu_0$, and thus never exceeds $\mu$. If we instead ask for the stronger constraint that the decoupling scale should be the strong IR scale of the previous sections, and not the $m_H$ scale, we need to impose the following constraint:

$$m_H^2(\mu_0) < \Lambda_{IR}^2 \left(\frac{\mu_0}{\Lambda_{IR}}\right)^{\gamma_0} , \tag{4.47}$$

where $\gamma_0$ is the one-loop coefficient of $\beta_{m_H^2}$ evaluated at $\mu_0$, i.e.

$$\gamma_0 = 4[\alpha_y(\mu_0) + \alpha_v(\mu_0) + 2\alpha_u(\mu_0)] . \tag{4.48}$$

Taking the IR scale to be the strong IR scale of the previous section, we get:

$$m_H^2(\mu_0) < \mu_0^2 \exp\left(-\frac{2-\gamma_0}{\beta_0 \alpha_g(\mu_0)}\right) . \tag{4.49}$$

This parameter choice ensures that the scale hierarchies computed in the previous section remain valid, when taking the scalar sector into account. One can imagine other possibilities that can lead to the generation of new intermediate scales

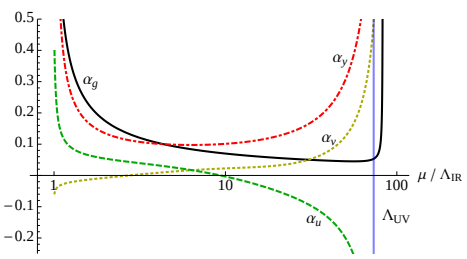


(a) NNLO running of the couplings

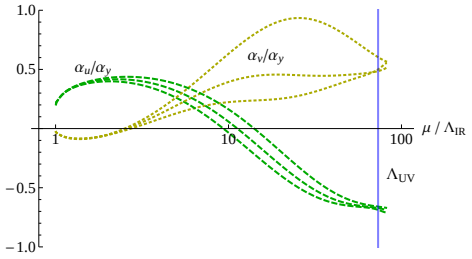


(b) NNLO running of coupling ratios

Figure 4.8: The evolution of the system of gauge, Yukawa, and quartic couplings for same values of parameters as in Fig 4.7. The running of the couplings is shown in (a), while the evolution of some ratios of the couplings are shown in (b). The conclusions are equivalent to that in Fig 4.7, however, he scale of IR divergence is now closer to the point where the couplings are initially defined, while the UV divergence is delayed by approximately the same amount. In addition, we also here see that the ratios between the quartic couplings and the Yukawa couplings stay well-defined, even when the couplings start to diverge, in accordance with the expected composite-like behavior of four-fermion interactions.

with interesting phenomenological applications that we, however, do not consider here. We illustrate the requirement Eq. (4.49) in Fig. 4.9 for the benchmark parameters mentioned above while varying $x$.

Finally we must ensure stability of the potential. The scalar fields are well-defined in the regime $\Lambda_{IR} < H < \Lambda_{UV}$. The scalar potential must for these values be positive to ensure the global minimum of the origin in field space. As shown in the appendix (cf. Eq. (.90)), in the large $N_F$ limit the constraint ensuring stability

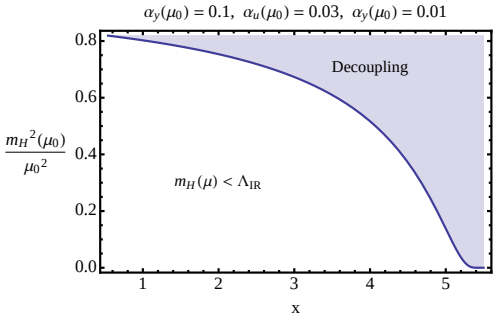


Figure 4.9: Initial mass values $m_H^2(\mu_0)$ which in the white region respect the requirement Eq. (4.49), ensuring that the scalars do not decouple above the scale $\Lambda_{IR}$.

of the potential reduces to

$$m_H^2 > 0\,. \tag{4.50}$$

Thus, if all the previous compositeness constraints are satisfied, the potential will automatically stay positive, in the entire domain of possible field values of $H$.

We have thus witnessed the emergence of a perturbative consistent picture of a subclass of gauge-Yukawa theories featuring Landau poles. We argued that these theories suggest a composite picture because they can me mapped directly into gNJL theories. We have furthermore shown that large scale hierarchies in these theories between the ultraviolet composite scale of the otherwise elementary scalar and the infrared scale leading to chiral symmetry breaking are a general feature. This result can be seen as the stepping stone towards realistic theories of SM fermion masses not at odds with flavour changing neutral currents constraints.

Since gauge-Yukawa theories can be equivalent to fermionic theories with composite scalars induced by a four-fermion interaction, it is intriguing to consider whether the Higgs in the standard model might be such a composite particle, which alterations should be made to the standard model and in turn which consequences this will have one the RG evolution of the parameters of the standard model.

# CHAPTER 5

# A NEUTRINO HIGGS CONDENSATE

The idea that the Higgs particle might be a composite particle in the spirit of the four-fermion interactions discussed in the previous chapter is not a new one. Even before the top quark was discovered, the non-discovery hinted towards a larger Yukawa coupling for the top quark than for the known quarks, maybe even large enough to fulfill the compositeness conditions mentioned above.

Many years ago it was thus proposed that the top quark Higgs-Yukawa (HY) coupling, $y_t$, might be large and governed by a quasi-infrared-fixed point behavior of the renormalization group [71,72]. This implied, using the minimal ingredients of the Standard Model, a top quark mass of order $220-240$ GeV for the case of a Landau pole in $y_t$ at a scale, $\Lambda$, of order the GUT to Planck scale. In light of the observed 173 GeV top quark mass, the fixed point prediction is seen to be within 25% of experiment. This suggests that small corrections from new physics might bring the prediction into a more precise concordance with experiment.

One of the main interpretations of the quasi-infrared fixed point was the compositeness of the Higgs boson. In its simplest form, the Higgs boson was considered to be a bound state containing a top and anti-top quark [13,73–77]. This was amenable to a treatment in a large-$N_c$ Nambu–Jona-Lasinio model [48], defined by a four-fermion interaction at a scale $\Lambda$, with a a large coupling constant, and a strong attractive $0^+$ channel. The theory requires drastic fine-tuning of quadratic loop contributions, which is equivalent to a fine-tuning of the scale-invariant NJL coupling constant . By tuning the NJL coupling close to criticality, the Higgs boson mass becomes small, creating an infrared hierarchy between the compositeness scale, $\Lambda$, and the electroweak scale embodied in $m_h$. Tuning the coupling slightly supercritical yields a vacuum instability and the Higgs boson acquires its vacuum expectation value (VEV).

Once the infrared hierarchy has been tuned, the remaining structure of the theory is controlled by renormalization group running of couplings [13]. The RG treatment indicates that a $\bar{t}t$ composite Higgs boson requires (i) a Landau pole at scale $\Lambda$ in the running top HY coupling constant, $y_t(\mu)$, (ii) the Higgs-quartic coupling $\lambda_H$ must also have a Landau pole, and (iii) compositeness conditions must be met, such as $\lambda_H(\mu)/y_t^4(\mu) \to 0$ and $\lambda_H(\mu)/y_t^2(\mu) \to$(constant) as $\mu \to \Lambda$,

[13]. This predicts a Higgs boson mass of order ~ 250 GeV with a heavy top quark of order ~ 220 GeV, predictions that come within a factor of 2 of reality.

While the $\bar{t}t$ minimal composite Higgs model is ruled out, it remains of interest to ask, "can we rescue an NJL–RG composite Higgs boson scenario with new physics?" and if so, "what are the minimal requirements of new physics needed to maintain a composite Higgs boson scenario?" In this chapter we address this issue and revisit a composite Higgs boson model based upon an attractive idea of S. P Martin, [78] (this has also been considered in a supersymmetry context by Leontaris, Lola and Ross [79]). Martin pointed out that the top quark HY is sensitive to right-handed neutrinos, $\nu_R^i$, that become active in loops above the large Majorana mass scale, $M$. The right-handed neutrinos are assumed to have HY couplings, $y_\nu^i \geq \mathcal{O}(1)$, and also have a Majorana mass of order $M \sim 10^{13}$, thus leading to the neutrino seesaw model at low energies [80,81]. Turning on the neutrino loops will generally pull a large $y_t(m_t)$ to a Landau pole at a scale of order $\Lambda \sim 10^{15} - 10^{19}$ GeV, and the large top quark mass becomes intertwined with neutrino physics above $M$. The strong dynamics that forms the boundstate Higgs boson for us is the dominant large coupling, $y_\nu^i$.

## 5.1 NJL Model

The effective UV model we have in mind is a variation on the Nambu–Jona-Lasinio model [48] and top condensation models [13, 73, 74]. We adapt this to a neutrino condensate with the four-fermion interaction Lagrangian:

$$\mathscr{L}' = \frac{g^2}{\Lambda^2}(\bar{L}_{Li}\nu_R^i)(\bar{\nu}_{Rj}L_L^j) + \frac{h^2}{\Lambda^2}(\bar{L}_{Li}\nu_R^i)(\bar{t}_{Ra}T_L^a) + h.c. \tag{5.1}$$

where $L_L^i = (\nu^i, \ell^i)_L$ ($\nu_{Ri}$) are left-handed lepton doublets (right-handed neutrino singlets), and $T_L$ ($t_R$) is the top quark doublet (singlet); $(i, j, ..)$ are generation indices running to $N_f = 3$ and $(a, b, ..)$ are color indices running to $N_c = 3$. The dominant large coupling constant in our scheme is $g$ and $h < g/N_f$. We will have additional smaller couplings involving the other quarks associated with light fermion mass generation and flavor physics, as well as charge conjugated terms like $(\bar{L}_{Li}\nu_R^i)g^{jk}(\bar{\nu}_{Rj}L_{Lk})^C$. These generate the charged lepton and quark masses and mixing angles, which we presently ignore.

Like in the previous chapter, we follow [13] and factorize the NJL interactions to write:

$$\mathscr{L}'_\Lambda = g\bar{L}_{iL}H\nu_R^i + g'\bar{T}_{aL}Ht_R^a - \Lambda^2 H^\dagger H \tag{5.2}$$

Here we define $g' = h^2/g$. Here we have introduced an auxillary field $H$ that reproduces eq.(5.1) by $H$'s equation of motion. This is the Lagrangian at the scale $\Lambda$, where the auxilliary field $H$ will become the dynamical Higgs boson boundstate at lower energies. We have ignored terms of order $g'^2$ which are generated when $H$ is integrated out to recover eq.(5.1).

We now use the RG to run the Lagrangian down to the Majorana mass scale, $M$, of the right-handed neutrinos, using only fermion loops. The result is formally:

$$\begin{aligned}\mathscr{L}'_M &= Z_H|DH|^2 - \widetilde{M}^2 H^\dagger H + \frac{\widetilde{\lambda}_H}{2}(H^\dagger H)^2 \\ &\quad + [g\bar{L}_{iL}H\nu^i_R + g'\bar{T}_{aL}Ht^a_R + \bar{\nu}^C_{Ri}M_{ij}\nu^j_R + \text{h.c.}]\end{aligned} \tag{5.3}$$

where the Majorana mass matrix, $M_{ij}$, is now incorporated by hand. The Higgs boson has acquired a logarithmic kinetic term and a quartic interaction due to the fermion loops, and the Higgs mass has run quadratically:

$$\begin{aligned}Z_H &= (4\pi)^{-2}(g^2N_f + g'^2N_c)\ln(\Lambda^2/M^2) \\ \widetilde{M}^2 &= \Lambda^2 - (4\pi)^{-2}(2g^2N_f + 2g'^2N_c)(\Lambda^2 - M^2) \\ \widetilde{\lambda}_H &= (4\pi)^{-2}(2g^4N_f + 2g'^4N_c)\ln(\Lambda^2/M^2)\end{aligned} \tag{5.4}$$

The quantities appearing in eq.(5.3) are, of course, unrenormalized. The renormalized couplings at the present level of approximation are:

$$y_\nu = \frac{g}{\sqrt{Z_H}} \qquad y_t = \frac{g'}{\sqrt{Z_H}} \qquad \lambda_H = \frac{\widetilde{\lambda}_H}{Z_H^2} \tag{5.5}$$

and we see that in the large $(N_f, N_c)$ limit the ratio $y_\nu^2/y_t^2$ is a constant.

For simplicity, we take the Majorana mass matrix to be diagonal, $M = \text{diag}\,(M_1, M_2, M_3)$. In the large $M/v_{weak}$ limit, where $v_{weak} \sim 175$ GeV, the masses of the three light neutrino states are given by the seesaw mechanism:

$$m^i_\nu = \frac{y_\nu^2 v^2_{weak}}{M_i}, \tag{5.6}$$

Assuming that $y_\nu$ is $\sim \mathcal{O}(1)$, and $\sim eV$ masses for the light neutrinos, we expect $M_i \sim 10^{13}$ GeV. Thus, in the RG evolution of the system, loops containing right-handed neutrinos occur only above the scales $M_i$. As an approximation, take the threshold of the $\nu^i_R$ in loops to be at a common Majorana mass scale $M$.

Note that the renormalized $\lambda_H = \widetilde{\lambda}_H/Z_H^2$ has the limits $\lambda_H/y_\nu^4 \to 0$ and $\lambda_H/y_\nu^2 \to$ (constant) as $\mu \to \Lambda$. The extent to which the top quark participates in the binding of the Higgs boson relative to the neutrinos is determined by $g'^2N_c/g^2N_f$ which we assume is of order $1/N_f$, and thus the dominant coupling at the UV scale is $g^2$. While we could keep the order $g'^2$ terms in the factorization of eq.(5.3), this would make a weakly boundstate doublet, $H'$ composed mainly of $\bar{t}t$, but since $g'^2$ is subcritical this state would remain a heavy dormant doublet with $m^2 \sim \Lambda^2$.

Below the Majorana mass scale $M$ the neutrinos decouple and the only significant running in the fermion loop approximation is the top quark. The electroweak scale is tuned by the choice of critical couplings. The quadratic running to a zero mass Higgs boson, $\widetilde{M}^2 = 0$ defines the critical coupling:

$$g^2N_f + g'^2N_c = 8\pi^2\left(1 + \frac{M^2}{\Lambda^2}\right) \tag{5.7}$$

The criticality, we assume, is due principally to the large value of $g^2$ and is only slightly modified by the top quark. We then choose $g^2$ slightly supercritical to produce the phenomenological tachyonic Higgs potential, $\widetilde{M}^2 = -M_H^2 Z_H(\Lambda/M_H)$.

The NJL model is schematic, and must itself be an approximation to some new dynamics in the UV. This structure suggests a new gauge interaction which leads to eq.(5.1) upon Fierz rearrangement, in analogy to topcolor models [82], as:

$$\frac{g^2}{\Lambda^2}\bar{L}_{Li}\nu_R^i\bar{\nu}_{Rj}L_L^j = -\frac{g^2}{\Lambda^2}\bar{L}_L\frac{\lambda^A}{2}\gamma^\mu L_L\bar{\nu}_R\frac{\lambda^A}{2}\gamma_\mu\nu_R + \ldots, \tag{5.8}$$

where the Gell-Mann matrices $\lambda^A$ now act on the flavor indices. The $g'$ term then requires some extension of the theory. A model such as this assigns an $SU(3)$ gauge group to lepton family number, and therefore gauge charges to the $\nu_{Ri}$, *i.e.*, the $\nu_{Ri}$ are no longer sterile. This would imply that the Majorana mass matrix must be generated by a VEV associated, *e.g.*, with additional $SU(3)$ scalar fields. With $\nu_{Ri}$ in the triplet representation, this requires $\{\bar{3}\}$ and/or $\{6\}$ scalar condensates, and would dictate the neutrino mass and mixing angle structure.

## 5.2 YUKAWA SECTOR

The above discussion is the Wilsonian renormalization group approach. To improve the calculation, we turn to the full RG equations which are used below the scale $\Lambda$, together with the matching conditions dictated by the fermion bubble approximation [13]. The full RG equations (for $N_f = 3$ these are a slight modification of ref. [78]) take the form:

$$\begin{aligned}
(4\pi)^2\frac{\beta_{y_t}}{y_t} &= \frac{9}{2}y_t^2 - 8g_3^2 + 3\theta_M(\mu - M)y_\nu^2 - \frac{9}{4}g_2^2 - \frac{17}{12}g_1^2, \\
(4\pi)^2\frac{\beta_{y_\nu}}{y_\nu} &= \theta_M(\mu - M)\left(\frac{9}{2}y_\nu^2 + 3y_t^2 - \frac{9}{4}g_2^2 - \frac{3}{4}g_1^2\right), \\
(4\pi)^2\frac{\beta_{g_1}}{g_1} &= \frac{41}{6}g_1^2, \quad (4\pi)^2\frac{\beta_{g_2}}{g_2} = -\frac{19}{6}g_2^2 \\
(4\pi)^2\frac{\beta_{g_3}}{g_3} &= -7g_3^2
\end{aligned} \tag{5.9}$$

where $g_1, g_2$, and $g_3$ are the gauge couplings of the $U(1)_Y$, $SU(2)_L$, and $SU(3)_c$ symmetries respectively, $y_t$ is the top HY coupling, and $y_\nu$ the HY coupling of the lepton doublets to right-handed neutrinos. We have introduced a step-function, $\theta_M = \theta(\mu - M)$, where $\theta(x) = 1$; $x \geq 0$ and $\theta(x) = 0$; $x < 0$. The step-function models the threshold of turning on the right-handed neutrino corrections at the scale of the Majorana mass matrix.

In Fig. 5.1 we demonstrate the running of the HY coupling for the top quark and the neutrino as described. We use the initial conditions for the gauge couplings $g_1(m_Z) = 0.36$, $g_2(m_Z) = 0.65$, $g_3(m_Z) = 1.16$, for the HY couplings:

$y_t(m_t) = 0.99$, and $y_\nu(M) = 1$, and for the masses $m_Z = 91.2$ GeV, $m_t = 173.2$ GeV, and $M = 10^{13}$ GeV.

The evolution in Fig. 5.1 clearly indicates the existence of a Landau pole for the HY couplings at a scale $\Lambda \sim 10^{20}$ GeV, in accord with what one would expect if the Higgs is a fermion pair condensate.

The Landau pole of the neutrino HY coupling is seen to pull the top HY towards a Landau pole at $\Lambda$. The neutrino HY coupling is always significantly larger than the top coupling for the scales where the perturbative result is valid. For the displayed example we find the ratio $y_\nu / y_t \geq 3$ for the region very close to the Landau pole.

To verify the consistency of this behavior of the top quark, consider the region below, but near, $\Lambda$. Here the RG equations for top and neutrino HY couplings can be approximated in the large $(N_f, N_c)$ limit by:

$$(4\pi)^2 \frac{d \ln y_t}{d \ln \mu} \approx (4\pi)^2 \frac{d \ln y_\nu}{d \ln \mu} \approx N_f y_\nu^2 + N_c y_t^2, \tag{5.10}$$

hence:

$$(4\pi)^2 \frac{d \ln (y_t / y_\nu)}{d \ln \mu} = 0 \tag{5.11}$$

This implies that $y_\nu(\mu)/y_t(\mu) \to$ (constant), as we approach the scale $\Lambda$. The ratio $y_t / y_\nu \sim g'/g$, so the role of the top quark role is only that of a spectator.

In this simplified setup, inserting an experimental neutrino mass in (5.6) yields $y_\nu(M)$ as a function of $M$. For a chosen $M$, this value may be used as an initial condition in the RG equation for $y_\nu$, and the scale $\Lambda$ may be read off from the solution to the RG equations. A simple analytic estimate is given by setting to zero

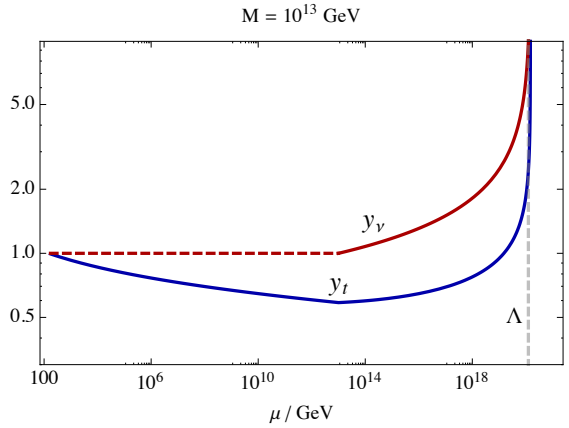


Figure 5.1: The RG evolutions of the top (solid) and neutrino (dashed) HY couplings with contributions from right-handed neutrinos for renormalization scales above the neutrino Majorana mass; $\mu > M = 10^{13}$ GeV.

all couplings except $y_\nu$, in which case one finds for the one loop solution

$$\Lambda = M \exp\left[\frac{(4\pi v_{weak})^2}{9\, m_\nu^{exp} M}\right]. \tag{5.12}$$

Here $v$ is again the Higgs VEV and $m_\nu^{exp}$ is the experimentally measured neutrino mass. The estimate (5.12) is in good agreement with the full numerical solution due to the fact that the neutrino coupling itself is what drives the divergence at $\Lambda$. The relation (5.12) also gives a lower bound on the possible compositeness scale $\Lambda_{min}$ for any neutrino mass given by

$$\Lambda_{min} \simeq 1.5 \times \left(\frac{m_\nu^{exp}}{\text{eV}}\right)^{-1} \times 10^{15}\ \text{GeV}. \tag{5.13}$$

We perform the numerical analysis as before using the RG equations above, and obtain the scale associated with the Landau pole for different values of $M$ given a specific mass of the light neutrino states in the eV range. In Fig. 5.2 we show numerical results concerning the relation between the Majorana mass and the $\Lambda$ scale for different values of the neutrino mass. The perturbative nature of our analysis does not allow us to extrapolate to infinite coupling values, so we instead take the naive estimate of the $\Lambda$ scale to be defined by $y_\nu(\Lambda) = 30$. We stress that this analysis is meant to provide a demonstration of principles rather than high precision results.

Two distinct behaviors are exhibited in Fig. 5.2: For smaller values of the Majorana mass, the scale $\Lambda$ is very sensitive to the choice of neutrino and Majorana mass. This is due to the fact that $y_\nu(m_t)$ is quite small for these values, and more RG time is needed to run to the Landau pole. For larger values of the masses, $y_\nu(m_t)$ also grows large in accordance with (5.6) and the Landau pole is shifted

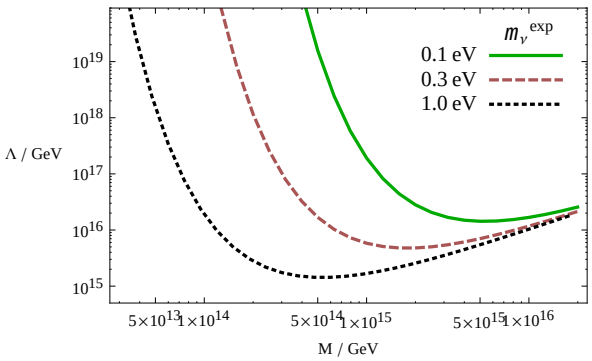


Figure 5.2: Numerical results displaying the relation between the Majorana mass and the scale associated with the Landau pole for the neutrino HY coupling for different values of the neutrino mass.

closer to the scale where the neutrino coupling becomes active in the RG equations.

## 5.3 SCALAR SECTOR

In the minimal version of a single composite Higgs boson, the physical Higgs mass prediction is larger than the observed ~ 125 GeV. The Higgs mass is controlled by the electroweak VEV, $v_{weak}$, and the quartic coupling. The Higgs compositeness conditions predict a Landau pole for the quartic scalar coupling at the compositeness scale $\Lambda$ [13]. However, the quartic coupling constant in the standard model is to be too low to match these conditions, and indeed, appears to decrease with scale potentially, becoming negative at ~ $10^{12}$ GeV as seen in Chapter 2 .

To achieve compositeness of the Higgs boson, we employ a simple modification by which the observed Higgs quartic coupling, $\lambda$, becomes only a low energy effective coupling, while the true quartic coupling, $\lambda_H$, is larger and can have the requisite Landau pole. The actual quartic coupling needs only be about 2× the observed $\lambda$ to achieve this, but requires additional physics at the ~ 1 TeV scale.

In the spirit of [83], we extend the scalar sector to include a complex singlet, $S$ and the new Higgs potential becomes:

$$\begin{aligned} V = &\frac{\lambda_H}{2}\left(H^\dagger H - v^2\right)^2 + \frac{\lambda_S}{2}\left(S^\dagger S - u^2\right)^2 \\ &+ \lambda_{HS}\left(H^\dagger H - v^2\right)\left(S^\dagger S - u^2\right), \end{aligned} \tag{5.14}$$

where we have assigned the vacuum expectation values

$$\langle H^\dagger H\rangle = v^2, \quad \langle S^\dagger S\rangle = u^2. \tag{5.15}$$

The VEVs (5.15) are the global minima of the potential when $\lambda_H, \lambda_S > 0$ and $\lambda_H\lambda_S > \lambda_{HS}^2$.

Expanding about the minimum of eq.(5.15), one finds the mass matrix for the massive scalars to be

$$\frac{\partial^2 V}{\partial\phi_i\phi_j} = 2\begin{pmatrix} \lambda_H v^2 & \lambda_{HS} vu \\ \lambda_{HS} vu & \lambda_S u^2 \end{pmatrix},$$

where $\phi_i$ refers to the direction of the VEV in $H$ and $S$. The eigenvalues are

$$m_\pm^2 = \lambda_H v^2 + \lambda_S u^2 \pm \kappa,$$

where $\kappa = \sqrt{(\lambda_H v^2 - \lambda_S u^2)^2 + 4\lambda_{HS} v^2 u^2}$. In the limit where $\lambda_H v^2 \ll \lambda_S u^2$, the lightest state mostly resides within $H$, and the mass can be approximated by

$$m_H^2 = m_-^2 = 2\left(\lambda_H - \frac{\lambda_{HS}^2}{\lambda_S}\right)v^2 + \mathcal{O}\left(\frac{\lambda_H v^2}{\lambda_S u^2}\right)v^2. \tag{5.16}$$

The effective quartic coupling, measured from the Higgs mass, is now:

$$\lambda = \lambda_H - \frac{\lambda_{HS}^2}{\lambda_S}, \tag{5.17}$$

which is intrinsically smaller than the coupling $\lambda_H$. Thus, the composite picture with a suitable Landau pole in $\lambda_H$ is now possible.

### 5.3.1 Singlet scalar extension

We now analyze the RG evolution of the full theory with an eye to the Landau pole in $\Lambda_H$. Assuming $S$ is an electroweak $SU(2)$ singlet, and $U(1)_Y$ sterile, the RG equations for the scalar sector are given by

$$\begin{aligned}
\beta_{\lambda_H} &= (12y_t^2 + 12\theta_M y_\nu - 3g_1^2 - 9g_2^2)\lambda_H - 12(y_t^4 + \theta_M y_\nu^4) \\
&\quad + \frac{3}{4}g_1^4 + \frac{3}{2}g_1^2 g_2^2 + \frac{9}{4}g_2^2 + 12\lambda_H^2 + 2\theta_u \lambda_{HS}^2, && (5.18)\\
\beta_{\lambda_{HS}} &= \left(6y_t^2 + 12\theta_M y_\nu - \frac{3}{2}g_1^2 - \frac{9}{2}g_2^2 + 6\lambda_H\right)\lambda_{HS} && (5.19)\\
&\quad + 4\theta_u(\lambda_S + \lambda_{HS})\lambda_{HS}, \\
\beta_{\lambda_S} &= 4\lambda_{HS}^2 + 10\theta_u \lambda_S^2, && (5.20)
\end{aligned}$$

where we have included the Heaviside function $\theta_u = \theta(\mu - u)$, to adjust for the fact that loops involving the $S$ state are not taken into account for scales below the VEV $\langle S\rangle = u$ which generates the mass for the $S$ state.

To accommodate the composite scenario, as first described in [13], both the quartic coupling and the HY coupling for the condensating fermions must diverge at a scale $\Lambda$. Furthermore, the nature with which the scalar becomes propagating at lower energy scales, sets the requirement

$$\lim_{\mu\to\Lambda} \lambda_H / y_\nu^4 = 0, \tag{5.21}$$

and we expect the common divergence to yield

$$\lim_{\mu\to\Lambda} \lambda_H / y_\nu^2 = \mathcal{O}(1). \tag{5.22}$$

In Fig. 5.3 we demonstrate the evolution of the quartic coupling for a specific choice of initial conditions. We choose a mass for the active neutrino $m_\nu^{exp} = 1$ eV, which yields a divergence of $y_\nu$ around $\Lambda = 10^{18}$ GeV, under the assumption that $M = 5\times 10^{13}$ GeV. At the scale where $y_\nu(\mu) = 10$, we then define the initial conditions for the quartic couplings $\lambda_H(\mu) = 98$, in accordance with (5.22), and the somewhat arbitrary choices $\lambda_{HS}(\mu) = 23$, $\lambda_S(\mu) = 1.7$. The assumed value for $u = 1$ TeV. The IR phenomenology features a large value for the Higgs quartic coupling $\lambda_H \sim 0.7$, while the effective coupling is considerably smaller $\lambda \sim 0.28$ corresponding to a Higgs mass $m_H \sim 130$ GeV.

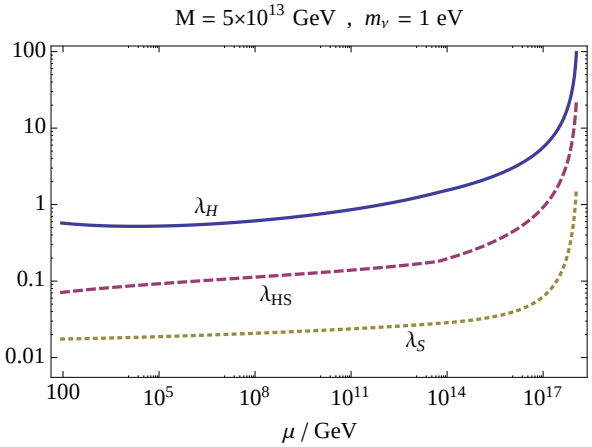


Figure 5.3: The RG evolution for the quartic couplings for a specific choice of initial conditions at the UV scale. The IR phenomenology features a large quartic for the Higgs, while the effective coupling leads to a light Higgs mass $m_H \sim 130$ GeV.

The RG system involves some degree of tuning to ensure the proper behavior of the two new quartic couplings. Specifically, we must tune $\lambda_S$ to be small, to ensure a large correction in $\lambda$ as seen in (5.16) while $\lambda_{HS}$ is also tuned, such that $\lambda_H > \lambda_{HS} > \lambda_S$ is satisfied for all RG scales, in order to ensure a valid value of $\lambda$ at small scales.

This model should merely serve as a proof of concept, displaying the possibility that the UV behavior of the Higgs quartic coupling can include a Landau pole. In this setup we have looked at the simplest possible scalar extension of the standard model with the standard Higgs mechanism in play for both scalars. The issues of tuned scalar couplings may then be alleviated if a different mechanism for symmetry breaking or a more complex scalar sector is considered. For a large class of more general gauge-Yukawa theories, a composite limit due to four fermion interactions at high energies is easily obtainable, as shown in [3], while we will focus on the simplest alternative solutions below.

## 5.4 ALTERNATIVE SCALAR EXTENSIONS

As we have introduced a tuning between the dimensionless coupling constants of the scalar sector in addition to the usual tuning for the Higgs mass parameter, it would be beneficial to find a mechanism to stabilize the IR phenomenology towards changes in the initial UV conditions. We expect that this might be found by connecting the symmetry breaking mechanisms for the scalar sector.

In the previous example, the role of the “portal" coupling $\lambda_{HS}$ was to supply a correction to the quartic Higgs coupling in the effective coupling by connect-

ing the two scalar sectors, while the symmetry breaking mechanism is that of the standard Higgs boson for both the $H$ and $S$ scalars.

### 5.4.1 Negative portal coupling

We can expand the role of the portal coupling by letting the portal interaction communicate symmetry breaking in the dark $S$ sector to the standard model. Setting $\lambda_{HS} < 0$ and assuming $\langle S \rangle \neq 0$ can trigger spontaneous symmetry breaking in the standard model, even if the mass term for the Higgs $m_H^2 \geq 0$, since the portal interaction will add a negative squared mass contribution for $H$. If the portal coupling is very small, then there can be a large hierarchy between the VEVs of $S$ and $H$, and the validity of eq.(5.16) is guaranteed.

The change from a positive portal coupling to a negative one can thus change the nature of the symmetry breaking for the Higgs particle. It allows for other values of the Higgs mass parameter, and specifically one can choose $m_H^2 = 0$ and still obtain a second order phase transition due to the portal interaction. The actual analysis of this alternative model is however almost identical to the original, since the stability constraint and mass prediction only involve $\lambda_{HS}^2$. The measured Higgs mass is still obtainable together with a Landau pole for $\lambda_H$, albeit tuning between the scalar couplings is needed.

### 5.4.2 Communicated Coleman-Weinberg symmetry breaking

Common to the scalar sectors discussed so far has been the feature that a mass scale has been inserted by hand into the potential, either for both scalars, or for one of them. This enables the generation of a vast interval of possible scalar masses, but intrinsically means that these are very sensitive to the input parameters. An alternative way to generate mass scales is the dynamical one, where the mass scales arise directly from the RG evolution. We will show in the following that Landau poles in the quartic couplings, in accordance with a composite picture, may also accommodate spontaneous symmetry breaking due to the Coleman-Weinberg(CW) mechanism as demonstrated for elementary scalars in [84].

It is central to the success of this model, that we now consider a dark[1] scalar doublet $S$, gauged under a new $SU(2)_X$ group[2]. Since we want all mass scales to be generated dynamically, the potential is given as

$$V = \frac{\lambda_H}{2}(H^\dagger H)^2 + \lambda_{HS}(H^\dagger H)(S^\dagger S) + \frac{\lambda_S}{2}(S^\dagger S)^2, \tag{5.23}$$

where we will investigate the cases where $\lambda_{HS} < 0$. Just as before, the requirement for stability of the potential is

$$\lambda_H > 0, \quad \lambda_S > 0, \quad \lambda_H \lambda_S > \lambda_{HS}^2. \tag{5.24}$$

[1] Similar models with a portal coupling to another scalar sector are often used to probe dark matter phenomenology.

[2] The critical property of the gauge group is asymptotic freedom, so any other gauge group with this property could have been used.

Spontaneous symmetry breaking then occurs dynamically in this setup via the Coleman-Weinberg mechanism when the RG evolution brings the system of coupling constants into violation of the stability conditions (5.24).

The driving force behind the symmetry breaking in this setup is the new gauge coupling $g_x$, related to the $SU(2)_X$ gauge symmetry. As this coupling becomes large at some scale due to asymptotic freedom, the quartic coupling $\lambda_S$ will be driven negative in the IR, due to the form of its beta function which is positive for any nonzero value of the couplings:

$$\beta_{\lambda_S} = 4\lambda_{HS}^2 + 12\lambda_S^2 + \frac{9}{4}g_x^4 - 9g_x^2\lambda_S. \tag{5.25}$$

Denoting by $s^*$ the scale at which $\lambda_S = 0$, and performing the approximation close to this scale that $\lambda_S \simeq \beta_{\lambda_S} \ln\left(\frac{s}{s^*}\right)$, the estimated value for the VEV of $S$ coming from the associated Coleman-Weinberg symmetry breaking mechanism is given by

$$\langle S \rangle = u = s^* e^{-1/4}. \tag{5.26}$$

In return, the negative portal coupling $\lambda_{HS}$ induces a VEV for $H$:

$$\langle H \rangle = v = u\sqrt{\frac{-\lambda_{HS}}{\lambda_H}}. \tag{5.27}$$

At this minimum, the mass matrix takes the form

$$v^2 \begin{pmatrix} 2\lambda_H & -2\sqrt{-\lambda_H\lambda_{HS}} \\ -2\sqrt{-\lambda_H\lambda_{HS}} & \lambda_{HS} - \beta_{\lambda_S}\frac{\lambda_H}{\lambda_{HS}} \end{pmatrix}. \tag{5.28}$$

Assuming that $v^2 \ll u^2$ which is to say $\frac{-\lambda_{HS}}{\lambda_H} \ll 1$, we may expand the eigenvalues to the leading order in $\frac{\lambda_{HS}}{\lambda_H}$ and obtain

$$m_1^2 = 2\lambda v^2, \quad m_2^2 = -\frac{\beta_{\lambda_S}\lambda_H}{\lambda_{HS}}v^2, \tag{5.29}$$

where the indices 1 and 2 relate to the state composed of mostly $H$ and $S$ respectively, and $\lambda = \lambda_H - \frac{\lambda_{HS}^2}{\beta_{\lambda_S}}$. This naturally resembles (5.16), and we see once again, how the effective quartic coupling is smaller than the true coupling for the Higgs.

So far, the setup seems to resemble the simple one given in the previous chapter. The key difference is that while a high degree of tuning was needed for the initial conditions in the simple setup to guarantee the correct hierarchy at smaller scales, this is no longer the case, since the dynamics at these scales are controlled mainly by the evolution of the new gauge coupling.

Our probes of the parameter space for this theory will follow the lines of logic from the previous section: Assuming a certain neutrino mass $m_\nu$ and Majorana mass $M$, the scale of compositeness scale $\Lambda$ is determined uniquely. We will then

impose the constraint (5.22), which fixes the quartic couplings at this scale[3]. The last remaining free parameter is the new gauge coupling $g_X$, which will be fixed at the mass of the Z boson. The only free parameters in our analysis are thus the two masses associated to the neutrino sector and the value $g_x(m_Z)$.

The RG equations for the remaining quartic coupling and the new gauge coupling is given to one loop by

$$\begin{aligned}
\beta_{\lambda_H} &= (12y_t^2 + 12\theta_M y_\nu - 3g_1^2 - 9g_2^2)\lambda_H - 12(y_t^4 + \theta_M y_\nu^4) \\
&\quad + \frac{3}{4}g_1^4 + \frac{3}{2}g_1^2 g_2^2 + \frac{9}{4}g_2^2 + 12\lambda_H^2 + 2\theta_u \lambda_{HS}^2, \qquad (5.30)\\
\beta_{\lambda_{HS}} &= \left(6y_t^2 + 6\theta_M y_\nu - \frac{3}{2}g_1^2 - \frac{9}{2}g_2^2 + 6\lambda_H\right)\lambda_{HS} \qquad (5.31)\\
&\quad + \left(6\lambda_S - \frac{9}{2}g_X^2\right)\lambda_{HS} + 4\lambda_{HS}^2, \\
\beta_{g_X} &= -\frac{43}{6}g_X^3. \qquad (5.32)
\end{aligned}$$

A numerical evaluation of the running of the couplings as described above will yield the VEVs of $H$ and $S$ as well as the masses of the respective eigenstates, through (5.26),(5.27), and (5.29), when the couplings are evaluated at the scale of symmetry breaking $s^*$.

A sample RG evolution yielding $v \simeq 175$ GeV and $m_H \simeq 125$ GeV is shown in Fig. 5.4, where the increase of the gauge coupling $g_X$ in the IR is displayed alongside the decrease of the dark quartic $\lambda_S$, which is the source of the symmetry breaking. We warn the reader that the value for $\langle S \rangle = u \simeq 227$ GeV, such that $v^2/u^2 \sim 0.6$ such that the approximation used in (5.29) may be invalid and a more complete analysis should be performed. Once again, we postpone this for other work, while aiming for a qualitative description for now.

For the RG evolution shown above all quartic values are fixed to be equal at the compositeness scale, and the tuning between is no longer needed. Instead, having settled on a specific neutrino mass, only the Majorana mass $M$ and $g_X(m_Z)$ require balancing in order to get the correct phenomenology in the Higgs sector. Keeping $g_X(m_Z)$ fixed while varying $M$ with respect to the sample calculation above, yields the Higgs VEV and mass depicted in Fig. 5.5. Interestingly, the Higgs mass seems to be stabilized around $\sim 130$ GeV for a range of different Majorana masses, while the VEV has a stronger dependence on $M$.

Varying $g_X(m_Z)$, one sees that in order to get values of $v$ and $m_H$ close to the correct values, one has to remain within the interval $g_X(m_Z) \in [5;6]$ with $M \sim 4 \times 10^{14}$ GeV for the chosen value of $m_\nu = 0.3$ eV. Thus the tuning problems within the parameters of the theory have been greatly reduced, and the interesting region of

[3] We will assume that all quartic couplings are large at this scale which would be true in a theory where all scalars are composite in the sense we have described here. This is not a necessary assumption, and it may be relaxed if one wishes to consider elementary scalar dark matter extensions.

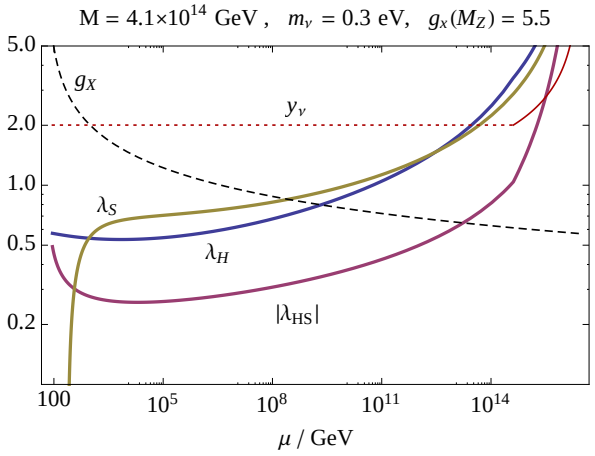


Figure 5.4: The RG evolution for the quartic couplings in the communicated CW setup. Choosing the active neutrino mass and Majorana mass, determines the compositeness scale, where the quartics are given values such that $\lambda_H = |\lambda_{HS}| = \lambda_S \approx y_\nu^2$ at this scale. The final assumption is that $g_X(m_Z) = 5.5$, which determines the IR behavior and symmetry breaking pattern. The evolution shown above yields $v \simeq 174$ GeV and $m_H \simeq 126$ GeV.

parameter space has been discovered. For the higher neutrino mass $m_\nu = 1$ eV, the relevant values of $M$ are centered at $M \sim 1.2 \times 10^{14}$ GeV, while for the lower mass $m_\nu = 0.1$ eV, realistic Higgs phenomenology requires $M \sim 1.2 \times 10^{15}$ GeV, while the value of $g_X(m_Z)$ is kept constant.

Along with the values for the Higgs mass and VEV, we obtain values for the mass of the other scalar state $m_s = m_2$ from (5.29) along with the mass for the dark matter candidate $M_X = g_X * u/2$, which are also shown in Fig. 5.5. For the choice of parameters corresponding to the values for the Higgs observables, marked with a grey line, we obtain $m_S \sim 190$ GeV and $M_X \sim 300$ GeV. The predictions for these dark matter observables are fairly independent on the choice of neutrino and Majorana mass in the setup.

The phenomenology of the model presented here is by construction virtually identical to the one of its elementary counterpart, as reviewed in [**?**]. The main effect of imposing the composite picture is that the absolute value for the portal coupling $\lambda_{HS}$ is larger in our setup.

## 5.5 PROSPECTS FOR A NEUTRINO HIGGS CONDENSATE

We have thus seen that the Higgs theory can be described by a condensate of neutrinos due to the possible large values for the neutrino Yukawa coupling. The composite theory may give the correct Higgs observables granted that a portal cou-

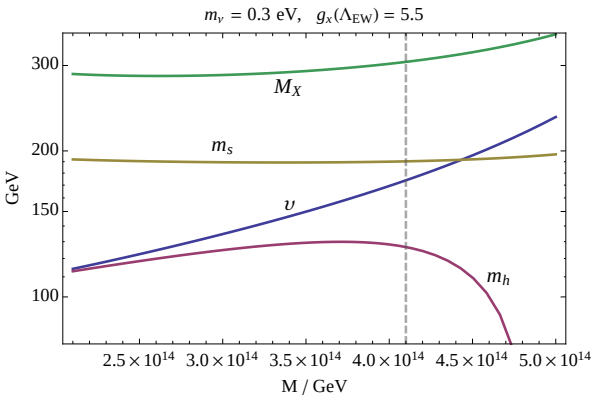


Figure 5.5: Values of the Higgs VEV ($v$) and mass ($m_h$) along with the mass of the extra scalar ($m_s$) and the dark gauge bosons ($M_X$) as the Majorana mass $M$ is varied, while the active neutrino mass $m_\nu = 0.3$ eV and $g_X(m_Z) = 5.5$. The grey dashes indicate the point where correct Higgs phenomenology is realized.

pling to a new scalar generates a smaller effective quartic coupling for the Higgs field. While large tuning is needed in the simplest setup, this may be alleviated if the symmetry breaking occurs due to the Coleman-Weinberg mechanism in the new scalar sector, and the predictions of the theory are then fairly unaffected by variance of the external parameters.

Since the structure of the neutrino sector is of the seesaw type, the model does not in this regard stand out from the bulk of neutrino theories. Tests of our setup should thus mainly be found within the Higgs and portal sectors.

# CONCLUSIONS

The renormalization group flow gives us information on the variations of different interaction strengths for gauge-Yukawa theories under a change of the relevant scale for the process. For theories with different types of couplings we derived consistency conditions relating the beta functions for the respective couplings to one another. This new structure is also present in the RG equations for the standard model, and result from the Weyl consistency conditions. These originate in the abelian nature of the Weyl anomaly, which in turn measures deviation from scale invariance. The consistency conditions relate terms occuring at different loop orders for different couplings to one another, and thus suggest an alternative perturbative counting in such theories. We have demonstrated that the effect on the question of stability of the electroweak vacuum are not large enough to change the conclusions on the matter of stability, although this may change with increased experimental precision.

We have investigated the stability of extensions of the standard model with well motivated dark matter candidates and shown that the electroweak vacuum may be stable in such theories due to extra contributions to the quartic Higgs coupling. The predictivity of these models is large due to approximate fixed points for some ratios of the couplings in the IR. It was also shown that these extensions could be consistent with a picture of asymptotic safety where the quartic couplings vanish around the Planck scale due to gravitational corrections to the beta functions for transplanckian momenta. This indicates that a large class of perturbative extensions to the standard model may posses this feature.

Alternative to the picture of fundamental scalars is one, where the scalars are sets of fermions held together by some four-fermion interaction. The correspondence between gauge-Yukawa theories and four-fermion theories has been demonstrated for a large class of QCD inspired gauge-Yukawa theories. We have demonstrated how the compositeness conditions are satisfied for the couplings of the theory and how a large ratio between the relevant scales in the theory can easily be accomplished. Finally we have determined the parameter space where such gauge-Yukawa theories are equivalent to a four-fermion theory at high energies.

As an application of the formalism derived for composite scalars above, we demonstrate how the Higgs particle could be composed of neutrinos. The neutrino Yukawa coupling stays small until contributions from heavy right-handed neutrinos modifies the running and introduces the divergence of the Yukawa cou-

pling natural to four-fermion equivalent theories. We show that even with the low Higgs mass measured at the LHC, the composite scenario is still viable if extra scalars exist. Specifically, we show that versions of popular dark matter models featuring Coleman-Weinberg symmetry breaking, are also consistent with the composite scenario, and natural values for the Higgs mass and VEV are easily obtained.

# ANALYTIC ANALYSIS OF THE COMPOSITENESS CONDITIONS FOR A GAUGE-YUKAWA THEORY AT ONE LOOP

It is possible to study the compositeness conditions in a general perturbative gauge-Yukawa theory analytically, by analyzing the gauge-Yukawa-quartic system of beta functions, at one-loop in all couplings. We will here consider the subspace of theories represented by the Lagrangian in Eqs. (4.14) and (4.15). The compositeness conditions on the couplings were given in Eq. (4.17) and read:

$$\lim_{\mu\to\Lambda_{UV}} \alpha_y^{-1} = 0\,, \qquad \lim_{\mu\to\Lambda_{UV}} \frac{\alpha_u}{\alpha_y^2} = \lim_{\mu\to\Lambda_{UV}} \frac{\alpha_v}{\alpha_y^2} = 0\,, \qquad \lim_{\mu\to\Lambda_{UV}} \frac{y^2}{m_H^2} = \frac{G}{\Lambda_{UV}^2}\,. \tag{.33}$$

We imagine a situation where the theory considered is valid perturbatively around some energy scale $\mu_0$. We can then investigate, using the one-loop running of the couplings, whether the compositeness conditions will be satisfied at some higher scale $\Lambda_{UV}$. The one-loop beta-functions in the Veneziano limit of the theory will in general take the form:

$$\beta_{\alpha_g} = \partial_t \alpha_g = -\beta_0 \alpha_g^2\,, \tag{.34}$$
$$\beta_{\alpha_y} = \partial_t \alpha_y = \alpha_y \left(c_y \alpha_y - c_g \alpha_g\right)\,, \tag{.35}$$
$$\beta_{\alpha_u} = \partial_t \alpha_u = \alpha_u \left(d_u \alpha_u + d_y \alpha_y\right) - d_{yy} \alpha_y^2\,, \tag{.36}$$
$$\beta_{\alpha_v} = \partial_t \alpha_v = \alpha_v \left(f_v \alpha_v + d_y \alpha_y + f_u \alpha_u\right) + f_{uu} \alpha_u^2\,, \tag{.37}$$

where $t = \ln \mu/\mu_0$ and all coefficients are positive definite in any gauge-theory, except for $\beta_0$. In infrared-free gauge theories $\beta_0 < 0$. Here we do not consider such theories, as we require the gauge sector to be perturbatively well-defined at the composite scale, and thus require $\beta_0 > 0$. Notice that the coefficient $d_y$ is the same in $\beta_{\alpha_u}$ and $\beta_{\alpha_v}$ for any gauge theory. Also notice that $\beta_{\alpha_u}$ is decoupled from $\alpha_v$, which holds to all orders in the Veneziano limit. The one-loop truncation of RG equations allows us to first solve the gauge sector, then the Yukawa sector, and finally the quartic sector sequentially.

## THE GAUGE SECTOR AND THE STRONG SCALE

The solution of $\alpha_g(t)$ is well known and reads:

$$\frac{1}{\alpha_g(t)} = \frac{1}{\alpha_g(0)} + \beta_0 t\,. \tag{.38}$$

It has a strong confinement scale at the point, where the left hand side vanishes, which reads:

$$t_s = \ln\frac{\Lambda_{IR}}{\mu_0} = -\frac{1}{\beta_0\alpha_g(0)}\,, \tag{.39}$$

where we defined $t_s$.

## THE YUKAWA SECTOR AND THE COMPOSITE SCALE

The beta function $\beta_{\alpha_g}$ can be used to reduce $\beta_{\alpha_y}$ to an ordinary differential equation in terms of $R_{gy} = \alpha_g/\alpha_y$, which for $c_g \neq \beta_0$ reads:

$$\frac{dR_{gy}}{d\ln\alpha_g} = a(R_{gy} - b)\,, \tag{.40}$$

where

$$a = 1 - \frac{c_g}{\beta_0}\,, \quad b = \frac{c_y}{c_g - \beta_0}\,. \tag{.41}$$

It follows that $a$ and $b$ have opposite signs and furthermore $a < 1$. The case $c_g = \beta_0$, where $b$ is not well-defined, will be considered in a moment.

It is easy to check that Eq. (.40) has the solution:

$$R_{gy}(t) = \big(R_{gy}(0) - b\big)\left(\frac{\alpha_g(t)}{\alpha_g(0)}\right)^a + b\,. \tag{.42}$$

The compositeness condition for $R_{gy}$ reads:

$$R_{gy}(t_L) = 0\,, \quad \text{for} \quad 0 < t_L = \ln\frac{\Lambda_{UV}}{\mu_0} < \infty\,, \tag{.43}$$

where we defined $t_L$. Due to asymptotic freedom the last condition on $t_L$ can also be stated in terms of $\alpha_g$:

$$R_{gy}(t_L) = 0\,, \quad \text{for} \quad 1 > \frac{\alpha_g(t_L)}{\alpha_g(0)} > 0\,. \tag{.44}$$

It can then be seen that if $a > 0$ (i.e. $c_g < \beta_0$), and thus $b < 0$, the compositeness condition will always be satisfied.

On the other hand, if $a<0$ (i.e. $c_g>\beta_0$) we have to impose an extra condition, since the composite scale in this case can be written as:

$$\left(\frac{\alpha_g(t_L)}{\alpha_g(0)}\right)^{|a|}=1-\frac{R_{gy}(0)}{b}\,. \tag{.45}$$

The lower bound $t_L>0$ (i.e. $\frac{\alpha_g(t_L)}{\alpha_g(0)}<1$) is always satisfied, since $\frac{R_{gy}(0)}{b}>0$. But the upper bound $t_L<\infty$ implies that $\frac{\alpha_g(t_L)}{\alpha_g(0)}>0$ and leads to a constraint on the parameter space:

$$R_{gy}(0)<b\,,\quad (\text{for } a<0)\,. \tag{.46}$$

Using the expression for $\alpha_g(t)$ in Eq. (.38) we can derive a general expression for the composite scale $\Lambda_{UV}$, for any $a$ and $b$ satisfying the compositeness conditions:

$$t_L=\ln\frac{\Lambda_{UV}}{\mu_0}=\frac{1}{\beta_0\alpha_g(0)}\left[\left(1-\frac{R_{gy}(0)}{b}\right)^{\frac{1}{a}}-1\right]\,. \tag{.47}$$

Finally, for the special case $a=0$, i.e. $c_g=\beta_0$, the RG equation for $R_{gy}$ reads:

$$\left.\frac{dR_{gy}}{d\ln\alpha_g}\right|_{c_g=\beta_0}=\frac{c_y}{\beta_0}\,. \tag{.48}$$

From the general solution

$$R_{gy}(t)=R_{gy}(0)+\frac{c_y}{\beta_0}\ln\frac{\alpha_g(t)}{\alpha_g(0)}\,, \tag{.49}$$

it is readily seen that the compositeness condition parametrized by

$$\alpha_g(t_L)=\alpha_g(0)\exp\left(-\frac{\beta_0}{c_y}R_{gy}(0)\right)<\alpha_g(0)\,, \tag{.50}$$

is always satisfied, since the coefficients in the exponential are positive definite. Furthermore the composite scale here reads:

$$t_L=\ln\frac{\Lambda_{UV}}{\mu_0}=\frac{1}{\beta_0\alpha_g(0)}\left[\exp\left(\frac{\beta_0}{c_y}R_{gy}(0)\right)-1\right]\,. \tag{.51}$$

This is not in contradiction with Eq. (.47), since it can be seen to be contained in that expression by noting that:

$$\lim_{a\to0}\left(1+a\frac{R_{gy}(0)}{-ab}\right)^{\frac{1}{a}}=\exp\left(\frac{R_{gy}(0)}{-ab}\right)=\exp\left(\frac{\beta_0}{c_y}R_{gy}(0)\right)\,. \tag{.52}$$

The hierarchy of scales between the composite and strong scales can now be computed:

$$t_L-t_s=\ln\frac{\Lambda_{UV}}{\Lambda_{IR}}=\frac{1}{\beta_0\alpha_g(0)}\left(1-\frac{R_{gy}(0)}{b}\right)^{\frac{1}{a}}=\frac{1}{\beta_0\alpha_g(0)}\left(1+R_{gy}(0)\frac{\beta_0-c_g}{c_y}\right)^{\frac{\beta_0}{\beta_0-c_g}}\,. \tag{.53}$$

As we noted before, the expression is regular for $(\beta_0-c_g)\to0$.

**The $SU(N)$ case**

Let us be specific and restrict to the case in Eq. (4.30) discussed in the paper, where:

$$\beta_0 = \frac{22-4x}{3}\,, \quad c_y = 2(1+x)\,, \quad c_g = 6\,. \tag{.54}$$

The parameters $a$ and $b$ then read:

$$a = \frac{2(1-x)}{11-2x}\,, \qquad b = \frac{3(x+1)}{2(x-1)}\,. \tag{.55}$$

For $x \leq 1$ we get that $a \geq 0$ and the compositeness conditions are always satisfied from the above analysis. For $x > 0$ we get that $a < 0$ and $b > 0$. The compositeness conditions are in this case only satisfied if furthermore $b > R_{gy}(0)$ or equivalently:

$$\frac{\alpha_y(0)}{\alpha_g(0)} > \frac{2(x-1)}{3(x+1)}\,. \tag{.56}$$

Since $\frac{\alpha_y(0)}{\alpha_g(0)} > 0$ is always true, this constraint holds automatically for $x \leq 1$. Thus for any $x < 11/2$ (such that $\beta_0 > 0$) we can uniquely impose the compositeness condition in Eq. (.56). Finally, the hierarchy of scales is given by:

$$\ln \frac{\Lambda_{UV}}{\Lambda_{IR}} = \frac{3\left(1+\frac{\alpha_g(0)}{\alpha_y(0)}\frac{(1-x)}{3(1+x)}\right)^{2\frac{11-2x}{2(1-x)}}}{2(11-2x)\alpha_g(0)}\,. \tag{.57}$$

## THE QUARTIC SCALAR SECTOR

From the compositeness conditions Eq. (.33) it follows that the quartic couplings may diverge only as fast as $\alpha_y$ at the composite scale. This specifically means that Landau poles in the quartic couplings entering before $t_L$, defined above, are not allowed. At the level of perturbation theory this is already implicit, since otherwise the above analysis would suffer from large corrections from the quartic couplings.

We consider, as before, the RG evolution of ratios. In particular, consider

$$R_{yu} = \frac{\alpha_y}{\alpha_u}\,, \quad R_{yv} = \frac{\alpha_y}{\alpha_v}\,. \tag{.58}$$

The RG equation for $R_{yu}$ can be written in terms of $R_{gy}$ as follows:

$$\frac{dR_{yu}}{d\ln R_{gy}} = \frac{d_u + c_g R_{gy} R_{yu} + (d_y - c_y) R_{yu} - d_{yy} R_{yu}^2}{c_y - (c_g - \beta_0) R_{gy}}\,. \tag{.59}$$

This equation is not well-defined at $c_y - (c_g - \beta_0) R_{gy} = 0$, which is a problem we will get back to. To investigate the compositeness conditions, however, we only need to understand the asymptotic behavior as $t \to t_L$, and since $R_{gy}(t_L) = 0$, and $c_y > 0$,

the above equation is well-defined in limit $t \to t_L$. The asymptotic RG behavior is thus given by:

$$\frac{dR_{yu}}{d\ln R_{gy}}\Big|_{t\to t_L} = \frac{d_u}{c_y} + \left(\frac{d_y}{c_y} - 1\right) R_{yu} - \frac{d_{yy}}{c_y} R_{yu}^2 = \rho_0 + \rho_1 R_{yu} - \rho_2 R_{yu}^2 \,, \tag{.60}$$

where to keep the notation light we introduced the coefficients $\rho_i$. Defining some intermediary scale $t_* \lesssim t_L$, where the asymptotic solution is viable, we can parametrize this solution by:

$$R_{yu}(t)\Big|_{t\approx t_L} = \frac{\rho_1 - \Delta_\rho \tanh\left(K - \frac{\Delta_\rho}{2}\ln\frac{R_{gy}(t)}{R_{gy}(t_*)}\right)}{2\rho_2} \,, \tag{.61}$$

where the discriminant $\Delta_\rho$ reads:

$$\Delta_\rho = \sqrt{\rho_1^2 + 4\rho_0\rho_2} \,. \tag{.62}$$

The integration constant $K$ is a number that has to be fixed by matching $R_{yu}(t_*)\Big|_{t\approx t_L}$ to the full solution given in terms of $R_{yu}(0)$ at the scale $t_*$, and is for this analysis unimportant. The important result is that the solution exists and that the ratio of couplings $R_{yu}$ at the composite scale is fixed, since $R_{gy}(t_L) = 0$ and $\tanh(\infty) = 1$, and reads:

$$R_{yu}(t_L) = \frac{\rho_1 - \Delta_\rho}{2\rho_2} \,, \tag{.63}$$

which is also a fixed-point of the RG equation (.60). Notice that this value is negative, meaning that $\alpha_u$ diverges to negative infinity as fast as $\alpha_y$ diverges to positive infinity, while keeping their ratio constant. This is potentially a problem for the stability of the potential near the composite scale. We shall comment on it after having considered the other quartic coupling $\alpha_v$ as well. Let us comment on the region of validity of the above approximation. Since $R_{yu}(t_L) \neq 0$ for any parameter value, the asymptotic solution will be a good approximation as long as $R_{gy}(t) \ll 1$. This can be expressed in terms of the initial conditions:

$$t_L > t_{asymp.} \gg \frac{1}{\beta_0 \alpha_g(0)} \left[\left(\frac{R_{gy}(0) - b}{1 - b}\right)^{\frac{1}{a}} - 1\right] \,, \tag{.64}$$

which for $a = 0$ exponentiates to:

$$t_L > t_{asymp.} \gg \frac{1}{\beta_0 \alpha_g(0)} \left[\exp\left(\frac{\beta_0}{c_y}\left(R_{gy}(0) - 1\right)\right) - 1\right] \,. \tag{.65}$$

Next we like to address the issue of divergence in Eq. (.59). The potential problem is that if for some $t_s < t < t_L$ the denominator goes to zero, i.e. $R_{gy}(t) = \frac{c_y}{c_g - \beta_0} = b$, then the quartic coupling will diverge at $t$. If $\beta_0 > c_g$ then it is automatically never

satisfied since $R_{gy}(t) > 0$. Let us consider the case $c_g > \beta_0$, meaning that $a < 0$ and $b > 0$. From the general solution it is readily found that $R_{gy}(t) = b$ only occurs for $t = t_s$, which is consistent and not a problem.

Finally, as a last condition on $\alpha_u$, we must ensure that it does not have Landau poles in the whole region $t_s < t < t_L$. We ensure this by negation: consider the case where $\alpha_u$ does have a pole at a scale $t_s < t_u < t_L$. Near this scale $\alpha_u$ is much bigger than $\alpha_y$, and to a good approximation the RG equation reads:

$$\beta_{\alpha_u} \approx d_u \alpha_u^2 \,. \tag{.66}$$

This is similar to the RG equation for $\alpha_g$, and analogously its strong scale reads:

$$t_u = \frac{1}{d_u \alpha_u(0)} \,. \tag{.67}$$

To ensure perturbation theory to be valid in the region $t_s < t < t_L$ thus requires that $t_u < t_s$ or $t_u > t_L$. Formally this gives:

$$d_u|\alpha_u(0)| < \begin{cases} \beta_0 \alpha_g(0) & \text{for } \alpha_u(0) < 0 \qquad (\Leftrightarrow t_u < t_s) \\ \beta_0 \alpha_g(0) \left[ \left( 1 - \frac{R_{gy}(0)}{b} \right)^{\frac{1}{a}} - 1 \right]^{-1} & \text{for } \alpha_u(0) > 0 \qquad (\Leftrightarrow t_u > t_L) \end{cases} \tag{.68}$$

One can also include the corrections to this, by including the term $\alpha_y(t)\alpha_u(t)$ in $\beta_{\alpha_u}$ and setting $\alpha_y(t) \approx \alpha_y(0)$, which is a good approximation for intermediary scales. One then finds the strong scale of $\alpha_u$ to be:

$$t_u = \frac{1}{d_y \alpha_y(0)} \log\left( 1 + \frac{d_y}{d_u} \frac{\alpha_y(0)}{\alpha_u(0)} \right) , \tag{.69}$$

which makes small corrections to the above bound on $\alpha_u(0)$. Finally, including all terms and assuming $\alpha_y(t) \approx \alpha_y(0)$, one can solve for $\alpha_u(t)$ exactly. Defining $A = d_u$, $B = d_y \alpha_y(0)$ and $C = -d_{yy} \alpha_y(0)^2$, and the discriminant $D = \sqrt{B^2 - 4AC}$, which is always real, since $C < 0$, the solutions reads:

$$\alpha_u(t)\Big|_{t_{intermed.}} = -\frac{B + D \tanh\left[ \frac{1}{2} D t - \tanh^{-1}\left( \frac{B + 2A\alpha_u(0)}{D} \right) \right]}{2A} \,. \tag{.70}$$

If the argument of tanh is real, there is never a Landau pole, since $\tanh \in [-1, 1]$ on the real domain. The argument can turn complex if $|B + 2A\alpha_u(0)| > D$, which potentially can lead to a Landau pole. Here one has to compute $t_u$ case by case and compare with $t_s$ and $t_L$. To avoid this, one can ensure that there is never a pole, by over-constraining the argument of tanh to always be real, i.e.:

$$|B + 2A\alpha_u(0)| < D \quad \Leftrightarrow \quad -B - D < 2A\alpha_u(0) < -B + D \tag{.71}$$

$$\Rightarrow -1 - \sqrt{1 + \frac{4 d_u d_{yy}}{d_y^2}} < 2\frac{d_u \alpha_u(0)}{d_y \alpha_y(0)} < -1 + \sqrt{1 + \frac{4 d_u d_{yy}}{d_y^2}} \,. \tag{.72}$$

We now move on to the coupling $\alpha_v$, through $R_{yv}$, as we did for $\alpha_u$ above. Its RG equation can be written as:

$$\frac{dR_{yv}}{d\ln R_{gy}} = \frac{\left(c_g R_{gy} - c_y + d_y\right) R_{yu}^2 R_{yv} + f_u R_{yu} R_{yv} + f_{uu} R_{yv}^2 + f_v R_{yu}^2}{\left(R_{gy}\left(\beta_0 - c_g\right) + c_y\right) R_{yu}^2} \,. \tag{.73}$$

This is in general not a useful description, however, asymptotically the equation simplifies to:

$$\frac{dR_{yv}}{d\ln R_{gy}}\Big|_{t\approx t_L} = \frac{f_{uu}}{c_y R_{yu}^2(t_L)} R_{yv}^2 + \left(\rho_1 - \frac{f_u}{c_y |R_{yu}(t_L)|}\right) R_{yv} + \frac{f_v}{c_y} = \eta_2 R_{yv}^2 + \eta_1 R_{yv} + \eta_0 \,, \tag{.74}$$

where we defined the coefficients $\eta_i$. Note that $\eta_0 > 0$ and $\eta_2 > 0$, while $\eta_1$ can take any real value, in general. The general solution reads:

$$R_{yv}(t)\Big|_{t\approx t_L} = -\frac{\eta_1 + \Delta_\eta \tanh\left(\frac{1}{2}\Delta_\eta \ln \frac{R_{gy}(t)}{R_{gy}(t_*)} + K_v\right)}{2\eta_2} \,, \tag{.75}$$

where $t_*$ is defined as before and

$$\Delta_\eta = \sqrt{\eta_1^2 - 4\eta_0\eta_2} > 0 \,. \tag{.76}$$

The positivity constraint on this expression is a requirement we have to impose to satisfy the compositeness conditions; for imaginary $\Delta_\eta$ the above expression switches from tanh to tan, and leads to Landau poles in $\alpha_v$ before the composite scale. This is therefore a constraint on the possible theory space of gauge-Yukawa theories we are considering. Furthermore we get that:

$$R_{yv}(t_L) = -\frac{\eta_1 - \Delta_\eta}{2\eta_2} \,. \tag{.77}$$

Finally, we repeat the exercise of removing possible parameter region that violates perturbation theory in the region $t_s < t < t_L$ by considering the strong scale of $\alpha_v$. To a first approximation it is simply:

$$t_v = \frac{1}{f_v \alpha_v(0)} \,, \tag{.78}$$

which leads to the equivalent bounds as in Eq. (.68). Perturbation theory is ensured if $t_v < t_s$ for $\alpha_v(0) < 0$ and $t_v > t_L$ for $\alpha_v(0) > 0$. Finally, we can again solve the full differential equation by assuming that at intermediate scales $\alpha_y(t) \approx \alpha_y(0)$ and $\alpha_u(t) \approx \alpha_u(0)$, which are good approximations in the composite phase space. Defining this time $A = f_v$, $B = d_y\alpha_y(0) + f_u\alpha_u(0)$ and $C = f_{uu}\alpha_u(0)^2$ and the discriminant $D = \sqrt{B^2 - 4AC}$, the solution is given by the same expression as for $\alpha_u$ in Eq. (.70). However, note that this time $C > 0$ and thus the discriminant can turn

complex, i.e. for $B^2 < 4AC$. Considering this case, the expression is rewritten in terms of tan:

$$\alpha_v(t)\Big|_{t_{intermed.}} = -\frac{B-(iD)\tan\left[\frac{1}{2}(iD)\,t+\tan^{-1}\left(\frac{B+2A\alpha_v(0)}{(iD)}\right)\right]}{2A}\,. \tag{.79}$$

In this case there are many poles, since $\tan(\pi/2+n\pi)=\pm\infty$ for all integer $n$. The scales at which these occur is given by:

$$t_v = \frac{\pi-2\tan^{-1}\left(\frac{B+2A\alpha_v(0)}{(iD)}\right)+n\cdot 2\pi}{(iD)}\,. \tag{.80}$$

This leads to the extra constraint, i.e. the smallest negativ $t_v$ has to be less than $t_s$ and the smallest positive $t_v$ has to be bigger than $t_L$. This constraint is relevant whenever $4f_vf_{uu} > \left(f_u + d_y\frac{\alpha_y(0)}{\alpha_u(0)}\right)^2$, while in the opposite case one should consider a constraint equivalent to Eq. (.71).

**The $SU(N)$ case**

Let us apply the above analysis to the case considered in the paper. The beta function coefficients read:

$$d_u = 8\,,\; d_y = 4\,,\; d_{yy} = 2x\,, \tag{.81}$$

$$f_v = 4\,,\; f_u = 16\,,\; f_{uu} = 12\,. \tag{.82}$$

From these we derive the relevant parameters:

$$\rho_0 = \frac{4}{1+x}\,,\; \rho_1 = \frac{1-x}{1+x}\,,\; \rho_2 = \frac{x}{1+x}\,,\; \Delta_\rho = \frac{\sqrt{(1-x)^2+16x}}{1+x}\,, \tag{.83}$$

$$\eta_0 = \frac{2}{1+x}\,,\; \eta_1 = -\frac{\sqrt{(1-x)^2+16x}}{1+x}\,,\; \eta_2 = \frac{24x^2}{(1+x)(x-1+\sqrt{(1-x)^2+16x})^2}\,. \tag{.84}$$

Notice that $\eta_1 < 0$ for any $x$. The expression for $\Delta_\eta$ takes a lengthy expression, but its constraint Eq. (.76) leads to:

$$x > -4+3\sqrt{3}-\sqrt{6(7-4\sqrt{3})} \approx 0.54\,. \tag{.85}$$

For a given $x$ it is always possible to find initial parameter values for $\alpha_g$, $\alpha_y$, $\alpha_u$ and $\alpha_v$ such that the constraints Eqs. (.56), (.68), (.71), (.76), and the ones related to Eq. (.78)-(.80) are satisfied. We consider the details in the paper.

We have furthermore found that the ratio of quartic couplings over $\alpha_y$ are completely fixed at the composite scale, independent of initial conditions, and given by Eq. (.63) and (.77).

## RUNNING MASS AND STABILITY OF THE POTENTIAL

The RG equation describing the running of the scalar mass term is given by

$$\beta_{m_H^2} = \partial_t m_H^2 = m_H^2(h_y\alpha_y + h_v\alpha_v + h_u\alpha_u)\,, \tag{.86}$$

where for $SU(N_C)$ the parameters read in the Veneziano limit: $h_y = 4$, $h_v = 4$, $h_u = 8$. This expression shows that, where it is valid, the scalar mass term can not change sign, since its beta function is proportional to the squared mass itself. The initial condition $m_H^2 > 0$, should then ensure that spontaneous symmetry breaking will not occur in the range where the above expression may be applied.

The further condition $m_H^2(\mu) < \mu^2$ should also be satisfied to make sure that no scalar states decouple at energies higher than the strong scale. However, this constraint is not related to compositeness and can be relaxed to instead read $m_H^2(\mu) < \mu_0$ such that the composite nature of the theory, which is probed for $\mu > \mu_0$ stays intact, while the IR physics defined by $\mu < \mu_0$ may have different phases. In our analysis we have constraint the IR phase to be dominated by strong gauge interactions.

Proceeding to study the stability conditions on the potential, we first note that the scalar fields are well-defined for field values $m_H(\mu) < H < \Lambda_{UV}$, where as argued above $m_H(\mu) < \mu_0$. For a positive mass-term it is clear that the potential has a minimum at the origin, $\langle H\rangle = 0$, which preserves the $U(N_F)\times U(N_F)$ symmetry of the classical theory. To ensure consistency of our analysis, we must make sure that this symmetry is obeyed for large field values as well and at every scale in the region $\mu_0 < \mu < \Lambda_{UV}$. It is enough to study the diagonal field $H = \mathrm{d}iag(h_1,\ldots,h_{N_F})$ since this can be rotated into any other $H$ by a $U(N_F)\times U(N_F)$ transformations. In terms of $h_i$ the potential reads:

$$V = m_H^2\sum_{i=1}^{N_F} h_i^2 + u\sum_{i=1}^{N_F} h_i^4 + v\left(\sum_{i=1}^{N_F} h_i^2\right)^2 . \tag{.87}$$

We consider the general case where $u$ and $v$ can take both positive and negative values. As argued before if all $h_i$ are small (i.e. $h_i \ll m_H$) then one sees that the minimum is at the origin, since $m_H > 0$. Let us now consider what happens for large values of some of the fields $h_i$, in particular take for $i = 1,\ldots,n$ the fields $h_i \to \Lambda_{UV}$, while for $i = n+1,\ldots,N_F$ keep $h_i \ll m_H$. Then the potential is dominated by the large fields and reads approximately:

$$V \approx m_H^2(n\Lambda_{UV}^2) + u(n\Lambda_{UV}^4) + v(n^2\Lambda_{UV}^4)\,. \tag{.88}$$

Positivity of this potential requires:

$$\frac{m_H^2}{n\Lambda_{UV}^2} + \frac{u}{n} + v \geq 0\,. \tag{.89}$$

In term of the rescaled couplings from Eq. (4.16), this becomes

$$\frac{m_H^2 N_F^2}{n(4\pi\Lambda_{UV})^2} + \frac{\alpha_u N_F}{n} + \alpha_v \geq 0 \quad \overset{N_F\to\infty}{\Longrightarrow} \quad m_H^2 > 0\,. \tag{.90}$$

Thus, in the large $N_F$ limit already assumed constraint $m_H^2 > 0$ ensures the potential to stay positive in the entire region of field values.

For completeness, let us discuss the finite $N_F$ case, and thus consider the unrescaled couplings. If $u$ is negative, then the strongest constraint comes from $n = 1$, yielding the constraint:

$$\frac{m_H^2}{\Lambda_{UV}^2} + v \geq -u \quad \text{for } u < 0\,. \tag{.91}$$

If $v$ is negative, the strongest constraint comes from $n = N_F$, thus:

$$\frac{m_H^2}{\Lambda_{UV}^2} + u \geq -v\,N_F \quad \text{for } v < 0\,. \tag{.92}$$

If both $u$ and $v$ are negative, one has to maximize the function $u + nv$ for $n$, and ensure that the general constraint Eq. (.89) is satisfied.

# BIBLIOGRAPHY


[1] O. Antipin, M. Gillioz, J. Krog, E. Mølgaard and F. Sannino, JHEP **1308**, 034 (2013) [arXiv:1306.3234 [hep-ph]].

[2] O. Antipin, J. Krog, M. Mojaza and F. Sannino, Nucl. Phys. B **886**, 125 (2014) [arXiv:1311.1092 [hep-ph]].

[3] J. Krog, M. Mojaza and F. Sannino, arXiv:1506.02642 [hep-ph].

[4] J. Krog and C. T. Hill, arXiv:1506.02843 [hep-ph].

[5] O. Antipin, J. Krog, E. Mølgaard and F. Sannino, JHEP **1309**, 122 (2013) [arXiv:1303.7213 [hep-ph]].

[6] M. E. Peskin and D. V. Schroeder, Reading, USA: Addison-Wesley (1995) 842 p

[7] [CMS Collaboration], CMS-PAS-HIG-13-005.

[8] D. J. Gross and F. Wilczek, Phys. Rev. Lett. **30**, 1343 (1973).

[9] H. D. Politzer, Phys. Rev. Lett. **30**, 1346 (1973).

[10] C. Wetterich, DESY-87-154.

[11] F. Bezrukov and M. Shaposhnikov, JHEP **0907**, 089 (2009) [arXiv:0904.1537 [hep-ph]].

[12] M. Shaposhnikov and C. Wetterich, Phys. Lett. B **683**, 196 (2010) [arXiv:0912.0208 [hep-th]].

[13] W. A. Bardeen, C. T. Hill and M. Lindner, Phys. Rev. D **41**, 1647 (1990).

[14] H. C. Cheng, B. A. Dobrescu and J. Gu, JHEP **1408**, 095 (2014) [arXiv:1311.5928 [hep-ph]].

[15] H. Osborn, Nucl. Phys. B **363**, 486 (1991).

[16] I. Jack and H. Osborn, Nucl. Phys. B **343**, 647 (1990).

[17] G. Degrassi, S. Di Vita, J. Elias-Miro, J. R. Espinosa, G. F. Giudice, G. Isidori and A. Strumia, JHEP **1208**, 098 (2012) [arXiv:1205.6497 [hep-ph]].

[18] M. Holthausen, K. S. Lim and M. Lindner, JHEP **1202**, 037 (2012) [arXiv:1112.2415 [hep-ph]].

[19] K. G. Chetyrkin and M. F. Zoller, JHEP **1206**, 033 (2012) [arXiv:1205.2892 [hep-ph]].

[20] L. N. Mihaila, J. Salomon and M. Steinhauser, Phys. Rev. Lett. **108**, 151602 (2012) [arXiv:1201.5868 [hep-ph]].

[21] C. Ford, I. Jack and D. R. T. Jones, Nucl. Phys. B **387**, 373 (1992) [Nucl. Phys. B **504**, 551 (1997)] [hep-ph/0111190].

[22] K. G. Chetyrkin and M. F. Zoller, JHEP **1**304, 091 (2013) [Erratum-ibid. **1309**, 155 (2013)] [arXiv:1303.2890 [hep-ph]].

[23] J. A. Casas, J. R. Espinosa and M. Quiros, Phys. Lett. B **342**, 171 (1995) [hep-ph/9409458].

[24] J. A. Casas, J. R. Espinosa, M. Quiros and A. Riotto, Nucl. Phys. B **436**, 3 (1995) [Nucl. Phys. B **439**, 466 (1995)] [hep-ph/9407389].

[25] G. Isidori, G. Ridolfi and A. Strumia, Nucl. Phys. B **609**, 387 (2001) [hep-ph/0104016].

[26] J. Beringer *et* al. [Particle Data Group Collaboration], Phys. Rev. D **86**, 010001 (2012).

[27] J. R. Espinosa, G. F. Giudice and A. Riotto, JCAP **0805**, 002 (2008) [arXiv:0710.2484 [hep-ph]].

[28] J. R. Espinosa, G. F. Giudice, E. Morgante, A. Riotto, L. Senatore, A. Strumia and N. Tetradis, JHEP **1509**, 174 (2015) [arXiv:1505.04825 [hep-ph]].

[29] K. Dissauer, M. T. Frandsen, T. Hapola and F. Sannino, Phys. Rev. D **87**, no. 3, 035005 (2013) [arXiv:1211.5144 [hep-ph]].

[30] M. T. Frandsen, F. Sannino, I. M. Shoemaker and O. Svendsen, Phys. Rev. D **89**, no. 5, 055004 (2014) [arXiv:1312.3326 [hep-ph]].

[31] F. Bezrukov, M. Y. Kalmykov, B. A. Kniehl and M. Shaposhnikov, JHEP **1210**, 140 (2012) [arXiv:1205.2893 [hep-ph]].

[32] H. An, S. L. Chen, R. N. Mohapatra, S. Nussinov and Y. Zhang, Phys. Rev. D **82**, 023533 (2010) [arXiv:1004.3296 [hep-ph]].

[33] T. Banks, J. F. Fortin and S. Thomas, arXiv:1007.5515 [hep-ph].

[34] E. Del Nobile, C. Kouvaris, P. Panci, F. Sannino and J. Virkajarvi, JCAP **1208**, 010 (2012) [arXiv:1203.6652 [hep-ph]].

[35] A. L. Fitzpatrick and K. M. Zurek, Phys. Rev. D **82**, 075004 (2010) [arXiv:1007.5325 [hep-ph]].

[36] O. Antipin, M. Mojaza and F. Sannino, Phys. Rev. D **89**, no. 8, 085015 (2014) [arXiv:1310.0957 [hep-ph]].

[37] S. R. Coleman, Phys. Rev. D **15**, 2929 (1977) [Phys. Rev. D **16**, 1248 (1977)].

[38] J. R. Espinosa and M. Quiros, Phys. Lett. B **353**, 257 (1995) [hep-ph/9504241].

[39] S. Weinberg, (1979). Ultraviolet divergences in quantum theories of gravitation. In "General Relativity: An Einstein centenary survey", ed. S. W. Hawking and W. Israel. Cambridge University Press. pp. 790Ð831

[40] D. F. Litim, PoS QG **-Ph**, 024 (2007) [arXiv:0810.3675 [hep-th]].

[41] R. Percacci and D. Perini, Phys. Rev. D **68**, 044018 (2003) [hep-th/0304222].

[42] M. Reuter, Phys. Rev. D **57**, 971 (1998) [hep-th/9605030].

[43] G. Narain and R. Percacci, Class. Quant. Grav. **27**, 075001 (2010) [arXiv:0911.0386 [hep-th]].

[44] S. P. Robinson and F. Wilczek, Phys. Rev. Lett. **96**, 231601 (2006) [hep-th/0509050].

[45] S. Folkerts, D. F. Litim and J. M. Pawlowski, Phys. Lett. B **709**, 234 (2012) [arXiv:1101.5552 [hep-th]].

[46] A. Rodigast and T. Schuster, Phys. Rev. Lett. **104**, 081301 (2010) [arXiv:0908.2422 [hep-th]].

[47] J. Elias-Miro, J. R. Espinosa, G. F. Giudice, H. M. Lee and A. Strumia, JHEP **1206**, 031 (2012) [arXiv:1203.0237 [hep-ph]].

[48] Y. Nambu and G. Jona-Lasinio, Phys. Rev. **124**, 246 (1961).

[49] A. Hasenfratz, P. Hasenfratz, K. Jansen, J. Kuti and Y. Shen, Nucl. Phys. B **365**, 79 (1991).

[50] P. Gerhold and K. Jansen, JHEP **0709**, 041 (2007) [arXiv:0705.2539 [hep-lat]].

[51] P. Gerhold, K. Jansen and J. Kallarackal, Phys. Lett. B **710**, 697 (2012) [arXiv:1111.4789 [hep-lat]].

[52] D. Y.-J. Chu, K. Jansen, B. Knippschild, C.-J. D. Lin and A. Nagy, Phys. Lett. B **744**, 146 (2015) [arXiv:1501.05440 [hep-lat]].

[53] S. Catterall and A. Veernala, Phys. Rev. D **87**, no. 11, 114507 (2013) [arXiv:1303.6187 [hep-lat]].

[54] R. S. Chivukula, M. Golden and E. H. Simmons, Phys. Rev. Lett. **70**, 1587 (1993) [hep-ph/9210276].

[55] W. A. Bardeen, C. T. Hill and D. U. Jungnickel, Phys. Rev. D **49**, 1437 (1994) [hep-th/9307193].

[56] M. Bando, T. Kugo, N. Maekawa and H. Nakano, Phys. Rev. D **44**, 2957 (1991).

[57] D. F. Litim and F. Sannino, JHEP **1412**, 178 (2014) [arXiv:1406.2337 [hep-th]].

[58] D. F. Litim, M. Mojaza and F. Sannino, arXiv:1501.03061 [hep-th].

[59] M. x. Luo, H. w. Wang and Y. Xiao, Phys. Rev. D **67**, 065019 (2003) [hep-ph/0211440].

[60] M. E. Machacek and M. T. Vaughn, Nucl. Phys. B **222**, 83 (1983).

[61] M. E. Machacek and M. T. Vaughn, Nucl. Phys. B **236**, 221 (1984).

[62] M. E. Machacek and M. T. Vaughn, Nucl. Phys. B **249**, 70 (1985).

[63] A. G. M. Pickering, J. A. Gracey and D. R. T. Jones, Phys. Lett. B **510**, 347 (2001) [Phys. Lett. B **535**, 377 (2002)] [hep-ph/0104247].

[64] L. N. Mihaila, J. Salomon and M. Steinhauser, Phys. Rev. D **86**, 096008 (2012) [arXiv:1208.3357 [hep-ph]].

[65] J. A. Gracey and R. M. Simms, Phys. Rev. D **91**, no. 8, 085037 (2015) [arXiv:1504.00186 [hep-ph]].

[66] T. A. Ryttov, Phys. Rev. D **90**, no. 5, 056007 (2014) [Phys. Rev. D **91**, no. 3, 039906 (2015)] [arXiv:1408.5841 [hep-th]].

[67] T. A. Ryttov, Phys. Rev. D **89**, no. 5, 056001 (2014) [arXiv:1311.0848 [hep-ph]].

[68] T. A. Ryttov and R. Shrock, Phys. Rev. D **86**, 065032 (2012) [arXiv:1206.2366 [hep-ph]].

[69] O. Antipin, S. Di Chiara, M. Mojaza, E. Mølgaard and F. Sannino, Phys. Rev. D **86**, 085009 (2012) [arXiv:1205.6157 [hep-ph]].

[70] O. Antipin, M. Gillioz, E. Mølgaard and F. Sannino, Phys. Rev. D **87**, no. 12, 125017 (2013) [arXiv:1303.1525 [hep-th]].

[71] B. Pendleton and G. G. Ross, Phys. Lett. B **98**, 291 (1981).

[72] C. T. Hill, Phys. Rev. D **24**, 691 (1981).

[73] Y. Nambu, report EFI 88-39 (July 1988), published in the Proceedings of the *Kazimierz 1988 Conference on New theories in physics*, ed. T. Eguchi and K. Nishijima; in the Proceedings of the *1988 International Workshop on New Trends in Strong Coupling Gauge Theories*, Nagoya, Japan, ed. Bando, Muta and Yamawaki (World Scientific, 1989); report EFI-89-08 (1989); see also H.Terazawa, in *Proc.XXII International Conf. on High Energy Physics*, Leipzig, 1984, edited by A. Meyer and E.Wieczorek, Vol.I, p.63.

[74] V. A. Miransky, M. Tanabashi and K. Yamawaki, Phys. Lett. B **221**, 177 (1989); *ibid*, Mod. Phys. Lett. A **4**, 1043 (1989). W. J. Marciano, Phys. Rev. Lett. **62** (1989) 2793.

[75] C. T. Hill and E. H. Simmons, Phys. Rept. **381**, 235 (2003) [Phys. Rept. **390**, 553 (2004)]

[76] G. Cvetic, Rev. Mod. Phys. **71**, 513 (1999) [hep-ph/9702381].

[77] G. von Gersdorff, E. Pontón and R. Rosenfeld, JHEP **1506**, 119 (2015) [arXiv:1502.07340 [hep-ph]].

[78] S. P. Martin, Phys. Rev. D **44**, 2892 (1991).

[79] G. K. Leontaris, S. Lola and G. G. Ross, Nucl. Phys. B **454**, 25 (1995) [hep-ph/9505402].

[80] M. Gell-Mann, P. Ramond and R. Slansky, Conf. Proc. C **790927**, 315 (1979)

[81] T. Yanagida, Prog. Theor. Phys. **64**, 1103 (1980).

[82] C. T. Hill, Phys. Lett. B **266**, 419 (1991).

[83] J. Elias-Miro, J. R. Espinosa, G. F. Giudice, H. M. Lee and A. Strumia, JHEP **1206**, 031 (2012)

[84] T. Hambye and A. Strumia, Phys. Rev. D **88**, 055022 (2013),